Characterization of a glycerophosphodiester phosphodiesterase in the human malaria parasite *Plasmodium falciparum*

Titilola Ifeoma Denloye

Dissertation submitted to the faculty of
Virginia Polytechnic Institute and State University
in partial fulfillment of the requirements for the degree of

Doctor of Philosophy
In
Biochemistry

Michael W. Klemba, Chair
Dennis R. Dean
Richard F. Helm
Marcy Hernick
Timothy J. Larson

April 25th, 2012
Blacksburg, VA

Keywords: *Plasmodium falciparum,* malaria, glycerophosphodiester phosphodiesterase, lipid metabolism**,** choline, fatty acid

Characterization of a glycerophosphodiester phosphodiesterase in the human malaria parasite *Plasmodium falciparum*

Titilola Ifeoma Denloye

ABSTRACT

Active lipid metabolism is a key process required for the intra-erythrocytic development of the malaria parasite, *Plasmodium falciparum*. Enzymes that hydrolyze host-derived lipids play key roles in parasite growth, virulence, differentiation, cell-signaling and hemozoin formation. Therefore, investigating enzymes involved in lipid degradation could uncover novel drug targets. We have identified in *P. falciparum,* a glycerophosphodiester phosphodiesterase (PfGDPD), involved in the downstream pathway of phosphatidylcholine degradation. PfGDPD hydrolyzes deacylated phospholipids, glycerophosphodiesters to glycerol-3-phosphate and choline. In this study, we have characterized PfGDPD using bioinformatics, biochemical and genetic approaches. Knockout experiments showed a requirement for PfGDPD for parasite survival. Sequence analysis revealed PfGDPD possesses the unique GDPD insertion domain sharing a cluster of conserved residues present in other GDPD homologues. We generated yellow fluorescent fusion proteins that revealed a complex distribution of PfGDPD within the parasite cytosol, parasitophorous vacuole and food vacuole. To gain insight into the role of PfGDPD, sub-cellular localization was modulated and resulted in a shift in protein distribution, which elicited no growth phenotype. Kinetic analyses suggest PfGDPD activity is Mg^{2+} dependent and catalytically efficient at the neutral pH environment of the parasitophorous vacuole. Next, our aim was to determine the upstream pathway that provides deacylated glycerophosphodiesters as substrate for PfGDPD. We identified via bioinformatics, a *P. falciparum* lysophospholipase (PfLPL1) that directly generates the substrate. Knockout clones were generated and genotyped by Southern and PCR analysis. The effects of PfLPL1 knockouts on parasite fitness were studied, and the results showed that PfLPL1was not required for parasite survival and proliferation.

ACKNOWLEDGMENTS

Words cannot express my gratitude to the people who have sincerely helped me attain my Ph.D. I pray that God will continually bless all your endeavours and grant you success in all you do.

I would first like to thank Dr. Michael Klemba for his guidance and teachings through my many bumpy years in graduate school and towards the completion of my dissertation. You are a brilliant scientist and I am grateful for all that I have learned from you. To my graduate committee members, Drs. Dennis Dean, Richard Helm, Tim Larson and Marcy Hernick, for your advice, patience, and constructive criticisms.

I would also like to thank members of the Klemba lab, Dr Seema Dalal, for her willingness to answer questions and her amazing ability to remember everything, Priscilla Krai, for our many conversations of old school Japanese music and TV shows and for your multiple kind gestures, and Alex Kullifay, for being the most amicable person I know. Also to Daniel Ragheb a recent graduate, helped me through my early years and was always a pleasure to have around.

In addition, my graduate career would not have been possible without the constant support of my friends. First and foremost, Adeseye Adekeye, I can honestly say I would not be writing this page if it weren't for you. Your unwavering friendship and support cannot be matched. Vinaya Raj, Brenna Traver, Rebecca Ortiz, we started graduate school as strangers and now we leave as more than friends. Phillip George, we had fun hanging out, major stress relief!

To my extended family in the US, The Adekoyas, Mrs Akinola, The Gbenros and The Okolos, thank you all for opening up your hearts and houses, and for your constant encouragements.

I definitely would not have been able to get this far without the love, encouragements and countless prayers of my Mom and Dad. I appreciate everything you have sacrificed for me to be where I am today and your tireless words of wisdom and truth, which have made me who I am today. To Tilewa and Soji, thank you both for being awesome siblings, I could not have asked for a better pair.

And last but not the least, thank you Lord Jesus Christ for Your guidance, protection and providence throughout my life. Your love and Grace has continually sustained me and I offer my gratitude, my heart and life for You.

ATTRIBUTION

I performed all the experiments presented in this dissertation except for the following:

Chapter 2: Parasite transfection and generation of PfGDPD C-terminal-YFP parasite lines were performed by Dr Seema Dalal

Chapter 4: Cloning and expression of PfLPL1 C-terminal-YFP fusions and PfLPL1 knockouts for *in vivo* experiments were performed by Dr Seema Dalal

TABLE OF CONTENTS

LIST OF FIGURES

Chapter 4

LIST OF TABLES

LIST OF ABBREVIATIONS

BiP	Binding immunoglobin protein
CAD	Conditional aggregation domain
CDP	Cytidine triphosphate
CFM	Choline-Free Media
CM	Complete RPMI 1640 (CM) medium
DHAP	Dihydroxyacetone phosphate
E63A	Glutamic acid63 to Alanine mutant
EDTA	Ethylenediaminetetraacetic acid
FA	Fatty acids
FASII	Type II fatty acid synthesis
FFA	Free fatty acids
ffBSA	Fatty acid free bovine serum albumin
FKBP	FK506 Binding protein
G3P	*sn*-glycerol-3-phosphate
G3PDH	Glycerol-3-phosphate dehydrogenase
gDNA	Genomic DNA
GDPD	Glycerophosphodiester phosphodiesterase
GDPD-I	GDPD insertion domain
GF	Gel filtration
GroPC	Glycerophosphocholine
hDHFR	Human dihydrofolate reductase
HEPES	4-(2-hydroxyethyl)-1-piperazineethanesulfonic acid
HPPA	3-(*p*-hydroxyphenyl)propionic acid
HRP	Horseradish peroxidase
IMAC	Immobilized metal affinity chromatography
IPTG	Isopropyl β-D-thiogalactopyranoside
KO	Knockout
LPC	Lysophosphatidylcholine
NADH	Nicotinamide adenine dinucleotide
PBS	Phosphate-buffered saline

PC	Phosphatidylcholine
PE	Phosphatidylethanolamine
PfGDPD	*P. falciparum* glycerophosphodiester phosphodiesterase
PfLPL1	*P. falciparum* Lysophospholipase 1
PL	Phospholipid
PS	Phosphatidylserine
PV	Parasitophorous vacuole
PVM	Parasitophorous vacuolar membrane
RBC	Red blood cells
RPMI	Albumax I free medium
SDPM	Serine-decarboxylation-phosphoethanolamine methyltransferase
SDS	Sodium dodecyl sulfate
SERA	Anti-serine-rich antigen
SM	Sphingomyelin
SmaseD	Sphingomyelinase D
TEV	Tobacco etch virus
TIM	Triosephosphate isomerase
ttGDPD	*Thermoanaerobacter tengcongensis* glycerophosphodiester phosphodiesterase
UTR	Un-translated region
WT	Wild-type
YFP	Yellow fluorescent protein

CHAPTER 1

Introduction

1.1 *Plasmodium falciparum* Malaria: An Ongoing Global Problem

Malaria is a disease that has plagued the world for centuries reported as far back as China in 2700 BC [1]. The human disease is caused by five species from the genus *Plasmodium* (*P. falciparum, P. vivax, P. ovale, P. malariae* and *P. knowlesi*), of which *P. falciparum* is the most virulent. The devastating effects of the disease during World War II pre-empted the establishment of the Malaria Control in War Areas (MCWA) in the United States, as an initiative to control the disease. In 1951, its successor, the Communicable Disease Center (now known as the Centers for Disease Control) succeeded at eradicating malaria from the United States using the available insecticide, dichlorodiphenyltrichloroethane (DDT) against the mosquito vector.

Unfortunately, the disease still remains a global problem, predominantly in tropical areas of sub-Saharan Africa, southern Asia and Central and South America, where an estimated 3.3 billion people are reportedly at risk of infection [2]. In 2010, the global deaths reported by the World Health Organization (WHO) was estimated at 655,000 [2], while an independent new study in the British Medical journal, the Lancet, reported a total number of 1.24 million deaths by the mosquito-borne disease [3]. The Lancet study observed a higher proportion of deaths, totalling 433,000 among older children and adults than reported by the WHO [3]. Despite the differences in reports, there has been a decline in mortality rates since 2004, which is attributed to the increase in accessible insecticide-treated mosquito nets (ITNs), indoor residual spraying (IRS), early detection rapid diagnostic tests and the use of artemisinin-based combination therapies (ACTs), as the currently preferred method of treatment. However, in light of these achievements, artemisinin resistance has emerged in countries in South-East Asia while resistance to pyrethroid, the insecticide used in ITNs and IRS have been reported in 24 African countries and 41 countries worldwide [2]. This undoubtedly requires new therapeutic drugs to combat the disease in a rapid and cost effective manner for long-term use.

Currently, there are no licensed anti-malarial vaccines available however, a single candidate vaccine RTS,S/AS01, is being assessed in Phase 3 clinical trials developed in partnership with GlaxoSmithKline and PATH Malaria Vaccine Initiative (Funded by the Bill & Melinda Gates Foundation). The vaccine has shown promising results with a 55 % reduction in incidence rate on clinical malaria over 12 months after the third dose and an efficacy of 35 % after variable follow-up from zero to 22 months after the third dose [4]. These trials are extensive and expensive and the vaccine efficacy rate lies below the WHO standard goal of at least 80 %.

Therefore, the need to develop therapeutic anti-malarial drugs remains the principal means of fighting the disease in a rapid, safe and cost effective manner.

1.2 Life Cycle of *P. falciparum*

The pathogenesis of malaria begins with the inoculation of sporozoite-stage parasites by an infected *Anopheles* mosquito into the blood stream. The parasites migrate to the liver and begin the exoerythrocytic phase where they invade hepatocytes and undergo asexual multiplication. After about a week, infected liver cells rupture and release thousands of merozoite-stage parasites, which traverse the blood stream and proceed to invade red blood cells (RBC). Within the RBC, the parasite is enclosed within a parasitophorous vacuole membrane (PVM) derived from the invagination of the RBC surface membrane, forming a barrier between the parasite and the host erythrocyte. The 48-hr replication cycle begins with the invasion of merozoites that mature from young ring-like structures to the trophozoite feeding stage and finally divide into multi-nucleated schizonts that eventually rupture and release between 8-32 daughter merozoites into the blood stream. The continuous process of erythrocyte reinvasion induces the manifestation of malaria clinical signs and symptoms. Since the parasite life cycle occurs between the human host and the mosquito vector, several stimuli trigger the induction of male and female gametocytes, which are taken up by the mosquito during a blood meal. A number of metabolic processes occur during the erythrocytic phase of development, some of which are vital and distinct to *P. falciparum* and serve as potential drug targets [5, 6]

1.3 *Plasmodium* Phospholipid Metabolism

Intra-erythrocytic replication requires actively controlled metabolic processes to ensure successful cell cycle development and multiplication. Of these, the lipid metabolic system play key roles in parasite growth, virulence, differentiation, cell signalling and hemozoin formation, to name a few [7, 8]. Red blood cells (RBCs) lack the necessary components to synthesize lipids or proteins, therefore the parasite relies on its own machinery in the synthesis of membranes of the permeable PVM, membranes of sub-cellular organelles, cytoplasmic membrane network, lipid signalling molecules and neutral lipid bodies. These membrane components are primarily comprised of glycerophospholipids and sphingolipids. Upon *P. falciparum* infection, there is a 6-fold increase in phospholipid (PL) content compared to non-infected erythrocytes.

Phosphatidylcholine (PC) is the most abundant PL, representing up to 40-50 %, followed by phosphatidylethanolamine (PE) (35-45 %) and phosphatidylinositol (PI) (4-11 %), whereas sphingomyelin (SM) and phosphatidylserine (PS) account for <5 % [9, 10]. There is however, little or no cholesterol present in the parasite [11]. Neutral lipids (including fatty acids (FA), diacylglycerol (DAG) and triacylglycerol (TAG), usually found in trace amounts in uninfected erythrocytes, are also increased upon *Plasmodium* infection [9, 10, 12, 13]. In addition to increased PL content, the parasite engages in remodelling host cell membrane, aiding in host immune evasion and consequent survival within infected erythrocytes. Prior to infection, PS molecules in erythrocytes exclusively localized to the inner leaflets of the lipid bilayer, are flipped to the outer leaflets of parasitized cells and contribute to cytoadherence of infected red cells to the vascular endothelium [7] to consequently evade the spleen. The increase in PL content coupled with PS asymmetry of host cell membrane aids in the pathogenesis of malaria.

To meet the demand of lipid species, the parasite synthesizes PL through *de novo* pathways using precursors procured from the host cytoplasm such as serine, choline, inositol, glycerol, and fatty acids [10, 11]. The synthesis of PC occurs via two metabolic pathways, namely the cytidine triphosphate (CDP)-choline pathway (Kennedy pathway) and the serine-decarboxylation-phosphoethanolamine methyltransferase pathway (SDPM) (Figure 1-1). In the CDP-choline pathway, choline is transported from the host through choline permease, phosphorylated into CDP-choline and acylated in a DAG-dependent reaction to yield PC. The SDPM pathway was elucidated from studies that indicated serine as an alternate precursor for PC and PE synthesis [14, 15]. In this pathway, serine is decarboxylated to ethanolamine, phosphorylated to phosphoethanolamine and either converted to phosphocholine by a methyltransferase and shuttled into the CDP-choline pathway to generate PC, or acylated via a DAG dependent reaction to yield PE through the CDP-ethanolamine pathway.

The considerable increase in lipid content upon *P. falciparum* infection is a direct correlation to increased amount of FA bound to the glycerol backbone [11]. A source of these fatty acids has been attributed to scavenging from the host milieu [16]. Studies have recently elucidated the importance of serum FA, but not phospholipid or neutral lipids for parasite survival [16, 17]. These FA are utilized to synthesize various phospholipids, neutral lipids and glycosylphosphatidylinositol [11]. The specific growth promoting serum FA have been identified as palmitic acid ($C_{16:0}$) and oleic acid ($C_{18:1\ n\text{-}9}$), which are provided in complex with serum

albumin [16, 18, 19]. In addition to host scavenging, the parasite encodes components of the type II fatty acid synthesis pathway (FAS II) within the apicoplast [20]. Though the presence of this pathway ensures *de novo* FA synthesis, the FAS II pathway is reportedly not essential in blood stages but required in the liver stages [21, 22]. This in turn suggests that the bulk of FA is acquired through the uptake of host serum FA [9, 16, 17, 23].

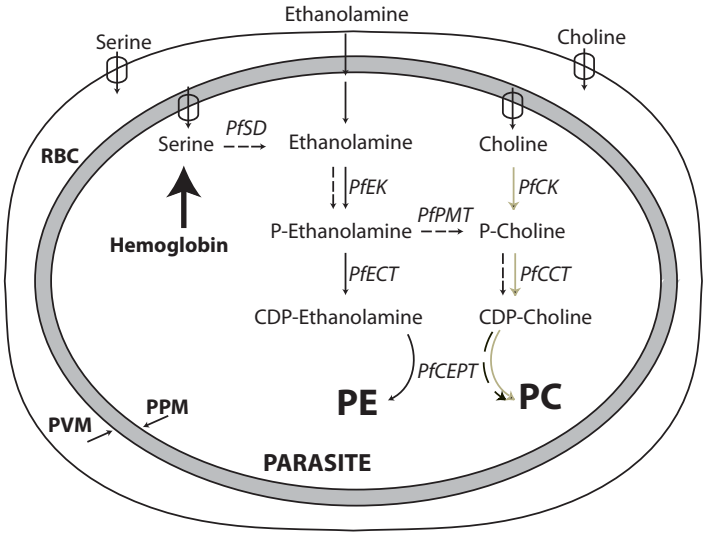

Figure 1-1. Phospholipid biosynthetic pathways in *P. falciparum*. The CDP-Choline pathway is depicted with gold arrows. The CDP-ethanolamine pathway is shown in black arrows and the SDPM pathway indicated with the broken arrows. *PC,* phosphatidylcholine; *PE*, phosphatidylethanolamine; *PfCK*, *P. falciparum* choline kinase; *PfCCT*, *P. falciparum* CTP phosphocholine cytidylyltransferase; *PfEK*, *P. falciparum* ethanolamine kinase; *PfECT*, *P. falciparum* CTP phosphoethanolamine cytidylyltransferase; *PfCEPT*, *P. falciparum* choline/ethanolamine-phosphate transferase; *PfPMT*, *P. falciparum* phosphoethanolamine methyltransferase; *PfSD*, serine decarboxylase; *PPM*, parasite plasma membrane; *PVM*, parasitophorous vacuolar membrane; *RBC*, red blood cell.

1.4 Lipases in *P. falciparum*

The synthesis and subsequent increase in *Plasmodium* phospholipids are undoubtedly important for parasite intra-erythrocytic growth and development. However, phospholipid degradation is also important for parasite growth and survival playing key roles in lipid homeostasis, hemoglobin degradation and hemozoin formation. Evidence for the catabolic activity of lipases have been detected and found to be associated with the degradation of hemoglobin, a process that is essential to parasite survival. Hemoglobin is the oxygen-carrying protein molecule in the red blood cell and its degradation provides the parasite with amino acids (of which only 16 % are incorporated into protein synthesis), space for parasite growth within the RBC and a potential mechanism of osmotic regulation to preserve host cell integrity [24-26]. Inhibition of this catabolic process causes enlarged food vacuole phenotypes and prevents

parasite maturation and replication [27]. A proposed model of the hemoglobin degradation suggests that hemoglobin is internalized through a mouth-like structure called the cytostome into a double membrane endocytic vesicle consisting of an outer plasma membrane (PM) and an inner parasitophorous vacuole membrane (PVM), which is then trafficked to the food vacuole and hydrolysed by resident proteases. Structural studies have elucidated the importance of phospholipases in degrading the inner PVM prior to hemoglobin release. The study of chloroquine treated parasites revealed that the outer PM fuses with the FV membrane to generate a single membrane bound organelle, which still remains intact within the food vacuole, implicating the presence of essential lipases within the parasite [28].

Another study correlated phospholipase activity with hemoglobin degradation in which parasites treated with gentamicin and amikacin were unable to degrade host hemoglobin due the inhibition of a Ca^{2+} independent phospholipase [29]. In addition to lipase activity, lipid degradation products have been associated with the crystallization of hemozoin, a by-product of hemoglobin catabolism. Heme crystallization is the target of available quinoline drugs, indicating the essential nature of this process. Studies have shown that efficient heme crystallization is suitable in a non-polar neutral lipid nanosphere and identified the lipid composition as DAG and TAG produced from PVM degradation by phospholipases [30].

A sphingomyelinase phospholipase C enzyme recently characterized in *P. falciparum,* was shown to be inhibited by scyphostatin, which severely impaired parasite stage progression from trophozoite to schizont [31]. These studies suggest the importance of lipases during intra-erythrocytic parasite growth, which can serve as potential drug targets against malaria parasites. The purpose of this study was to characterize lipases that contribute to the growth and development of *P. falciparum*. We have identified a glycerophosphodiester phosphodiesterase (*Pf*GDPD) which we hypothesize plays a role in phospholipid metabolism during intra-erythrocytic replication.

1.5 The Study of *P. falciparum* Glycerophosphodiester Phosphodiesterase

Glycerophosphodiester phosphodiesterase (GDPD) hydrolyze glycerophosphodiesters into glycerol-3-phosphate and corresponding alcohol head group. GDPD domain family are ubiquitous enzymes found in both prokaryotes and eukaryotes [32-34]. The enzyme was first

characterized in *E.coli* and shows specificity to a variety of glycerophosphodiesters, which include glycerophosphocholine, glycerophosphoethanolamine, glycerophosphoglycerol [35, 36].

In this study, we discuss the bioinformatics approach in identifying GDPD in *P. falciparum* (PfGDPD) and detail its characterization in Chapter 2 and 3. In Chapter 2 we will present data based on the localization, genetic and kinetic characterization of PfGDPD. Attempts to modulate protein levels within the parasite and the subsequent effects on parasite proliferation will be presented in Chapter 3. Chapter 4 will feature the characterization of a lysophospholipase, that we hypothesize is responsible for generating the PfGDPD substrate, glycerophosphocholine.

1.6 REFERENCES

1. Cox, F.E., *History of human parasitology.* Clin Microbiol Rev, 2002. **15**(4): p. 595-612.
2. *World Malaria Report 2011*, World Health Organization: Geneva.
3. Murray, C.J.L., et al., *Global malaria mortality between 1980 and 2010: a systematic analysis.* The Lancet, 2012. **379**(9814): p. 413-431.
4. *First Results of Phase 3 Trial of RTS,S/AS01 Malaria Vaccine in African Children.* New England Journal of Medicine, 2011. **365**(20): p. 1863-1875.
5. Bannister, L.H., Margos, G. M., and Hopkins, J. M, *Making a Home for Plasmodium Post-Genomics: Ultrastructural Organization of the Blood Stages*, in *Molecular Approaches to Malaria*, I.W. Sherman, Editor 2005, American Society for Microbiology Press: Washington, D.C. p. 24-49.
6. Sherman, I.W., *The Life of Plasmodium: an Overview*, in *Molecular Approaches to Malaria*, I.W. Sherman, Editor 2005, American Society for Microbiology Press: Washington, Dc. p. 3-11.
7. Eda, S. and I.W. Sherman, *Cytoadherence of malaria-infected red blod cells involves exposure of phosphatidylserine.* Cell Physiol. Biochem., 2002. **12**: p. 373-384.
8. Katherine, E.J., et al., *Food vacuole-associated lipid bodies and heterogeneous lipid environments in the malaria parasite, Plasmodium falciparum.* Molecular Microbiology, 2004. **54**(1): p. 109-122.
9. Vial, H.J. and M.L. Ancelin, *Malarial Lipids: an overview.* Subcell. Biochem, 1992. **18**: p. 259-306.
10. Holz, G.G., *Lipids and the malaria parasite.* Bull. World Health Organ. (WHO), 1977. **55**: p. 237-248.
11. Vial, H.J.a.B.M., C., *Plasmodium Lipids: Metabolism and Function*, in *Molecular Approaches to Malaria*, I.W. Sherman, Editor 2005, American Society for Microbiology Press: Washington, D.C. p. 327-352.
12. Sherman, I.W., *Biochemistry of Plasmodium (malarial parasites).* Microbiol Rev, 1979. **43**(4): p. 453-95.
13. Vial, H.J., et al., *Biosynthesis and dynamics of lipids in Plasmodium-infected mature mammalian erythrocytes.* Blood Cells, 1990. **16**(2-3): p. 531-55; discussion 556-61.

14. Elabbadi, N., M.L. Ancelin, and H.J. Vial, *Phospholipid metabolism of serine in Plasmodium-infected erythrocytes involves phosphatidylserine and direct serine decarboxylation.* Biochem. J., 1997. **324**(2): p. 435-445.
15. Pessi, G., G. Kociubinski, and C.B. Mamoun, *A pathway for phosphatidylcholine biosynthesis in Plasmodium falciparum involving phosphoethanolamine methylation.* Proceedings of the National Academy of Sciences of the United States of America, 2004. **101**(16): p. 6206-6211.
16. Mitamura, T., et al., *Serum factors governing intraerythrocytic development and cell cycle progression of Plasmodium falciparum.* Parasitology International, 2000. **49**(3): p. 219-229.
17. Vielemeyer, O., et al., *Neutral lipid synthesis and storage in the intraerythrocytic stages of Plasmodium falciparum.* Molecular and Biochemical Parasitology, 2004. **135**(2): p. 197-209.
18. Mi-ichi, F., S. Kano, and T. Mitamura, *Oleic acid is indispensable for intraerythrocytic proliferation of Plasmodium falciparum.* Parasitology, 2007. **134**(12): p. 1671-1677.
19. Mi-ichi, F., K. Kita, and T. Mitamura, *Intraerythrocytic Plasmodium falciparum utilize a broad range of serum-derived fatty acids with limited modification for their growth.* Parasitology, 2006. **133**(04): p. 399-410.
20. Waller, R.F., et al., *Nuclear-encoded proteins target to the plastid in Toxoplasma gondii and Plasmodium falciparum.* Proceedings of the National Academy of Sciences, 1998. **95**(21): p. 12352-12357.
21. Vaughan, A.M., et al., *Type II fatty acid synthesis is essential only for malaria parasite late liver stage development.* Cellular Microbiology, 2009. **11**(3): p. 506-520.
22. Yu, M., et al., *The Fatty Acid Biosynthesis Enzyme FabI Plays a Key Role in the Development of Liver-Stage Malarial Parasites.* Cell Host & Microbe, 2008. **4**(6): p. 567-578.
23. Krishnegowda, G. and D.C. Gowda, *Intraerythrocytic Plasmodium falciparum incorporates extraneous fatty acids to its lipids without any structural modification.* Molecular and Biochemical Parasitology, 2003. **132**(1): p. 55-58.
24. Krugliak, M., J. Zhang, and H. Ginsburg, *Intraerythrocytic Plasmodium falciparum utilizes only a fraction of the amino acids derived from the digestion of host cell cytosol*

for the biosynthesis of its proteins. Molecular and Biochemical Parasitology, 2002. **119**(2): p. 249-256.

25. Allen, R.J.W. and K. Kirk, *Cell volume control in the Plasmodium-infected erythrocyte.* Trends in Parasitology, 2004. **20**(1): p. 7-10.
26. Lew, V.L., T. Tiffert, and H. Ginsburg, *Excess hemoglobin digestion and the osmotic stability of Plasmodium falciparum-infected red blood cells.* Blood, 2003. **101**(10): p. 4189-4194.
27. Rosenthal, P.J. and S.R. Meshnick, *Hemoglobin catabolism and iron utilization by malaria parasites.* Mol Biochem Parasitol, 1996. **83**(2): p. 131-9.
28. Yayon, A., et al., *Effects of chloroquine on the feeding mechanism of the intraerythrocytic human malarial parasite Plasmodium falciparum.* The Journal of Protozoology, 1984. **3**: p. 367-372.
29. Krugliak, M., Z. Waldman, and H. Ginsburg, *Gentamicin and amikacin repress the growth of Plasmodium falciparum in culture, probably by inhibiting a parasite acid phospholipase.* Journal of Life Science, 1987. **40**(13): p. 1253-7.
30. Pisciotta, J.M., et al., *The role of neutral lipid nanospheres in Plasmodium falciparum haem crystallization.* Biochem J, 2007. **402**(1): p. 197-204.
31. Hanada, K., et al., *Plasmodium falciparum Phospholipase C Hydrolyzing Sphingomyelin and Lysocholinephospholipids Is a Possible Target for Malaria Chemotherapy.* The Journal of Experimental Medicine, 2002. **195**(1): p. 23-34.
32. Tommassen, J., et al., *Characterization of two genes, <i>glpQ and <i>ugpQ , encoding glycerophosphoryl diester phosphodiesterases of <i>Escherichia coli</i&gt.* Molecular and General Genetics MGG, 1991. **226**(1): p. 321-327.
33. Fisher, E., et al., *Glycerophosphocholine-dependent Growth Requires Gde1p (YPL110c) and Git1p in Saccharomyces cerevisiae.* Journal of Biological Chemistry, 2005. **280**(43): p. 36110-36117.
34. van der Rest, B., et al., *Glycerophosphocholine Metabolism in Higher Plant Cells. Evidence of a New Glyceryl-Phosphodiester Phosphodiesterase.* Plant Physiol., 2002. **130**(1): p. 244-255.

35. Larson, T.J., M. Ehrmann, and W. Boos, *Periplasmic glycerophosphodiester phosphodiesterase of Escherichia coli, a new enzyme of the glp regulon.* Journal of Biological Chemistry, 1983. **258**(9): p. 5428-5432.

36. Larson, T.J. and A.T. van Loo-Bhattacharya, *Purification and characterization of glpQ-encoded glycerophosphodiester phosphodiesterase from Escherichia coli K-12.* Archives of Biochemistry and Biophysics, 1988. **260**(2): p. 577-584.

CHAPTER 2

Characterization of a glycerophosphodiester phosphodiesterase expressed in *P. falciparum*

2.1 ABSTRACT

Glycerophosphodiester phosphodiesterases (GDPD) are ubiquitous enzymes present in both prokaryotes and eukaryotes, which catalyze the hydrolysis of phospholipid-derived glycerophosphodiesters into glycerol-3-phosphate and the corresponding alcohol head group i.e. choline. GDPDs are involved in a variety of metabolic processes including phospholipid and glycerol metabolism. Through bioinformatics approach, we have identified a single GDPD homologue in *P. falciparum*, which encodes a 56 kDa protein possessing an N-terminal signal sequence. Sequence alignment with *E.coli* and *Thermoanaerobacter tengcongensis* GDPD homologues, revealed a characteristic GDPD insertion domain with conserved residues important in catalysis and metal binding. Genetic studies revealed an important role for PfGDPD during intra-erythrocytic replication. Reporter tag fusion experiments localize PfGDPD to the parasite cytosol, food vacuole and parasitophorous vacuole. Kinetic analyses on both recombinant and native enzymes showed characteristic bivalent metal ion dependency preference as $Mg^{2+} > Mn^{2+} > Co^{2+}$. Steady state parameters indicated efficient catalysis of glycerophosphocholine with a K_m of 3.4 ± 1.6 mM, k_{cat} of 27 ± 6 $s^{-1}$and k_{cat}/K_m of (8.7 ± 4.1) x 10^3 $M^{-1}•s^{-1}$.

2.2 INTRODUCTION

Phospholipid catabolism is an important element of cellular lipid homeostasis that contributes to the growth and multiplication of the malaria parasite, *Plasmodium falciparum*. In the asexual blood stage of the parasite, enzymes that hydrolyze phospholipids may contribute to the breakdown of membranes in the lumen of the food vacuole, generating neutral lipids that can catalyze hemozoin crystallization, an essential process that prevents oxidative damage to the parasite by detoxifying free heme. Therefore, investigating essential lipolytic enzymes could uncover novel drug targets to combat this infectious disease. Accordingly, we have identified a *P. falciparum* homolog of the enzyme glycerophosphodiester phosphodiesterase (PfGDPD) expressed during blood stages, involved in the downstream degradation of phospholipids.

Glycerophosphodiester phosphodiesterases (GDPD) (EC 3.1.4.46) are ubiquitous enzymes found in prokaryotes and eukaryotes with diverse biological functions, such as phospholipid metabolism, cytoskeletal modification, motor neuron differentiation, and as a virulence factor [1-4]. They catalyze the hydrolysis of deacylated glycerophosphodiesters to *sn*-glycerol-3-phosphate (G-3-P) and the corresponding alcohol moiety (Figure 2-1). The alcohol product can be any of several alcohols, which include choline, ethanolamine, or serine, either of which can be shuttled into phospholipid synthesis [5]. Glycerol-3-phosphate has several metabolic fates, to which it can be converted to lysophosphatidic acid and shuttled into phospholipid synthesis, converted to dihydroxyacetone phosphate (DHAP) and acylated for phospholipid synthesis, or shuttled into glycolysis through conversion to DHAP and glyceraldehyde-3-phosphate, or dephosphorylated to glycerol and inorganic phosphate.

GDPDs were initially characterized in bacteria to generate G-3-P as a source of carbon and phosphate and are present as two isoforms, GlpQ and UgpQ, [5, 6]. GDPD in *Haemophilus influenzae*, GlpQ, is considered an important virulence factor contributing to pathogenesis [7]. Studies in a rat otitis model show that *H. influenzae* GlpQ mutants required approximately 100-fold higher inoculum than the parental strain to induce otitis media after injection [7]. Seven mammalian GDPDs, termed GDEs, have been identified to date and are involved in variety of metabolic processes such as osteoblast and neuronal differentiation, phospholipid metabolism, signal transduction, cytoskeletal regulation and osmotic regulation [8].

Available crystal structures of GDPD from various organisms including *E.coli* GlpQ, *Thermotoga maritma* and *Thermoanaerobacter tengcongensis*, (ttGDPD) share the conventional

triosephosphate isomerase (TIM) barrel protein fold [9]. There is a small insertion domain within the TIM barrel fold, unique to the GDPD family and referred to as GDPD-insertion domain (GDPD-I) [10].

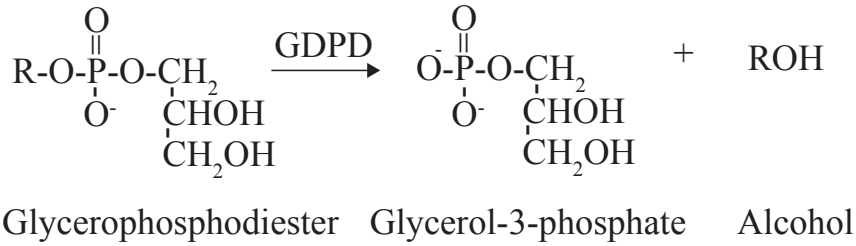

Figure 2-1. Enzymatic reaction of glycerophosphodiester phosphodiesterase. GDPDs hydrolyze the phosphodiester bond of glycerophosphodiesters such as glycerophosphocholine or glycerophosphoethanolamine, to glycerol-3-phosphate and the corresponding alcohol.

Catalysis is mediated by metal ion binding residues and two catalytic histidine residues that are involved in the stabilization and hydrolysis of phosphodiester bond in glycerophosphodiesters via an acid-base mechanism (Figure 2-2) [11, 12]. These conserved residues are located within a cleft at the C terminus of the barrel and considered as the active region in the TIM-barrel super family [11, 13]. GDPDs have been shown to require bivalent metal ions for enzyme activation. In *E.coli*, GlpQ requires Ca^{2+} [5], while UgpQ is activated by Mg^{2+}, Co^{2+} or Mn^{2+} [14], similarly, ttGDPD ahs been reported as a Mg^{2+} dependent enzyme [12]. In *P. falciparum*, we identified only one homologue GDPD (UnitProt ID Q8IM31) in the *Plasmodium* genome (gene ID PF14_0060). We present here the results of our localization studies and gene knockout strategies. Biochemical characterizations of enzyme kinetics and metal ion preference are also discussed.

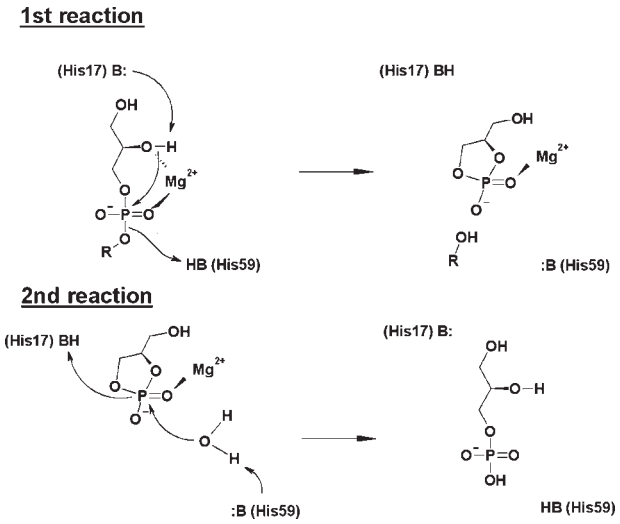

Figure 2-2. Proposed catalytic mechanism of *Thermoanaerobacter tengcongensis* glycerophosphodiester phosphodiesterase [12]. The catalytic histidine residues are located at position 17 and 59. The mechanism is a two-step reaction, where His17 accepts a proton form the OH2 group of glycerol acting as a general base, attacking phosphorous. Simultaneously, His59 acts a general base by donating a proton to the oxygen of the alcohol leaving group. Magnesium ion acts as an electrophile in stabilizing the intermediate. The second reaction follows with the deprotonation of the water molecule by His59, which initiates a nucleophilic attack on cyclic phosphate intermediate. His17 donates a proton to release glycerol-3-phosphate.

2.3 EXPERIMENTAL PROCEDURES

2.3.1 Generation of Constructs

To determine the distribution of PfGDPD in *P. falciparum,* we tagged the chromosomal gene at the C-terminus with yellow fluorescent protein (YFP) to generate PfGDPD-YFP plasmid construct. 3'-1- kb fragments from the PfGDPD sequence excluding the stop codon were PCR amplified from the genomic DNA (gDNA) of *P. falciparum* 3D7 strain, which were cloned upstream of YFP encoding sequence into XhoI/AvrII restriction sites of the vector pPM2CIT2. To disrupt the endogenous PfGDPD copy, we employed a homologous recombination technique using a single crossover truncation plasmid and a double crossover knockout (KO)/negative selection plasmid. Truncation constructs were generated by amplifying the internal bases 299-1108 of the PfGDPD open reading frame from 3D7 gDNA and cloned into XhoI/AvrII sites of pPM2CIT2, upstream of YFP coding sequence. The KO plasmid was constructed by amplifying bases 1-604 to generate a 5' fragment and bases 845-1427, as the 3' fragment. The 5' and 3' inserts were digested and cloned respectively into SacII/SpeI and NcoI/AvrII sites, positioned to flank the positive selection cassette, human *dihydrofolate reductase* (h*DHFR*) in pCC1 vector (Table 2-1).

To obtain recombinant enzyme for kinetic analyses, three types of PfGDPD variants were cloned and expressed. An amino-terminal hexa-histidine fusion protein was generated by amplifying residues 23-475 from 3D7 gDNA, excluding the predicted signal peptide. Inserts were digested and cloned into BamHI/NotI sites of the T7 expression vector pET45b (Novagen). To generate un-tagged and a carboxyl-terminal hexa-histidine fusion protein, sequences were amplified from residues 19-475, digested with BspHI/NotI and cloned into NcoI/NotI sites of pET45b. Site-directed mutagenesis was used to generate mutant PfGDPD in which glutamic acid at position 63 was substituted with alanine (E63A) using the QuikChange XL site directed mutagenesis kit (Agilent Technologies). Mutant protein was cloned as two variants, one with an amino-histidine tag and the other as a carboxyl-histidine fusion protein described similarly to wild-type. Human glycerol-3-phosphate dehydrogenase (G3PDH) was used as the coupling enzyme to assay PfGDPD activity. The sequence was cloned with an N-terminal hexa-histidine tag from complementary DNA clone MGC-34464 (Mammalian Gene Collection ATCC) and digested into BamHI/NotI sites of pET45b. A list of primer sequences used for PCR amplification is shown in Table 2-1. All coding sequences were in-frame and verified by DNA sequencing.

2.3.2 Parasite Culture and Transfection

All tissue culture experiments were performed under aseptic conditions in a biosafety cabinet using sterile tissue culture plates. Parasite cultures were maintained in a 5 % CO_2 incubator, cultured in human O^+ erythrocytes (Interstate Blood Bank) at 2% hematocrit in complete RPMI 1640 (CM) supplemented with 27 mM sodium bicarbonate, 11 mM glucose, 0.37 mM hypoxanthine, 10 μg/mL gentamycin and 5 g/L Albumax I (Invitrogen) [15]. For plasmid transfection, synchronous 3D7 ring cultures were obtained by centrifuging12 mL cultures for 3 min at 863 x g and incubating the recovered pellet with 4 mL 5 % sorbitol [16] for 5 min, vortexing 2- 3 times. Cultures were spun for 3 min at 863 x g and the pellet was re-suspend in 12 mL complete media. Sorbitol treatment was repeated 2-3 times to obtain tight synchronicity. 3D7 ring stage parasites were transfected with 75-100 μg plasmid DNA in 2mm BTX cuvettes (Harvard Apparatus) at 310 volts, 950 μF [17]. Parasites were positively selected with 10 nM WR99210 drug (Jacobus Pharmaceuticals) 48 hours post transfection. After 18-24 days, emerging parasites underwent drug cycling, whereby WR99210 was removed from media for 21

days and reapplied to enrich for plasmid integration [18]. Emerged resistant parasites expressing PfGDPD-YFP were observed microscopically after two drug cycles, while parasites targeted for gene disruption were cycled three times on/off drug. In addition, parasites transfected with the knockout (KO)/negative selection plasmid underwent negative selection, where 100 nM 5-fluorocytosine was added to WR resistant parasites after each cycle.

Table 2-1. Primers used for PCR amplification of PfGDPD and G3DPH gene fragments for creating/confirming fusion tags, gene disruption and site directed mutation.

Description	Direction	Sequence	Restriction Site
PfGDPD Target			
1.Fusion tag			
YFP-Fusion	Forward	GCACGCTCGAGATAATCAGAAAAAATATTCTTCCTTAAC	XhoI
	Reverse	GCACGCCTAGGTATTGTGTCGTTTTCTTTTATACCTT	AvrII
N-terminal Histidine	Forward	GCACGGGATCCCGAAAACCTGTATTTTCAGAGCAGTGC ATCAATCGTTGGTCATAGAG	BamH1
	Reverse	GTACGGCGGCCGCTTATATTGTGTCGTTTTCTTTTATACCT	NotI
C-terminal Histidine	Forward	GCACGTCATGAGTTCTCCTAGTGCATCAATCG	BspHI
	Reverse	CGTACGCGGCCGCTCAGTGATGATGGTGATGATGGCTCT GAAAATACAGGTTTTCTATTGTGTCGTTTTCTTTTATACCT	NotI
Untagged	Forward	GCACGTCATGAGTTCTCCTAGTGCATCAATCG	BspHI
	Reverse	GTACGGCGGCCGCTTATATTGTGTCGTTTTCTTTTATACCT	NotI
2. Gene Disruption			
Truncation	Forward	GTACGCTCGAGTTGAAGAATTAAATTTAGATGAGATACAA	XhoI
	Reverse	GCACGCCTAGGATCATCTGAGAAAAGAAGTGCTACAG	AvrII
5' fragment KO	Forward	GGCTTCCGCGGATGATATATTTTTTGCTTTTTATTTGTATC	SacII
	Reverse	GGCTTACTAGTCAATATATTCGGTATCATTAATAGGTTC	SpeI
3' fragment KO	Forward	GTACGCCATGGTTGAACTTAAAGGTAACAAAGAAGATCT	NcoI
	Reverse	TATAACCTAGGTATATTGTGTCGTTTTCTTTTATACCTTG	AvrII
3. E63A mutant	Forward	ATGTTGACGGAGTAGCATTGGACGTATGGCTAACG	
	Reverse	CGTTAGCCATACGTCCAATGCTACTCCGTCAACAT	
4. Southern Probe	Forward	GTACGCCATGGTTGAACTTAAAGGTAACAAAGAAGATCT	
	Reverse	TATAACCTAGGTATATTGTGTCGTTTTCTTTTATACCTTG	
5. Truncation Confirmation			
499	Forward	TATTATACACGTGTACACATTATAAC	
529	Reverse	CGTAATTATTTTCATTAAATGTTTTTCC	
HSPRI	Reverse	TATATATGTATATTGGGGTGATG	
6. KO Confirmation			
499	Forward	TATTATACACGTGTACACATTATAAC	
233	Reverse	TATAACCTAGGTATATTGTGTCGTTTTCTTTTATACCTTG	
G3PDH Target			
N-terminal Histidine	Forward	GCACGGGATCCCAGCATGGCTAGCAAGAAAGTCTGCATTG	BamH1
	Reverse	GTACGGCGGCCGCTCACATATGTTCTGGATGATTCTGCA	NotI

To generate parasite clones expressing PfGDPD-YFP, parasitemia was determined by Giemsa stained smears and the culture was diluted 2-4 %. The culture was further diluted 10^4-fold and inoculated into mixture of 24 mL media and 1mL 50 % red blood cell according to the formula below:

volume (μL) of 10^4-fold diluted culture = [25000/(80 x % parasitemia)] x 2.5

200 μL of diluted culture was aliquoted into round bottom 96 well plates, whereby media was changed every two days and resuspended in ~ 170 μL of fresh media. Every 6 days, parasites were split 1:1 with media containing fresh red blood cells at 2 % hematocrit. Individual clones appeared after 10 days and were identified by Giemsa stained smears. Clones D9 and E8 were used in this study.

Gametocytes expressing PfGDPD-YFP were induced from asynchronous clone D9 parasites using the following procedure. Parasites were inoculated at a low parasitemia of ~0.5 % at 6 % hematocrit in a 5 ml culture volume, placed in a cake jar and gassed with 5 % O_2, 5 % CO_2, 90 % N_2 mixture, for 3 min. Media was changed daily and after 3-4 days, media volume was increased to 7.5 mL, with continuous daily media changes. Late stage gametocytes were observed after 15-18 days, at which point images were collected.

2.3.3 Parasite Fractionation

Trophozoite stage parasites from clone E8 and 3D7 were obtained using a MACS magnetic column (Miltenyi Biotech). The column was washed with 5mL complete RPMI media and allowed to flow through. 12 mL of culture were centrifuged for 3 min at 863 x g. The collected pellet was re-suspended in 5 mL complete RPMI media and loaded onto the column. Due to the presence of significant amounts of hemozoin in trophozoite/schizont-infected red blood cells, these parasites are bound to the column, while ring stage parasites and un-infected erythrocytes flow through. The column was removed from the magnet and bound parasites were eluted in 3 mL complete RPMI media and centrifuged for 3 min at 863 x g. The pellet was re-suspended in 2 mL Dulbecco's phosphate-buffered saline (PBS) and split into 1 mL aliquots. Following centrifugation, one pellet was set aside on ice as whole cell pellet extract, while the other pellet was treated with 2x pellet volume of 1.5 mg/ml saponin diluted in PBS for 15 min on ice. Parasite lysate was spun at 1940 x g for 10 min at 4 ^oC and separated into soluble and pellet fractions. Pellet fractions were washed twice in ice cold PBS. Both soluble and pellet extracts

were taken up to a volume of 80 µL PBS containing the following inhibitor cocktail: 10 µM pepstatin, 10 µM N-(trans-epoxysuccinyl)-L-leucine 4-guanidinobutylamide (E-64), 0.5 mM 4-(2-aminoethyl)benzenesulfonyl fluoride (AEBSF) and 1 mM sodium ethylenediaminetetraacetic acid (EDTA). Samples were solubilized in 20 µL 5x loading buffer (250 mM Tris-HCl pH 6.8, 10% SDS, 50% glycerol, 25% ®-mercaptoethanol and 0.5% bromophenol blue), pulse-vortexed and immediately boiled in a water bath for 1.5 min (performed 2 x). Samples were spun at 16,000 x *g* for 2 min to remove any insoluble material and analyzed by immunoblotting.

To confirm the presence of PfGDPD in the parasitophorous vacuole, mature clones D9 were cultured to parasitemia between 5-7 %. A 1 mL culture aliquot was spun at 863 x g for 3 min and the pellet was re-suspended in 40 µL (0.1 % w/v) saponin prepared in RPMI 1640 complete media. The culture was incubated for 10 min at room temperature (RT) then diluted with 1 mL media and spun at 1940 x g for 10 min, RT. Pellet was washed twice in 1 ml media and taken up in 200 µL of media into 96 well plate flat bottom plate and imaged immediately.

2.3.4 Southern Blot and PCR Analysis

To confirm integration of YFP plasmid into PfGDPD gene locus, genomic DNA (gDNA) was collected from saponin-treated PfGDPD-YFP clones and 3D7 wild-type parasites. 24 mL parasite culture were washed in 40 mL PBS and centrifuged for 3 min at 863 x g. Collected pellet was treated with 40 mL cold 0.1 % saponin in PBS and mixed by inverting the tube several times. The culture was incubated for 10 min on ice and centrifuged at 1940 x g, 10 min at 4 ^{o}C. Parasite pellet was washed in cold PBS at 1940 x g, 10 min at 4 ^{o}C and stored at -80 ^{o}C. gDNA was extracted from using the QiaAmp DNA blood mini kit (Qiagen) according to the manufacturer's instruction. 50 µL of gDNA (2 µg) and YFP plasmid (1 µg) were digested in a 100 µL reaction containing 10 µL10x NEB Buffer 4, 10 µL 10x bovine serum albumin (BSA), 1 µL EcoRI restriction enzyme and 29 µL MilliQ-H_20. Reaction was incubated for 3 hrs at 37 ^{o}C and purified using the QiaAmp nucleotide removal kit (Qiagen) in 30 µL elution buffer. DNA fragments were resolved on a 0.6 % agarose gel (200 mL) without ethidium bromide, run overnight at 30 volts for ~17 hours. 1kb markers were loaded in an edge lane and after electrophoresis, the marker lane was cut off, stained for 20 minutes in 0.5 µg/mL ethidium bromide and photographed with a fluorescent ruler. Following separation, DNA fragments were depurinated in 0.25 M HCl for 15 min, denaturing in 0.5 M NaOH, 1.5 M NaCl for 30 min and

neutralizing in 1 M Tris-HCl pH 8, 1.5 M NaCl for 30 min, rinsed in water after each step. DNA was transferred to an Immobilon Nytran^{+} membrane (Millipore) using a Turboblotter for a minimum of 3 hrs in 20x SSC buffer containing 3.0 M NaCl and 0.3 M sodium citrate. Membrane was blocked using 20 µL AlkPhos Direct pre-hybridization reagent in a hybridization oven tube rotating for 1 hr at 55 ºC. After blocking, PfGDPD locus was detected by incubating the membrane overnight at 55 ºC using 100 ng probe complementary to the 3' end of the gene, listed in Table 2-1. Probe labeling and detection were performed using AlkPhos direct labeling kit (GE Biosciences) and signal was detected by autoradiography.

Genotyping of PfGDPD gene disruption parasites were performed by PCR analysis using 5 ng/µL gDNA. Primers used are indicated in Table 2-1. To confirm single crossover truncation integration, we designed forward primers 499, specific to the 5' UTR and reverse primers HSPR1, specific to the YFP sequence. As a positive control, we designed reverse primers 529, specific to the internal coding region, which was paired with forward primer 499. Knockout parasites were analyzed with forward primers 499 and reverse primers 233, specific to PfGDPD 3' coding region.

2.3.5 Fluorescence Microscopy

Images were collected on a Zeiss AxioImager M1 equipped with an MRm Axiocam digital camera using a 100x/1.4NA objective lens. 40 µL of live parasites were incubated with 1 µL 5 µM Hoescht 33342 nuclear stain for 5 min at 37 ^{o}C. 1000 millisecond exposure time was used in the YFP channel and 2 millisecond in the DAPI channel, set to a camera gain of 4 and a fluorescence index of 2. Images were converted to TIFF files and contrast was adjusted using Adobe Photoshop CS4.

2.3.6 Antibodies and Immunodetection

Recombinant PfGDPD was used as the immunogen raised as anti-sera in rats (Cocalico Biologicals). Serum was purified on an affinity column using AminoLink Coupling Resin (Pierce) according to the manufacturer's instructions. Purified Anti-PfGDPD antibodies were dialyzed overnight in PBS pH 7.4, flash frozen in liquid nitrogen and stored at -80 ^{o}C in 1 mg/mL BSA and 0.02% sodium azide.

SDS extracts of ~1 x 10^7 parasites were loaded on a 10 % SDS-polyacrylamide gel. The resolved bands were transferred to nitrocellulose membrane for 40 min at constant current (0.4Amp) and blocked with 2% (w/v) bovine serum albumin (BSA) in Tris-Buffered Saline Tween-20 (TBST) buffer for 1 hour. Immunoblotting was carried out with primary antibody anti-PfGDPD (1:5,000 dilution in 2 % (w/v) BSA/TBST) followed by a 1 hour incubation in anti-rat horseradish peroxidase-conjugated secondary antibody (1:10,000 dilution in 2 % (w/v) BSA/TBST). After three 5-minute washes in TBST, chemiluminescent signal was developed with Amersham ECL kit (GE Bio-sciences), and detected on a photographic film. To assess saponin permeabilization treatment, blots were stripped and re-probed with rabbit anti-binding immunoglobin protein (BiP) (1:10,000 dilution in 2 % (w/v) BSA/TBST) [19] and mouse anti-serine-rich antigen (SERA) (1:38,000 dilution in 2 % (w/v) BSA/TBST) [20].

2.3.7 Recombinant Protein Expression and Purification

E. coli BL21(DE3) Rosetta 2 cells (Novagen) were transformed with either PfGDPD and G3PDH expression plasmids were grown in Luria-Bertani (LB) media. Expression and purification of PfGDPD was performed in the presence of 10 mM $MgCl_2$ as a metal ion supplement. 3 L of *E. coli* cells were grown to A_{600} value of 0.8 (PfGDPD) and 1.5 (G3PDH) and induced with 1 mM isopropyl β-D-thiogalactopyranoside (IPTG) for 4 hrs at 25 ^oC. Bacterial cell pellets were harvested by centrifugation at 7,000 X g for 30 min and lysed in immobilized metal affinity chromatography (IMAC) buffer (500 mM NaCl, 30 mM imidazole, 20 mM NaH_2PO_4 pH 7.4) containing 1 mM 4-(2-aminoethyl)benzene-sulfonyl fluoride and 1 mg/mL hen egg white lysozyme. After 30 min incubation on ice, cells were sonicated and lysates were recovered by centrifugation at 20,000 X g for 15 min at 4 ^oC. To precipitate out nucleic acids, protamine sulfate was added to the supernatant at 16 mg/g of cell pellet wet weight, stirred on ice for 15 min and clarified lysates were obtained by centrifugation at 20,000 X g for 15 min at 4 ^oC. The collected supernatant was filtered with a 0.45μM syringe filter (Millipore) and loaded onto a Ni^{2+}-charged His-Trap column (GE Healthcare) equilibrated in IMAC buffer and eluted at a 15 min linear gradient of 30 mM to 500 mM imidazole at a flow rate of 1mL/min. Fractions were collected in 1 mL 96 deep well plates (USA Scientific) at a rate of 0.33 min/fraction. Peak fractions determined by Coomassie staining, were diluted in gel filtration (GF) buffer (50 mM Tris-HCl, pH 7.5, 200 mM NaCl) to lower the concentration of imidazole and further

concentrated to ~300 μL by centrifugation at 1940 x g at 4 °C in an Ultra-4 centrifugal device (Amicon). Retentate was injected onto a Superdex 200 10/30 GF column (GE Healthcare) equilibrated in GF buffer, which ran for 60 min at a flow rate of 0.5 mL/min. Eluted protein fractions were collected at a rate of 0.66 min/fraction. PfGDPD peak fractions were determined at 280 nm on a NanoDrop 1000 spectrophotometer (Thermo Scientific), pooled and snap frozen in liquid nitrogen and stored at -80 °C. G3PDH peak fractions were determined on a 10% SDS-polyacrylamide gel and fractions were pooled and an aliquot was stored at 4 °C in 50 % glycerol and the remaining was snap frozen in liquid nitrogen and stored at -80 °C.

PfGDPD E63A mutant and wild-type enzyme were expressed simultaneously in 1.5 L *E.coli* BL21 (DE3) Rosetta 2 cells in LB/10 mM $MgCl_2$ and grown to A_{600} value of 0.8. Cells were induced with 1 mM IPTG and induced with for 5 hrs at 25 °C. Pellets were harvested and lysed as described above. Lysates were clarified at 20,000 x g for 15 min at 4 °C and supernatants were filtered and proteins were sequentially purified on a Ni^{2+}-charged IMAC column and eluted at a linear gradient of imidazole from 30 mM to 500 mM. PfGDPD wild-type peak fraction was determined at 280 nm absorbance. Peak fraction F18 from both protein variants were exchanged into 100 mM HEPES pH 7.5 and concentrated to ~150 μl.

2.3.8 Partial Purification of Native PfGDPD

P. falciparum 3D7 parasites were grown to 20-24 % parasitemia. 864 mL of schizont and trophozoite stage parasites were lysed with 1.5 mg/mL saponin diluted in PBS supplemented with inhibitors (10 μM E-64, 10uM pepstatin and 1 mM AEBSF) for 15 min on ice. Parasite lysate was spun at 1940 x g for 10 min at 4 °C. Membrane fractions were removed at 100,000 x g for 1 hr to and filtered through a 0.45 μM syringe filter (Millipore) and immediately injected onto an Mono Q 5/50 GL (GE Healthcare) column equilibrated in 20 mM bis-tris•HCl pH 6.0. Bound protein was eluted with linear gradient from 0 to1 M NaCl. Protein was eluted a flow rate of 0.75 mL/min an eluted around 400 mM NaCl. Fractions were collected at a rate of 0.75 min/fraction. Immuno dot-blot analysis with anti-PfGDPD was used to determine peak fractions, which were pooled and loaded on to a Superdex 200 10/30 GF column equilibrated in 50 mM Tris-HCl pH 7.5, 200 mM NaCl. Protein concentration of a peak fraction from anion exchange purification was calculated by quantitative immunoblotting using a standard curve generated with known concentrations of recombinant PfGDPD.

2.3.9 Enzyme Assays and Kinetic Analysis

PfGDPD activity was analyzed using two end-point assay techniques; 1) glycerol-3-phosphate (G3PDH) coupled spectrophotometric assay and 2) Choline oxidase assay. G3PDH coupled assay measures the production of glycerol-3-phosphate (G-3-P) produced by the reversible oxidation of G-3-P to dihydroxyacetone phosphate (DHAP) and reduction of nicotinamide adenine dinucleotide (NAD^+) to NADH at an absorbance of 340 nm, catalyzed by G3PDH (Figure 2-3) [5, 21]. To move the reaction in a forward favorable direction, buffer containing 0.2 M hydrazine pH 9.5, was used to DHAP through a Schiff base mechanism [21].

The 1^o assay master mix containing 10 µL 200 mM 4-(2-hydroxyethyl)-1-piperazineethanesulfonic acid (HEPES) pH 7.5 or 200 mM sodium acetate pH 5.5, 2 µL 100 mM $MgCl_2$, and 1. 5 µL 0.69 µM of recombinant PfGDPD or 1.3 µM of native PfGDPD, was pre-incubated in a Bio-Rad S1000 thermocycler for 15 min at 37 ^oC, after which 6.5 µL glycerophosphocholine (GroPC) (Sigma) substrate mix containing 150 mM NaCl and MilliQ-H_20, was added at a concentration range of 0 mM to 10 mM. The 20 µL reaction was allowed to proceed for 30 min at 37 ^oC, after which was heat quenched at 95 ^oC for 5 min and cooled to 25 ^oC. 13.7 µL from 1^o assay was transferred to a 2^o assay mix with a total volume of 30 µL containing 15 µL 0.4 M hydrazine/ 1 M glycine/ 5 mM EDTA buffer pH 9.5, 1.16 µL 60 mM NAD^+ and 0.15 µL 10 µg/ µL G3PDH. After 30 min incubation at 25 ^oC in a 96 well plate microplate, NADH produced was determined at 340 nm on a Spectramax microplate reader or a Nanodrop spectrophotometer. To ensure enzyme activity was within the linear range, purified PfGDPD was serially diluted and assayed at 0, 3,10 and 30 ng with 2 mM GroPC substrate, as described above. The estimated glycerol-3-phosphate concentration in the 2^o assay is ~91.3 µM. 30 ng PfGDPD resulted in ~ 5 % substrate cleavage, which was determined by the absorbance of 50 µM glycerol-3-phosphate standard. NADH concentration was determined using an extinction coefficient of 6300 $M^{-1} \bullet cm^{-1}$. Kinetic parameters (K_m, k_{cat}, k_{cat}/K_m) were determined using Kaleidagraph 4.1, by a non-linear regression fit to Michaelis-Menten equation:

$$\nu = \frac{[E]_o[S]k_{cat}}{K_m + [S]}$$

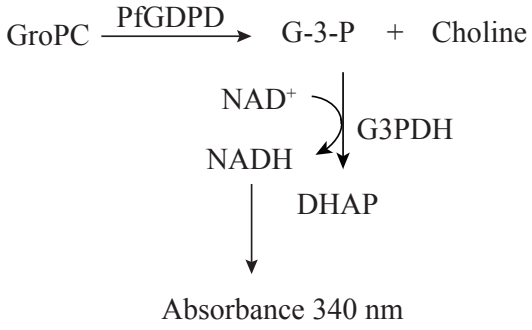

Figure 2-3. Schematic of G3PDH coupled spectrophotometric assay. The phosphodiester bond of glycerophosphocholine (GroPC) is hydrolyzed to release glycerol-3-phosphate (G-3-P) and choline. In a redox reaction, G-3-P is oxidized to dihydroxyacetone phosphate (DHAP) by glycerol-3-phosphate dehydrogenase (G3PDH) and nicotinamide adenine dinucleotide (NAD^+) is reduced to NADH and absorbance is recorded at 340 nm.

Choline oxidase assay detects the production of choline. This assay was employed to assess PfGDPD activity against GroPC and lysophosphatidylcholine (LPC); 1-Lauroyl-2-Hydroxy-*sn*-Glycero-3-phosphocholine (LPC6:0) and 1-Hexanoyl-2-Hydroxy-*sn*-Glycero-3-phosphocholine (LPC12:0) (Avanti Polar Lipids). 50 μL of 10 mg/mL LPC in chloroform were transferred to glass vials and dried under a stream of nitrogen. The lipid residue was further desolvated for 1 hr 20 min in a CentriVap concentrator (LabConco) and reconstituted in 352 μL (LPC6:0) and 284 μL (LPC12:0) of solvent containing 125 mM Tris pH 8.5, 5 mM $MgCl^{2+}$ to a final concentration of 4 mM. The 1^o assay buffer mix consisted of 45 μL 250 mM Tris buffer pH 8.5, 6.75 μL 2 M NaCl, 9 μL 100 mM $MgCl_2$ and 0.75 μL MilliQ-H_20. PfGDPD was added at a volume of 6 μL to the buffer mix at different amounts (6, 12, and 24 ng), incubated at 37 ^oC for 15 min in a Bio-Rad S1000 thermocycler. To start the reaction, 22.5 μL of 1 mM LPC substrate was added to the enzyme mix and incubated for 30 min at 37 ^oC. The reaction was heat inactivated at 95 ^oC for 5 min and cooled to 25 ^oC, after which 10 μL of the 2^o assay master mix was added to 1^o reaction at a total volume of 100 μL. The 2^o mix consisted of a 10 x stock containing 1 μL of 100 U/ml choline oxidase, 1 μL of 100 mM 3-(*p*-hydroxyphenyl)propionic acid (HPPA) and 1 μL 18 U/ml horseradish peroxidase (HRP). Reaction proceeded for 10 min on bench-top in a 96 well half-area plate (Corning), after which oxidized HPPA was recorded at 340 nm using a Victor^3 microplate fluorometer (PerkinElmer).

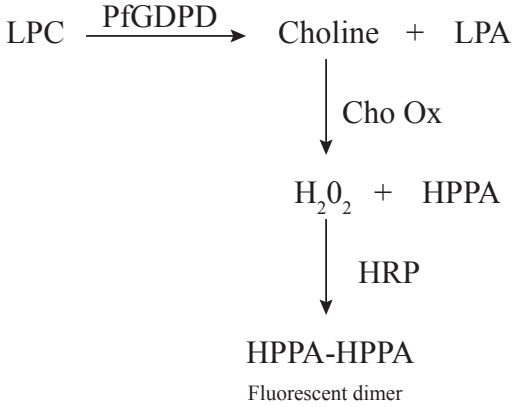

Figure 2-4. Schematic of choline oxidase assay. Lysophosphocholine (LPC) is hydrolyzed to lysophophatidic acid (LPA) and choline. Choline is oxidized by choline oxidase (Cho ox) to generate hydrogen peroxide (H_20_2), which serves as the oxidizing agent for horse radish peroxidase (HRP) oxidation of 3-(*p*-hydroxyphenyl)propionic acid (HPPA), which forms a fluorescent dimer that can be detected at an emission wavelength of 340 nm.

2.3.10 PfGDPD Metal Ion Dependency

The metal ion preference for native enzyme was examined with 10 mM Mg^{2+}, 0.1 mM Co^{2+}, 1 mM Mn^{2+} and Zn^{2+} and Cu^{2+} at concentrations of 0.1 mM and 1 mM, The volume of enzyme to yield 10 % substrate cleavage was estimated by comparing absorbance of 3-fold serial dilutions of enzyme assayed against 2 mM GroPC to an internal control of 50 μM glycerol-3-phosphate. 3 μL of enzyme was incubated with 12 μL 10x metal stock, 60 μL 200 mM HEPES pH 7.5 and 33 μL MilliQ-H_20 for 15 min at 37^{o}C. After with 12 μL of 20 mM GroPC substrate was added and incubated for 30 min at 37 ^{o}C. Reaction was heat quenched at 95 ^{o}C for 5 min and 91.3 μL from the 1^o assay was added to the 2^o assay containing 7.7 μL 60 mM NAD^+, 100 μL 0.4 M hydrazine/ 1 M glycine/ 5 mM EDTA buffer pH 9.5 and 1 μL 10μg/ μL G3PDH.

The metal ion preference of recombinant PfGDPD was assessed by incubating 1.5 μL of 0.72 μM PfGDPD with 12 μL of Mg^{2+} or Ca^{2+} (10 mM and 100 mM) and 10 mM EDTA, 60 μL 200 mM HEPES pH 7.5, 9 μL 2 M NaCl and 25.5 μL MilliQ-H_20. The enzyme mix was incubated for 1 hour at 30 ^{o}C, after which 12 μL of 20 mM GroPC substrate was added to start the 30 min reaction at 37 ^{o}C. Reaction was heat quenched and a 91.3 μL aliquot from 1^o assay was added to the 2^o assay containing 7.7 μL 60 mM NAD^+, 100 μL 0.4 M hydrazine/1 M glycine/5 mM EDTA buffer pH 9.5 and 1 μL 10μg/ μL G3PDH.

2.4 RESULTS

2.4.1 Sequence Analysis

To identify lipolytic enzymes targeted to the food vacuole, we employed a bioinformatics approach and performed a homology and a text search for phospholipases and lipases annontated in the *Plasmodium* genome (PlasmoDB.org). Prior studies of food vacuole enzymes suggest these enzymes have a transmembrane domain and/or a signal peptide, which directs proteins to localiztion. Accordingly, we performed a limited follow up search using these criteria and identified 6 candidate genes: PF14_0060, PF14_0015, PF14_0250, PFC0065C, PF11_0276 and MAL13P1.285. Reporter tag constructs were generated and protein distribution was analyzed microscopically, revealing only one highly expressed protein, previously annotated as putative lipase and re-annotated as a glycerophosphodiester phosphodiesterase, termed PfGDPD. The protein consists of 475 amino acid residues encoded by a 1.4 kilo base single-exon gene (gene ID: PF14_0060) on chromosome 14 with a predicted molecular mass of 56 kDa. Orthologues are found in genome sequences of *Plasmodium* species, *P. vivax, P. chabaudi, P. knowlesi and P. berghei.* Sequence analysis of PfGDPD revealed a GDPD-insert (GDPD-I) domain of 88 amino acids at the amino-terminus found within the conventional triosephosphate isomerase (TIM) barrel protein fold, unique to GDPDs [9]. Conserved residues were identified as His29, Arg30, Gly31, Glu45, Glu63, Asp65, Lys70, Asp71, His78, Glu107 (Figure 2-5). The proposed catalytic histidine residues were identified as His29 and His78 and residues Glu44, Asp46 and Glu119, were identified as the metal binding residues. Analysis of the first 70 residues with the signal peptide prediction algorithm SignalP 4.0 revealed a putative signal peptide from residues 1 to 16, which have been identified in other GDPD homologues [6, 22, 23].

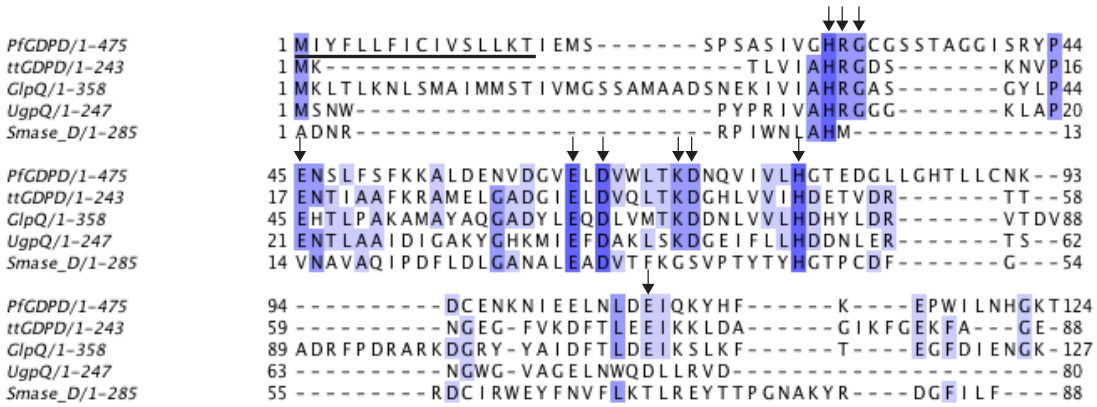

Figure 2-5. Alignment of the N-terminal region of GDPD homologues. *Pf*GDPD (*P. falciparum*); ttGDPD (*T. t*engcongensis); GlpQ (*E.coli*); UgpQ (*E.coli*); spider venom sphingomyelinase D (SmaseD) from *Loxosceles laeta*. Conserved residues are indicated with the arrows. Underlined sequence indicates the predicated PfGDPD signal sequence The alignment was generated with T-coffee multiple alignment server [24] and colored using Jalview 2.4 ([25]

2.4.2 PfGDPD Localization

To assess the cellular distribution of PfGDPD, we generated stable parasite lines expressing PfGDPD fused to YFP (PfGDPD-YFP), via a single crossover homologous recombination approach (Figure 2-4A). Since multiple parasites can infect a single red blood cell (RBC), we generated parasite lines derived from a single infected RBC, designated as clones F12, B5, E8 and D9. The parasite clones were subsequently genotyped using Southern blotting to confirm integration of PfGDPD-YFP plasmid into the chromosome. To differentiate plasmid integration events, our analysis employed EcoRI restriction enzyme digest with probes specific to 3'end of the gene and 3D7 wild-type parasites as a negative control (Figure 2-6A). In the event of plasmid integration into PfGDPD locus, the 3' end of the gene would be duplicated; and therefore would be detected as two bands at the expected sizes of 3.0 kb and 10 kb. In contrast, a non-integration event would be detected at a size of 5.9 kb. As expected, our analysis revealed the chromosomal insertion of PfGPDP-YFP plasmid into the PfGDPD gene locus, indicated by presence of 3 kb and 10 kb bands, of which is clearly absent from 3D7 wild-type parasites (Figure 2-6B). With the genotype confirmed, we assessed PfGDPD protein distribution in clone D9 parasites.

Microscopic analysis, revealed the expression of the fusion protein throughout the intra-erythrocytic asexual stages within the cytosol, encircling the parasite in the parasitophorous vacuole (PV) space and less intensely within the acidic food vacuole (FV) (Figure 2-7A). Since

our aim was to identify lipolytic enzymes potentially trafficked to the FV, we were interested in confirming PfGDPD food vacuole distribution. To achieve this, we took advantage of the reversible acid-base equilibrium of YFP between the non-fluorescent dark state and fluorescent states [26, 27], by photobleaching the cytosolic fluorescent species through repetitive exposures in an attempt to visualize the YFP species in the FV. As illustrated in Figure 2-7B, the presence of PfGDPD in the food vacuole is clearly visible, and our analysis of PfGDPD enzymatic activity within the lumen will be discussed further.

In addition to confirming protein localization to FV, we also assessed PfGDPD distribution in the PV cellular compartment, a space that surrounds the parasite, isolating it from the host cell within a semi-permeable membrane. Accordingly, we addressed PV localization by incubating parasites with saponin, a pore-forming detergent that permeabilizes both erythrocyte and PV membranes that results in the leakage of PV contents, identifiable as a loss of rim fluorescence. Following centrifugation, parasites were immediately imaged and PfGDPD fluorescence was observed strictly confined in the cytosol, thus confirming PV distribution (Figure 2-7C). In addition to PfGDPD expression in the intra-erythrocytic stages, the fusion protein was also expressed in gametocytes, but only observed as a cytosolic distribution (Figure 2-7D).

To support our PfGDPD fluorescence studies, we assessed protein cellular distribution by immnoblotting. 3D7 and clone E8 parasites were fractionated into whole cell (WC) extracts, supernatant (S) and pellet (P) parasite extracts, of which the latter two were obtained by saponin treatment. An average of 1 $x10^7$ parasites were loaded in each extract and subjected to immunoblotting with affinity purified anti-PfGDPD antibody generated in rats. PfGDPD was detected in 3D7 extracts at the native size of 50 kDa, however in the clonal extracts, we observed the presence of both the intact 75 kDa fusion protein in the all fractions and the 50 kDa protein the pellet extract (Figure 2-7E).

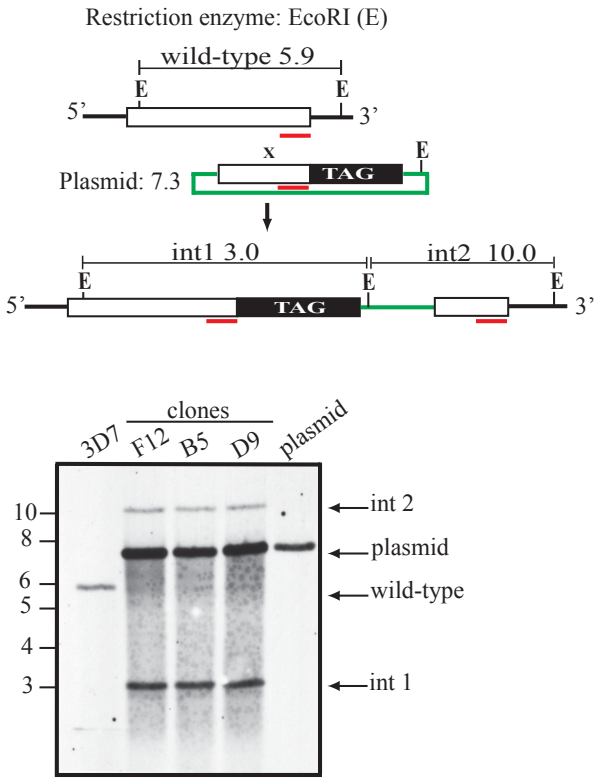

Figure 2-6. **Homologous recombination strategy and Southern analysis of PfGDPD-YFP clones.** A) Schematic diagram of a single crossover homologous recombination approach to generate parasites expressing fluorescently tagged PfGDPD fusion protein. Diagram depicts the sites of EcorRI (E) restriction digest and hybridization site with 3' gene-specific Southern probes, as indicated by the red bar. Expected fragment sizes are indicated in kilobases for the endogenous PfGDPD locus (wild-type), YFP plasmid and the event of a single-crossover integration (int1 and int2). The white box represents the PfGDPD coding region, the black box indicates the YFP fusion tag, the green line corresponds to the plasmid backbone. The diagrams are not drawn to scale. B) Southern analysis of 2 μg total DNA isolated from 3D7 parasites and PfGDPD-YFP parasite clones, F12, B5 and D9 and 1 μg of plasmid control. The plasmid band in PfGDPD-YFP clonal lines indicates the integration of episomal concatemers, which when digested, produces the same size band as the plasmid.

The faint 50 kDa band results from the clipping of the 25 kDa YFP tag. Several studies have observed this phenomenon, which has been attributed to the presence of active proteases within acidic compartments as the food vacuole [28-30]. Therefore, the untagged protein reflects the presence of PfGDPD in the food vacuole as previously observed in our fluorescence studies. In addition, PV localization is confirmed, as observed in supernatant fractions that consist of soluble PV and RBC content generated from saponin treatment.

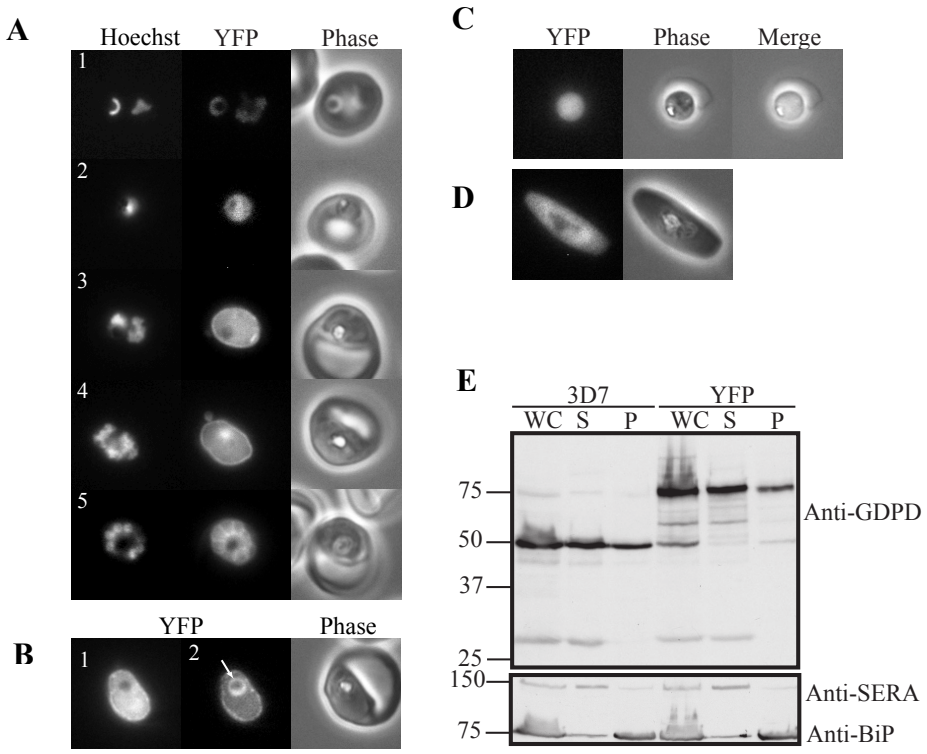

Figure 2-7. Localization of PfGDPD in intra-erythrocytic *P. falciparum.* A) Fluorescence microscopy of live clone D9 parasites expressing a complex distribution of PfGDPD-YFP; *1. Rings. 2. Young trophozoite. 3. Mature trophozoite. 4. Schizont. 5. Segmenters.* B) Photobleaching of clone D9 parasites obtained after 3 consecutive imaging (Exposure 1) to reveal YFP fluorescence in the food vacuole (Exposure 2), indicated by the arrow. C) Saponin treated trophozoite stage D9 parasites showing expression of cytosolic expression of PfGDPD-YFP and loss of parasitophorous vacuolar rim fluorescence. D) PfGDPD-YFP clone E8 induced late stage gametocytes showing cytosolic protein expression. E) Western blot analysis of purified whole cell (WC) trophozoite stage 3D7 and PfGDPD-YFP clone E8 parasites, treated with saponin and separated into supernatant (S) and pellet (P) fractions. An average of 1 x10 ^{7} parasites were loaded in each extract and protein expression was detected by immunoblotting with affinity purified anti-PfGDPD antibody generated in rats. Molecular size markers in kDa are shown on the left. The endoplasmic reticulum compartment marker, anti-binding immunoglobin protein (BiP) and the parasitophorous vacuole compartment marker, anti-serine-rich antigen (SERA), are indicated in the lower panel.

2.4.3 PfGDPD Gene Disruption

The complex distribution of PfGDPD suggests multiple roles in each compartment or a single in all compartments. These functions however, may not be important for successful survival of parasites replicating within RBCs. Therefore, we evaluated the importance of PfGDPD by targeting the endogenous gene using a homologous recombination system to generate, 1) a truncated gene via single-crossover and 2) gene knockout (KO) via double-crossover/negative selection approach (Figure 2-8). The truncation plasmid comprised of a 1-kb internal PfGDPD sequence fused to YFP, while the KO plasmid consisted of two homology regions of the 5' and 3' ends of the gene. Both plasmids carry the human dihydrofolate reductase

gene cassette that generates multiple copies of the plasmid, allowing for positive selection with the anti-folate inhibitor WR99210. A secondary means of selection, we included a cytosine deaminase cassette in KO plasmid which when expressed converts innocuous 5-fluorocytsoine to the highly toxic compound 5-fluouracil, which inhibits parasite DNA synthesis.

Wild-type 3D7 parasites were transfected with the plasmid and were cycled for a minimum of 3 weeks to enrich for plasmid integration by removing WR99210 from the media to allow lose of episome after which drug pressure was re-applied to select for drug resistant parasites with chromosomal integrated episomes. Following 3 rounds of cycling, PfGDPD gene disruption was examined by PCR analysis. Earlier indications of non-disruption were revealed when parasites were analyzed microscopically for YFP expression and were found to be non-fluorescent, indicating that truncated PfGDPD proteins were not expressed. To confirm our observation, primers were designed to specifically amplify the PfGDPD gene locus and exclude amplification of plasmid. Resulting primers 499/HSPR1, were specific to the 5'UTR of the gene and YFP sequence on the plasmid, respectively. Gene amplification would result in a 1.8 kb band indicating successful gene integration of the truncation plasmid and a band size of 2.1 kb, which is only observed in parasites expressing full length PfGDPD-YFP (Figure 2-8A). Genomic DNA obtained from two independent transfection lines (A and B), 3D7 wild-type and PfGDPD-YFP clone D9 parasites, were examined and our results indicated that PfGDPD gene was not disrupted, however it is evident the gene is amenable to tagging.

To determine the occurrence of PfGDPD gene knockout, we designed primers specific to the 5' UTR and 3' coding region, which would result in the amplification of two distinct sized bands of 1.4 kb, representing the intact coding sequence seen in control 3D7 parasites and a 3 kb band, indicating an integration event (Figure 2-8B). Consistent with prior gene disruption analysis, there was no evidence of PfGDPD gene disruption, which remained as an intact 1.4 kb sequence. The inability to disrupt PfGDPD coding sequence suggests the protein plays a yet unidentified role in *P. falciparum* intra-erythrocytic stages. Biochemical analysis to probe the enzymatic ability of PfGDPD within acidic food vacuole and near neutral pH environment of the parasitophorous vacuoles, were examined and are discussed below.

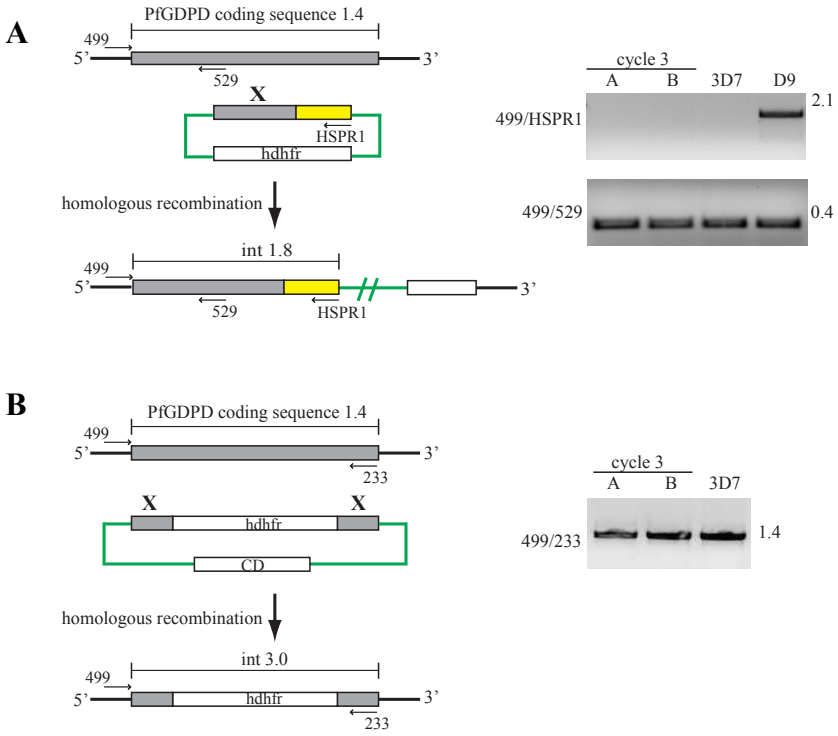

Figure 2-8. **PCR analysis of PfGDPD gene disruption parasite lines.** Left panel depicts the homologous recombination strategies and shown in the right panel are the results of PCR analysis of 5 ng/μL genomic DNA A) Single-crossover approach to generate a truncated PfGDPD gene sequence. PCR analysis of parasites designated as A and B are from two independent transfections cycled 3 times. 3D7 and D9 were included as controls. B) Schematic of double-crossover knockout approach. PCR analysis of two independent transfections (A and B) after 3 cycles. Primers are indicated as numbers and primer positions are designated by the corresponding arrows. Predicted sizes of intact PfGDPD coding sequence and disrupted coding sequence (int) are indicated in kilo bases. The diagrams are not drawn to scale. The grey box represents the PfGDPD coding region, the yellow box indicates YFP coding sequence, and the green line corresponds with the plasmid backbone.

2.4.4 Purification of Native PfGDPD

PfGDPD was partially purified from soluble trophozoite extract using the established protocol described in section 2.3.8. The protein was enriched through sequential steps of anion exchange and gel filtration chromatography (Figure 2-9). Immunoblot analysis of PfGDPD separated by SDS-PAGE detected a single band with an apparent minimum subunit molecular weight of 50 kDa, which is comparable to the predicted molecular mass of 56 kDa using the ExPasy Protparam tool. The monomeric structure of PfGDPD was confirmed from the gel filtration elution profile and calculated from a calibration curve of standard proteins of known sizes. Enzyme activity of PfGDPD was lower after gel filtration purification, probably due to the adsorption of low quantities of the enzyme to the surface walls. Therefore only PfGDPD purified over anion exchange column was profiled.

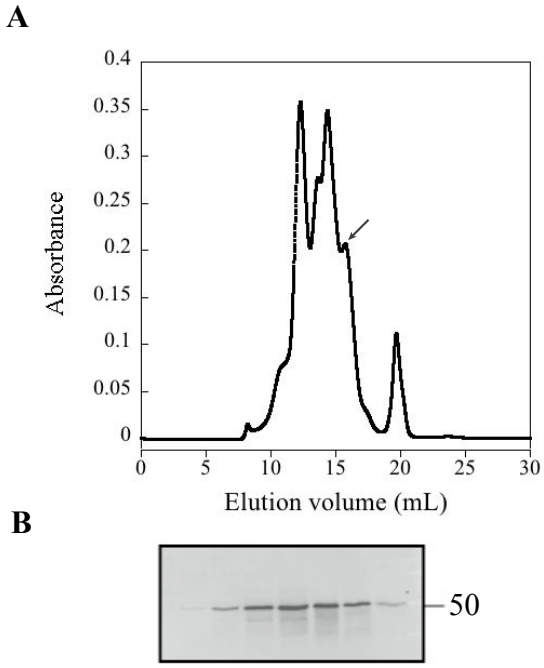

Figure 2-9. Gel filtration profile of native PfGDPD. A) Gel filtration elution profile of native PfGDPD following anion exchange chromatography. The arrow indicates peak corresponding to elution of native PfGDPD. B) Anti-PfGDPD immunoblot of eluted peak fractions.

2.4.5 Metal Ion Dependency of Native PfGDPD

Studies of GDPDs have indicated a requirement for bivalent ions, however the metals differ between species. Ca^{2+} is a potent activator of *E.coli* GlpQ [5], whereas Mg^{2+} activates *E.coli* UgpQ and mammalian GDE1 [14, 31]. Native PfGDPD, termed (nPfGDPD), was incubated with Zn^{2+} and Cu^{2+} at concentrations of 0.1 mM and 1 mM, 10 mM Mg^{2+}, 0.1 mM Co^{2+} and 1 mM Mn^{2+} and metal ion dependency was examined using the G3PDH coupled assay (Figure 2-3) and assayed against 2 mM glycerophosphocholine (GroPC) substrate using G3PDH coupled assay. Enzyme activation was observed in 10 mM Mg^{2+}, 1 mM Mn^{2+} and 0.1 mM Co^{2+} (Figure 2-10) and inhibition in Cu^{2+} and Zn^{2+}. In a separate assay, PfGDPD activity was also inhibited by 1 mM Ca^{2+}.

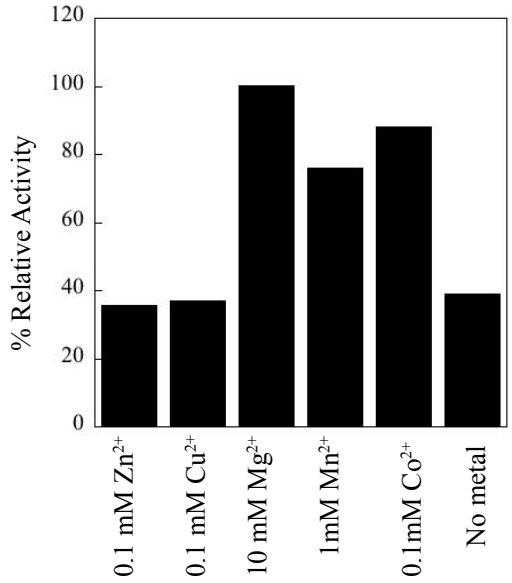

Figure 2-10. Metal ion assay of native PfGDPD. Graph represents results of native PfGDPD activity in the presence of 0.1 mM Zn^{2+}, 0.1 mM Cu^{2+}, 10 mM Mg^{2+}, 0.1 mM Co^{2+} and 1 mM Mn^{2+}. Data are shown as the percentage activity compared to 10 mM addition of $MgCl_2$. Native PfGDPD was purified using gel filtration chromatography. 3 µL of enzyme was assayed against 2 mM glycerophosphocholine in 100 mM HEPES pH 7.5 and transferred to 2° assay reaction containing 0.2 M hydrazine/500 mM glycine/2.5 mM EDTA buffer pH 9.5, 2.3 mM NAD^+ and 0.05 µg/µL G3PDH. Data are shown as the percentage activity compared to 10 mM addition of $MgCl_2$ and are the results from a single assay.

2.4.6 Steady Sate Parameters of Native PfGDPD

Localization studies showed PfGDPD is highly expressed in the PV and cytosol and less abundant within the food vacuole Therefore, we examined enzyme functionality within the two different compartment, at the near neutral pH of the PV [32] and at pH 5.5, which falls within the pH range of 5.2-5.7 estimated for the food vacuole [33-36]. A single peak fraction from anion exchange purification was used for analysis and protein concentration 6.1 x 10^{-3} mg/mL, was estimated by immnoblotting with anti-PfGDPD using a standard curve of known of recombinant PfGDPD concentration. 0.1 µM nPfGDPD was incubated with 0-5 mM GroPC and kinetic analysis was examined at pH 7.5 (100 mM HEPES, 150 mM NaCl, 10 mM Mg^{2+}) and pH 5.5 (100 mM sodium acetate, 150 mM NaCl, 10 mM Mg^{2+}), using G3PDH coupled assay. At pH 7.5, GroPC hydrolysis followed Michaelis–Menten kinetics, however, at pH 5.5, we observed inefficient catalysis of substrate (Figure 2-11). The kinetic parameters at pH 7.5 showed a K_M of 2.2 mM, substrate turnover (k_{cat}) rate of 7.2 s^{-1} and catalytic efficiency value of 3.6 x 10^3 $M^{-1} \bullet s^{-1}$ expressed as the ratio of k_{cat} over K_M (Table 2-2). These values demonstrate a functional role of PfGDPD in the parasite PV as opposed to the food vacuole. The presence of the protein within

the food vacuole is therefore questionable. One possible explanation could result from the passive transport of PfGDPD during hemoglobin uptake in cytostomal vesicles that extend from the parasite plasma membrane and PV membrane. This process has previously been described in the trafficking of a plasmodial enzyme, plasmpepsin II [30]

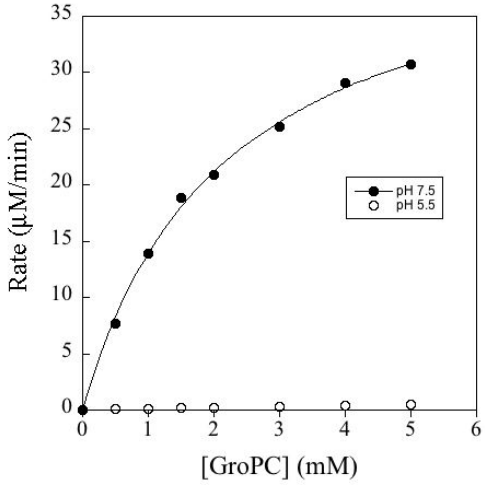

Figure 2-11. Comparison of native PfGDPD activity at pH 7.5 and pH 5.5. 0.1 μM native PfGDPD was incubated with 0-5 mM glycerophosphocholine (GroPC) in the presence of 10 mM $MgCl_2$ in 100 mM HEPES pH 7.5 and 100 mM sodium acetate pH 5.5. Lines are non-linear regression fits to the Michaelis-Menten equation and represent the results from a single experiment.

2.4.7 Purification of Recombinant PfGDPD

The limitations in biochemically characterizing native PfGDPD prompted the purification of recombinant enzyme in order to generate greater quantities of protein with high purity. However, we encountered several set backs our attempts to obtain recombinant enzyme due to the constant low level of activity observed. We addressed several potential problem areas, which include re-assessing the induction time and temperature during protein expression in *E.coli* cells, re-positioning the hexa-histidine (His_6) fusion tag and employing several combination of purification techniques, however protein activity remained unchanged even when assays were supplemented with 10 mM Mg^{2+} and 1 mM Mn^{2+}, metal ions shown to activate native enzyme activity. In contrast, the addition 10 mM Mg^{2+} and 1 mM Mn^{2+} during protein expression and purification yielded a much more active recombinant enzyme specifically in 10 mM Mg^{2+}. Accordingly, expression and purification of recombinant PfGDPD included 10 mM in liquid broth and buffers. Briefly, recombinant enzyme, termed rPfGDPD was expressed as a soluble protein in *E. coli* purified by immobilized metal affinity chromatography (IMAC) and gel filtration chromatography. A His_6 tag was placed at the N-terminus followed by a linker

containing the tobacco etch virus (TEV) protease cleavage site. Attempts to cleave the His_6 tag at the TEV protease recognition site yielded a small proportion of cleaved protein. However, activity assays indicated both cleaved and uncleaved protein variants were equally active, therefore characterization proceeded with uncleaved protein. Enzyme was purified to homogeneity as shown on the coomassie stained gel of eluted gel filtration fractions (Figure 2-12A). Comparison of protein mobility between rPfGDPD and native enzyme on an SDS-polyacrylamide gel showed a slight shift in size between the two protein species (Figure 2-12B), which may have resulted from proteolytic post-translational modifications of the native enzyme.

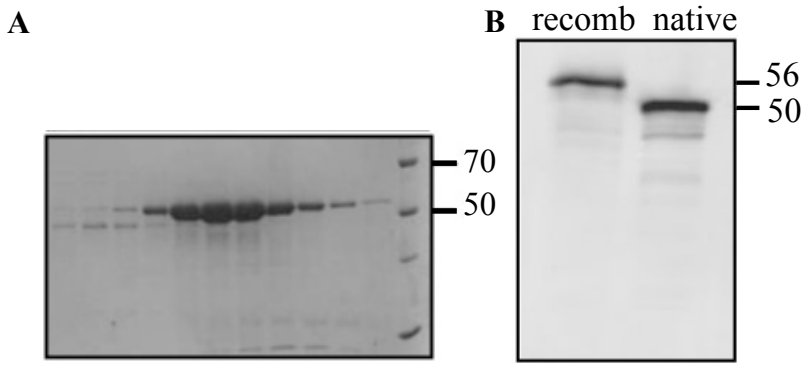

Figure 2-12. Purification of recombinant PfGDPD. A) Coomassie staining of 10 % polyacrylamide gel of purified recombinant PfGDPD gel filtration fractions. B) Anti-PfGDPD immunoblot of SDS-denatured native and recombinant (recomb) PfGDPD. Size markers are indicated on the right panels.

2.4.8 Metal Ion Dependency of Recombinant PfGDPD

The metal ion preference for nPfGDPD is represented as $Mg^{2+} > Mn^{2+} > Co^{2+}$, while relatively low inhibition was observed with Ca^{2+}, Cu^{2+} and Zn^{2+}. To determine if the same metal preference held true for the recombinant enzyme, we examined the effects of Mg^{2+} and Ca^{2+} on rPfGDPD activity. Mg^{2+} was chosen due to the high level of activation observed, whereas the physiological relevance of Ca^{2+} over Cu^{2+} and Zn^{2+} presented the most obvious choice. At pH 7.5, 9 nM rPfGDPD was incubated with 1 mM Mg^{2+}, 10 mM Mg^{2+}, 1 mM Ca^{2+}, 10 mM Ca^{2+} and 1 mM EDTA. As expected, strong activation was observed with Mg^{2+} whereas inhibitory effects were seen with Ca^{2+} (Figure 2-13). We observed a 5-fold activation in 10 mM Mg^{2+} and a 2-fold difference in 1mM Mg^{2+}. Relative to activity in 10 mM Mg^{2+}, we observed approximately 20 % activity in the absence of added metal and a loss in activity with EDTA treatment. Metal ion

dependency of rPfGDPD is therefore consistent with results obtained with nPfGDPD, thus confirming activation of PfGDPD activity by Mg^{2+}.

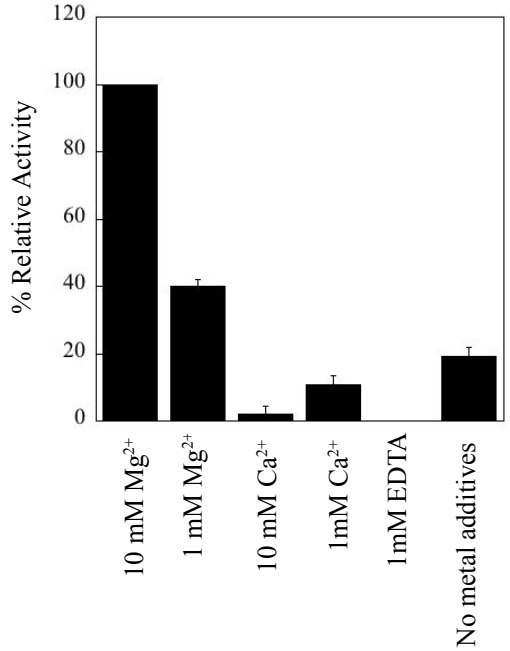

Figure 2-13. Recombinant PfGDPD is maximally stimulated by Magnesium (II) ions. Graph showing results of 9 nM rPfGDPD activity in the presence of 10 mM Mg^{2+}, 1 mM Mg^{2+}, 10 mM Ca^{2+}, 1 mM Ca^{2+} in buffer containing 100 mM HEPES pH 7.5, 150 mM NaCl and transferred to 2° assay containing 0.2 M hydrazine/500 mM glycine/2.5 mM EDTA buffer pH 9.5, 2.3 mM NAD^+ and 0.05 μg/μL G3PDH. Data are shown as the percentage activity compared to 10 mM addition of $MgCl_2$ and are the average of triplicate assays.

2.4.9 Steady State Parameters of rPfGDPD Activity

Though nPfGDPD exhibited efficient catalysis of GroPC, it can be argued that other enzyme impurities could contribute to the since PfGDPD was only partially purified. To address this, the catalytic activity of recombinant enzyme was therefore examined. 52 nM of rPfGDPD was incubated with 0-10 mM GroPC at pH 7.5 supplemented with 10 mM Mg^{2+}. GroPC hydrolysis followed Michaelis–Menten kinetics (Figure 2-14). The kinetic parameters revealed a K_m of 3.4 ± 1.6 mM, k_{cat} of 27 ± 6 s^{-1} and a catalytic efficiency (k_{cat}/K_m) of (8.7 ± 4.1) x 10^3 $M^{-1}•s^{-1}$. (Table 2-2). rPfGDPD activity represents a reflection of native catalytic ability. Additionally, these rates are comparable to *E. coli* UgpQ [14], with ~8-fold difference in substrate turnover and catalytic efficiency values within the same order of magnitude. In comparison to *E. coli* GlpQ (K_m = 0.28 mM), an11-fold difference is observed in substrate affinity.

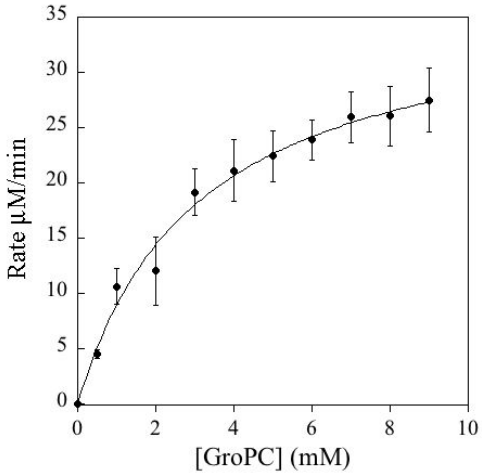

Figure 2-14. Michaelis-Menten curve for the hydrolysis of glycerophosphocholine by PfGDPD at pH 7.5. 52 nM of recombinant PfGDPD was incubated with 0-10 mM glycerophosphocholine (GroPC) in the presence of 10 mM $MgCl_2$ at pH 7.5 in 100mM HEPES, and 150 mM NaCl. Lines are non-linear regression fits to the Michaelis-Menten equation and represent the average of triplicate experiments.

Table 2-2. Kinetic parameters for the hydrolysis of GroPC by PfGDPD and *E.coli* UgpQ homolog. Data values were determined with 52 nM PfGDPD at pH 7.5 at 37 ^{o}C in the presence of 10 mM $MgCl_2$. [a]*E. coli* enzyme was assayed in the presence of 3 mM $MgCl_2$.

Enzyme	K_m (mM)	k_{cat} (s^{-1})	k_{cat}/K_m ($M^{-1} \bullet s^{-1}$)	Ref.
rPfGDPD	3.4 ± 1.6	27 ± 6	(8.7 ± 4.1) x 10^3	This study
nPfGDPD	2.0	7.2	3.6 x 10^3	This study
[a]*E.coli* UgpQ	2.0	3.2	1.6 x 10^3	[14]

The comparable kinetic parameters of rPfGDPD to *E.coli* GDPD, we questioned the possibility of bacteria contamination, contributing to rPfGDPD activity. To rule out the possibility of an *E.coli* GDPD contamination, we attempted to generate a mutant variant of PfGDPD. Mutational studies in *Thermoanaerobacter tengcongensis* (ttGDPD) show complete inactivity with alanine (Ala) substitution at each metal binding residues (Glu44, Asp46 and Glu119) [12]. Sequence alignment of rPfGDPD to ttGDPD and other GDPD homologues, indicate Glu63, Asp65 and Glu107 as the metal binding residues in PfGDPD (Figure 2-1). Accordingly, we generated a Glu63-Ala mutant with an N-terminal His_6 tag. Mutant and wild-type enzymes were expressed and purified simultaneously under the same conditions. Mutant enzyme was expressed as a soluble protein when analyzed by immunoblot analysis, however when purified over Ni^{2+} IMAC column, the elution profile indicated the protein did not bind to the column. In the event the mutant protein eluted in lower imidazole concentration, purification

was repeated in the absence of the elution agent. Unable to obtain protein, we addressed issues pertaining to the orientation of the His_6 tag and Ni^{2+} resin by generating a C-terminal His_6 tag protein and switching to a Co^{2+} column. These modifications proved unsuccessful in purifying mutant enzyme, although the possibility persisted that bacteria GDPD could still be present in the IMAC protein fractions even in the absence of mutant enzyme. Therefore, an eluted fraction from 'mutant' PfGDPD was assayed for the presence contaminating bacterial enzyme activity. The concentration of a peak fraction from wild-type was determined at an absorbance of 280 nm and assayed at 0.14 μM. The corresponding fraction from the "mutant" pool was assayed using 1) the same volume as wild-type enzyme and 2) ten times the volume as wild-type enzyme. Fractions were assayed with 2 mM GroPC in 100 mM HEPES pH 7.5, 150 mM NaCl and10 mM Mg^{2+}. Activity was not observed in the 'mutant' fractions, which therefore suggests hydrolysis of GroPC is solely due to rPfGDPD.

2.4.10 Lysophosphatidylcholine as a Possible Substrate

Crystallography studies on GDPDs indentified several structurally similar proteins with distinct functions include copper homeostasis protein (Cutcm; 1X71), tryptophan synthase (2TYS), pyridoxine 5' phosphate synthase (1HO1), pyruvate kinase (1A49) and sphingomyelinase (1XX1). Of these, sphingomyelinase was of interest because of its lipolytic activity on the membrane phospholipid, sphingomyelin [37]. Spider venom sphingomyelinase D (SMaseD) from the genus *Loxosceles* and bacterial Spider SMaseD, reportedly originated by divergence from GDPD domain family [38]. Previous studies have also reported an intrinsic lysophospholipase D activity in Spider SMaseD towards lysophosphatidylcholine to yield choline and lysophsohatidic acid, which is known to induce proinflammatory responses, platelet aggregation, endothelial hyperpermeability [39]. Importantly, SMaseDs share broad similarities with GDPD, which include similar TIM barrel structure and catalytic mechanism. Structural studies indicate that catalysis is mediated by metal ion binding and two histidine residues involved in stabilization and hydrolysis of substrate (Figure 2-5) [38, 40, 41]. We therefore examine the catalytic activity of PfGDPD against lysophosphatidylcholine (LPC). We prepared two LPC substrates, each with either a 6-carbon fatty acid chain (LPC6:0) or 12-carbon chain esterified at *sn*-1 position. These substrates have been reported as substrates for SMaseD [37, 39].

We assayed the hydrolytic activity of rPfGDPD by measuring the amount of choline released from LPC using the choline oxidase assay described in section 2.3.9 (Figure 2-4). Enzyme was incubated at different amounts if 6, 12 and 24 ng, in 125 mM TRIS pH 8.5, 150 mM NaCl and 10 mM Mg^{2+} for 15 min at 37 ^{o}C. Following incubation, 1 mM LPC was added to start the 30 min reaction at 37 ^{o}C, after which PfGDPD activity was inactivated and an enzyme cocktail of 1 U/mL choline oxidase, 1 mM HPPA and 0.18 U/mL HRP was added to the mixture, which proceeded for 10 min at 25 ^{o}C. As an internal control, 1 Mm GroPC was included in the assay reactions and hydrolysis showed a linear increase in activity with increasing enzyme concentration (Figure 2-15). In contrast, we observed much lower levels of activity with LPC that showed an enzyme preference for the shorter fatty acid chain, LPC6:0 over LPC12:0. Low activity observed with LPC12:0, could be due to the formation of lipid micelles as the concentration of lipid used in the assay was higher than the Critical Micelle Concentration value of 0.2 mM.

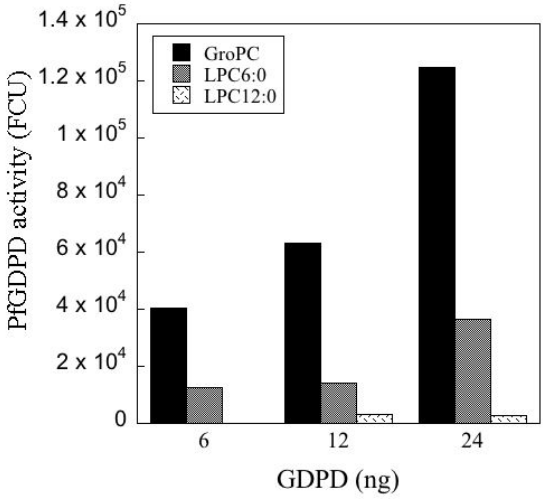

Figure 2-15. Substrate preference of recombinant PfGDPD. rPfGDPD at 6, 12 24 ng, was incubated with 1mM glycerophosphocholine (GroPC) and lysophosphatidylcholine at 1 mM LPC6:0 and 1mM LPC12:0, in a buffer containing 125 mM TRIS pH 8.5, 150 mM NaCl and 10 mM Mg^{2+} for 15 min at 37 ^{o}C, after which cocktail mix of 1 U/mL choline oxidase, 1 mM HPPA and 0.18 U/mL HRP was added and proceeded for 10 min at 25 ^{o}C. PfGDPD enzyme concentration is plotted against enzyme activity, expressed in fluorescent cell units (FCU). Data presented are from a single experiment.

2.5 DISCUSSION

The emergence of drug resistant *Plasmodium falciparum* parasites combined with the lack of available vaccines in treating malaria, presents an urgent need to identify and develop novel anti-malarial drugs. Phospholipid catabolism is an important metabolic process, required for the growth and development of *P. falciparum* within the erythrocytic host cell. Lipolytic enzymes play key roles in parasite growth, virulence, differentiation, cell signaling and hemozoin formation [42, 43]. Accordingly, the goal of this study was to identify enzymes involved in phospholipid degradation. Our current study describes a glycerophosphodiester phosphodiesterase homologue in *P. falciparum* (PfGDPD), involved in the downstream hydrolysis of phosphatidylcholine, a major lipid of parasite membranes. PfGDPD hydrolyzes glycerophosphodiester to glycerol-3-phopshate and the corresponding alcohol, both of which have different metabolic fates.

Similar to other GDPD homologues, PfGDPD contains the unique GDPD insertion domain and conserved catalytic histidine and metal binding residues. Similarly, PfGDPD also contains a putative signal peptide sequence. Multiple attempts to disrupt the endogenous coding region were unsuccessful implicating a yet unidentified role in parasite development within human erythrocytes, which may involve either phospholipid metabolism or shuttling glycerol-3-phosphate into the glycolysis metabolic pathway. Our localization studies complicate a means of attributing a specialized function of PfGDPD as we observed a complex distribution in the parasitophorous vacuole (PV), cytosol and less intensely in the food vacuole, which were further confirmed by immoblot analysis of fractionated parasite extracts. It is therefore possible that PfGDPD may have multiple roles in theses compartments or a sole function in the parasite. The presence of a signal peptide, which functions to direct proteins through the secretory pathway destined for a cellular location, renders protein distribution in the cytosol intriguing. One explanation could stem from the presence of an alternate transcription site, where two different mRNA transcripts are expressed to produce two pools of PfGDPD. Another could be the result of an alternate translation site, where more than one initiation methionine within close proximity could serve as an alternate start site. Present in the N-terminal extension of PfGDPD are two methionines (Met1, Met19), either of which could serve as translation start site, generating a species with or without a signal peptide, targeted respectively to the PV or cytosol.

Biochemical characterization of PfGDPD required the availability of active purified enzyme. Partially purified native enzyme was obtained, however, due to limited quantities, recombinant enzyme was purified and profiled for enzyme activity. After multiple attempts, active recombinant enzyme was obtained when Mg^{2+} was supplemented with during expression and purification steps.

Kinetic analysis of both native and recombinant enzyme revealed efficient hydrolysis of glycerophosphocholine and a modest hydrolysis of lysophosphadtylcholine of shorter fatty acid chain length in the presence of Mg^{2+} at pH 7.5, reflective of the parasitophorous vacuole lumen and therefore suggests a functional role for PfGDPD in this environment. PfGDPD also hydrolyzed. In contrast, low activity of native enzyme was observed at pH 5.5 of the food vacuole, indicating a non-functional role in at that pH or perhaps a different substrate preference in that environment. Therefore, attributing a physiological role would shed some light in understanding the contribution of PfGDPD during development. The next chapter highlights the attempted strategy to attribute a functional role for PfGDPD.

2.6 REFERENCES

1. Rao, M. and S. Sockanathan, *Transmembrane Protein GDE2 Induces Motor Neuron Differentiation in Vivo.* Science, 2005. **309**(5744): p. 2212-2215.
2. Nogusa, Y., et al., *Isolation and characterization of two serpentine membrane proteins containing glycerophosphodiester phosphodiesterase, GDE2 and GDE6.* Gene, 2004. **337**(0): p. 173-179.
3. Yanaka, N., et al., *Novel Membrane Protein Containing Glycerophosphodiester Phosphodiesterase Motif Is Transiently Expressed during Osteoblast Differentiation.* Journal of Biological Chemistry, 2003. **278**(44): p. 43595-43602.
4. Fernández-Murray, J.P. and C.R. McMaster, *Glycerophosphocholine Catabolism as a New Route for Choline Formation for Phosphatidylcholine Synthesis by the Kennedy Pathway.* Journal of Biological Chemistry, 2005. **280**(46): p. 38290-38296.
5. Larson, T.J., M. Ehrmann, and W. Boos, *Periplasmic glycerophosphodiester phosphodiesterase of Escherichia coli, a new enzyme of the glp regulon.* Journal of Biological Chemistry, 1983. **258**(9): p. 5428-5432.
6. Tommassen, J., et al., *Characterization of two genes, glpQ and ugpQ , encoding glycerophosphoryl diester phosphodiesterases of Escherichia coli.* Molecular and General Genetics MGG, 1991. **226**(1): p. 321-327.
7. AhrÈn, I.L., et al., *Protein D expression promotes the adherence and internalization of non-typeable Haemophilus influenzae into human monocytic cells.* Microbial Pathogenesis, 2001. **31**(3): p. 151-158.
8. Yanaka, N., *Mammalian Glycerophosphodiester Phosphodiesterases.* Bioscience, Biotechnology, and Biochemistry, 2007. **71**(8): p. 1811-1818.
9. Rao, K.N., et al., *Crystal structure of glycerophosphodiester phosphodiesterase from <I>Agrobacterium tumefaciens</I> by SAD with a large asymmetric unit.* Proteins: Structure, Function, and Bioinformatics, 2006. **65**(2): p. 514-518.
10. Santelli, E., et al., *Crystal structure of a glycerophosphodiester phosphodiesterase (GDPD) from <I>Thermotoga maritima</I> (TM1621) at 1.60 ≈ resolution.* Proteins: Structure, Function, and Bioinformatics, 2004. **56**(1): p. 167-170.

11. Heinz, D.W., et al., *Crystal Structure of Phosphatidylinositol-Specific Phospholipase C from Bacillus cereus in Complex with Glucosaminyl(α 1→6)-d-myo-inositol, an Essential Fragment of GPI Anchors †, ‡*. Biochemistry, 1996. **35**(29): p. 9496-9504.
12. Liang, S., et al., *Crystal structure of glycerophosphodiester phosphodiesterase (GDPD) from <I>Thermoanaerobacter tengcongensis</I>, a metal ion-dependent enzyme: Insight into the catalytic mechanism.* Proteins: Structure, Function, and Bioinformatics, 2008. **72**(1): p. 280-288.
13. Nagano, N., C.A. Orengo, and J.M. Thornton, *One Fold with Many Functions: The Evolutionary Relationships between TIM Barrel Families Based on their Sequences, Structures and Functions.* Journal of Molecular Biology, 2002. **321**(5): p. 741-765.
14. Ohshima, N., et al., *Escherichia coli Cytosolic Glycerophosphodiester Phosphodiesterase (UgpQ) Requires Mg2+, Co2+, or Mn2+ for Its Enzyme Activity.* J. Bacteriol., 2008. **190**(4): p. 1219-1223.
15. Trager, W. and J. Jensen, *Human malaria parasites in continuous culture.* Science, 1976. **193**(4254): p. 673 - 675.
16. Lambros C, V.J., *Synchronization of Plasmodium falciparum erythrocytic stages in culture.* Journal of parasitology, 1979. **65**(3): p. 418-420.
17. Fidock, D.A. and T.E. Wellems, *Transformation with human dihydrofolate reductase renders malaria parasites insensitive to WR99210 but does not affect the intrinsic activity of proguanil.* Proceedings of the National Academy of Sciences, 1997. **94**(20): p. 10931-10936.
18. Wu, Y., L.A. Kirkman, and T.E. Wellems, *Transformation of Plasmodium falciparum malaria parasites by homologous integration of plasmids that confer resistance to pyrimethamine.* Proceedings of the National Academy of Sciences, 1996. **93**(3): p. 1130-1134.
19. Kumar, N., et al., *Induction and localization of Plasmodium falciparum stress proteins related to the heat shock protein 70 family.* Molecular and Biochemical Parasitology, 1991. **48**(1): p. 47-58.
20. Li, J., et al., *Differential localization of processed fragments of Plasmodium falciparum serine repeat antigen and further processing of its N-terminal 47 kDa fragment.* Parasitology International, 2002. **51**(4): p. 343-352.

21. Bublitz, C. and O. Wieland, *Glycerokinase: Glycerol+ATP→L- α -Glycerophosphate+ADP*, in *Methods in Enzymology*, P.C. Sidney and O.K. Nathan, Editors. 1962, Academic Press. p. 354-361.
22. Shevchenko, D.V., et al., *Membrane Topology and Cellular Location of the Treponema pallidum Glycerophosphodiester Phosphodiesterase (GlpQ) Ortholog.* Infect Immun, 1999. **67**(5): p. 2266-2276.
23. Shang, E.S., et al., *Sequence analysis and characterization of a 40-kilodalton Borrelia hermsii glycerophosphodiester phosphodiesterase homolog.* Journal of Bacteriology, 1997. **179**(7): p. 2238-46.
24. Notredame, C., D.G. Higgins, and J. Heringa, *T-coffee: a novel method for fast and accurate multiple sequence alignment.* J Mol Biol, 2000. **302**(1): p. 205-217.
25. Waterhouse, A.M., et al., *Jalview Version 2—a multiple sequence alignment editor and analysis workbench.* Bioinformatics, 2009. **25**(9): p. 1189-1191.
26. Haupts, U., et al., *Dynamics of fluorescence fluctuations in green fluorescent protein observed by fluorescence correlation spectroscopy.* Proceedings of the National Academy of Sciences, 1998. **95**(23): p. 13573-13578.
27. Kneen, M., et al., *Green Fluorescent Protein as a Noninvasive Intracellular pH Indicator.* Biophysical Journal, 1998. **74**(3): p. 1591-1599.
28. Dalal, S. and M. Klemba, *Roles for Two Aminopeptidases in Vacuolar Hemoglobin Catabolism in Plasmodium falciparum.* Journal of Biological Chemistry, 2007. **282**(49): p. 35978-35987.
29. Klemba, M., I. Gluzman, and D.E. Goldberg, *A Plasmodium falciparum Dipeptidyl Aminopeptidase I Participates in Vacuolar Hemoglobin Degradation.* Journal of Biological Chemistry, 2004. **279**(41): p. 43000-43007.
30. Klemba, M., et al., *Trafficking of plasmepsin II to the food vacuole of the malaria parasite Plasmodium falciparum.* J Cell Biol, 2004. **164**(1): p. 47-56.
31. Zheng, B., et al., *GDE1/MIR16 is a glycerophosphoinositol phosphodiesterase regulated by stimulation of G protein-coupled receptors.* Proceedings of the National Academy of Sciences of the United States of America, 2003. **100**(4): p. 1745-1750.

32. Klonis, N., et al., *Evaluation of pH during cytostomal endocytosis and vacuolar catabolism of haemoglobin in Plasmodium falciparum.* Biochem J, 2007. **407**(3): p. 343-354.
33. Bennett, T.N., et al., *Drug resistance-associated pfCRT mutations confer decreased Plasmodium falciparum digestive vacuolar pH.* Mol Biochem Parasitol, 2004. **133**(1): p. 99-114.
34. Klonis, N., et al., *Evaluation of pH during cytostomal endocytosis and vacuolar catabolism of haemoglobin in Plasmodium falciparum.* Biochem J, 2007. **407**(3): p. 343-54.
35. Krogstad, D.J., P.H. Schlesinger, and I.Y. Gluzman, *Antimalarials increase vesicle pH in Plasmodium falciparum.* J Cell Biol, 1985. **101**(6): p. 2302-9.
36. Kuhn, Y., P. Rohrbach, and M. Lanzer, *Quantitative pH measurements in Plasmodium falciparum-infected erythrocytes using pHluorin.* Cell Microbiol, 2007. **9**(4): p. 1004-13.
37. Lee, S., and Lynch, K.R., *Brown recluse spider (Loxosceles reclusa) venom phospholipase D (PLD) generates lysophosphatidic acid (LPA).* Biochem. J., 2005. **391**: p. 317-323.
38. Cordes, M.H.J. and G.J. Binford, *Lateral gene transfer of a dermonecrotic toxin between spiders and bacteria.* Bioinformatics, 2006. **22**(3): p. 264-268.
39. van Meeteren, L.A., et al., *Spider and Bacterial Sphingomyelinases D Target Cellular Lysophosphatidic Acid Receptors by Hydrolyzing Lysophosphatidylcholine.* Journal of Biological Chemistry, 2004. **279**(12): p. 10833-10836.
40. Binford, G.J., M.H.J. Cordes, and M.A. Wells, *Sphingomyelinase D from venoms of Loxosceles spiders: evolutionary insights from cDNA sequences and gene structure.* Toxicon, 2005. **45**(5): p. 547-560.
41. Murakami, M.r.T., et al., *Structural insights into the catalytic mechanism of sphingomyelinases D and evolutionary relationship to glycerophosphodiester phosphodiesterases.* Biochemical and Biophysical Research Communications, 2006. **342**(1): p. 323-329.
42. Eda, S. and I.W. Sherman, *Cytoadherence of malaria-infected red blod cells involves exposure of phosphatidylserine.* Cell Physiol. Biochem., 2002. **12**: p. 373-384.

43. Katherine, E.J., et al., *Food vacuole-associated lipid bodies and heterogeneous lipid environments in the malaria parasite, Plasmodium falciparum.* Molecular Microbiology, 2004. **54**(1): p. 109-122.

CHAPTER 3

Effects of modulating the sub-cellular location of glycerophosphodiester phosphodiesterase in *Plasmodium falciparum*

3.1 ABSTRACT

Kinetic analysis of *P. falciparum* enzyme, glycerophosphodiester phosphodiesterase (PfGDPD) revealed PfGDPD efficiently hydrolyzes glycerophsophocholine to generate free choline and glycerol- 3-phosphate, which are actively utilized by the parasite. However, knockout strategies to define a function for PfGDPD during parasite intra-erythrocytic replication were unattainable. In an attempt to determine a physiological role for PfGDPD, we modified the sub-cellular distribution using a conditional aggregation domain (CAD) system, which confers aggregation and endoplasmic reticulum (ER) retention of fused proteins in a ligand-reversible manner. We generated parasites expressing PfGDPD-YDP-CAD fusion protein and when observed in the absence of ligand, fusion protein was not strictly localized to the ER but rather distributed as punctate structures within the parasite. Furthermore, immunoblot analysis of cellular fractions detected the leakage of fusion protein in the parasitophorous vacuole. The effect of the resulting shift in protein distribution showed no growth inhibition of parasites cultured in complete RPMI medium. To determine a phenotype, we developed a more stringent media, termed Choline Free Medium, in which we probed the ability CAD fusion protein in generating choline from exogenously added choline esters. Choline Free Medium supplemented with different choline esters sustained wild-type 3D7 parasite proliferation, and elicited no growth phenotype in PfGDPD-YDP-CAD expressing parasites.

3.2 INTRODUCTION

The clinical manifestations of malaria occur as the human malaria parasite asexually replicates within the host erythrocyte. Studies suggest *P. falciparum* requires the presence of certain factors in the human serum for successful proliferation [1]. The parasite has the ability to scavenge metabolites from the host required for several metabolic processes including phospholipid metabolism. Serine, choline, ethanolamine and free fatty acid (FFA) bound to serum albumin are examples of host-derived precursors necessary for lipid synthesis. *In vitro* culturing of *P. falciparum* blood stages provide the necessary nutrients and a suitable environment needed to maintain parasite culture in an attempt to gain insights into the biology, biochemistry and immunology of this organism [2].

Current cultivation techniques employ the method of Trager & Jenson using serum supplemented RPMI 1640 media within a buffered system in an atmosphere of raised carbon dioxide and lowered oxygen levels [3]. RPMI 1640 is a basal medium and consists of inorganic salts, amino acids, vitamins, glutathione, glucose and a pH indicator (Phenol Red). As the medium contains no proteins or growth promoting elements, serum supplementation is required to render it a "complete" medium. Human serum is the most favorable supplement to support parasite growth [3], but due to cost, reproducibility and possible presence of inhibitory immune factors, commercially available lipid rich bovine serum, AlbuMAX I and AlbuMAX II, are now available and have been proven to serve as alternatives to human serum [4, 5].

Recent studies examined the serum specific growth promoting factors as free fatty acids (FFA) in complex with the lipid carrier albumin [6]. The study indicated that the essential FFA were required as a pair of unsaturated and saturated species. The best combination comprised of the two most abundant FFA in human plasma, palmitic acid ($C_{16:0}$) and oleic acid ($C_{18:1\ n\text{-}9}$) [6-9]. Notably, mixtures of FFA and not individual molecules were shown to sustain parasite growth [6, 8, 10, 11]. The parasite can metabolize host acquired FFA into phosphatidylcholine, phosphatidylethanolamine, phosphatidylserine, phosphatidylinositol, diacylglycerol, and triacylglycerol [9, 12]. Though the parasite possesses the machinery for a type II fatty acid synthesis system (FASII) in the apicoplast [13, 14], the scavenging pathway has been demonstrated as the dominant system in procuring FFA for lipid synthesis [15-18].

In addition to FFA, parasite acquires phospholipid precursors, serine and choline, through uptake from the host via a carrier-mediated process [19-21]. In addition, serine is readily

available through the degradation of host hemoglobin [22, 23] and choline can be generated through the hydrolysis of choline esters i.e glycerophosphocholine and lysophosphatidylcholine.

In this chapter, we attempt to define a role for *P. falciparum* glycerophosphodiester phosphodiesterase (PfGDPD), an enzyme that generates choline as one of its products by hydrolyzing glycerophosphocholine. We have previously demonstrated the inability to disrupt the PfGDPD gene coding sequence, establishing an important function during parasite intra-erythrocytic replication. To further examine the contribution of PfGDPD, we attempted to modulate the sub-cellular localization of PfGDPD within the parasite to elicit a phenotypic effect. We used a conditional aggregation domain (CAD) system to generate a fusion protein that confers aggregation of the fused protein in a reversible manner using a small anti-aggregation ligand. We generated parasites expressing PfGDPD-YFP-CAD and assessed the effects of the altered protein distribution on parasite proliferation in a chemically defined basal media termed Choline-Free Media (CFM). We developed this media in an attempt to examine the choline releasing capabilities of PfGDPD-YFP-CAD parasites by exogenously supplementing CFM with specific choline-containing compounds.

3.3 EXPERIMENTAL PROCEDURES

3.3.1 Generation of Constructs

To generate conditional aggregation domain (CAD) sequence, forward primer GTACGGCTAGCCAAGAGGGCAGTGCCTCTAGAG and reverse primer GTACGGCGGCCGCCTCTTCTGACGGTTTCAAGCACTAGTTTCCAG were designed to amplify 4 tandem repeats of mutated FK506 binding protein (FKBP) from the template pC_4S_1-F_M4-FCS-hGH (RPD™ Regulated Secretion/Aggregation Kit). FKBP has a mutation at the Phe36 position, which converts the normally monomeric protein into a ligand-reversible dimer [24]. Inserts were digested with NheI/NotI (underlined) and cloned into the same sites of pPM2CIT2 plasmid, downstream of PfGDPD-YFP sequence generating a PfGDPD-YFP-CAD plasmid construct. Human dihydrofolate reductase (hDHFR) gene, a positive selection cassette that confers resistance to the anti-folate drug WR 99210 was included in the plasmid construct.

3.3.2 Parasite Transfection

All tissue culture experiments were performed under aseptic conditions in a biosafety cabinet. Unless stated otherwise, parasite cultures were maintained in a 5 % CO_2 incubator, cultured in human O^+ erythrocytes (Interstate Blood Bank) at 2% hematocrit in complete RPMI 1640 (CM) medium supplemented with 27 mM sodium bicarbonate, 11 mM glucose, 0.37 mM hypoxanthine, 10 μg/mL gentamycin and 5 g/L AlbuMAX I (Invitrogen) [3]. To obtain synchronous 3D7 ring cultures for plasmid transfection, 12 mL cultures were centrifuged for 3 min at 863 x g. The recovered pellet was incubated with 4 mL 5 % sorbitol [25] for 5 min, vortexed 2- 3 times and spun for 3 min at 863 x g. Supernatant was aspirated and the culture was re-suspend in 12 mL complete media. Sorbitol treatment was repeated 2-3 times to obtain tight parasite synchrony. Isolated 3D7 ring parasites were transfected with 75-100 μg of PfGDPD-YFP-CAD plasmid DNA using low voltage electroporation conditions. 48 hr post-transfection, parasites were positively selected with 10 nM WR 99210 drug. Resistant parasites appeared after 3 weeks and were cycled once in the presence of 1μM AP21998 anti-aggregation ligand [24, 26] and were maintained in CM prior to growth analysis. AP21998 is a monovalent synthetic compound designed to bind with high affinity to FKBP mutants with mutations at position 36.

3.3.3 Fluorescence Microscopy

Live images of parasites expressing PfGDPD-YFP-CAD were collected by incubating 40 μL of with 1 μL 5 μM nuclear stain Hoechst 33342 for 5 min at 37 ^oC. 10 μL of parasite cultures were mounted under a coverslip and images were collected on a Zeiss AxioImager M1 equipped with an MRm Axiocam digital camera using a 100x/1.4NA objective lens. Images were converted to TIFF files and contrast was adjusted using Adobe Photoshop CS4.

3.3.4 Southern Blot Analysis

To obtain parasites for genomic DNA (gDNA) extraction, 24 mL cultures were washed in 40 mL PBS, centrifuged for 3 min at 863 x g to remove supernatant. Pellet cultures were treated with 40 mL cold 0.1 % saponin in PBS and mixed by inverting the tube several times. The culture was incubated for 10 min on ice and centrifuged at 1940 x g, 10 min at 4 ^oC. Parasite pellet was washed in cold PBS at 1940 x g, 10 min at 4 ^oC and stored at -80 ^oC. To confirm chromosomal integration of PfGDPD-YFP-CAD plasmid, gDNA was extracted from saponin-

treated 3D7 and transfected parasites using the QiaAmp DNA blood mini kit (Qiagen). 50 μL of gDNA (2 μg) and KO plasmid (1 μg) were digested in a 100 μL reaction containing 10 μL 10x EcoRI Buffer, 10 μL 10x bovine serum albumin (BSA), 1 μL EcoRI restriction enzyme and 29 μL MilliQ-H_20. Reaction was incubated for 3 hrs at 37 ºC and purified using the QiaAmp nucleotide removal kit (Qiagen) in 30 μL elution buffer. DNA fragments were resolved on a 0.6 % agarose gel (200 mL) without ethidium bromide, run overnight at 30 volts for ~17 hours. 1kb markers were loaded in an edge lane and after electrophoresis, the marker lane was cut off, stained for 20 minutes in 0.5 μg/mL ethidium bromide and photographed with a fluorescent ruler. DNA fragments were depurinated in 0.25 M HCl for 15 min, denatured in 0.5 M NaOH, 1.5 M NaCl for 30 min and neutralized in 1 M Tris-HCl pH 8, 1.5 M NaCl for 30 min, and rinsed in water after each step. DNAwas transferred to an Immobilon Nytran$^+$ membrane (Millipore) using a Turboblotter for a minimum of 3 hrs in 20x SSC buffer containing 3.0 M NaCl and 0.3 M sodium citrate. Membrane was blocked using 20 μL AlkPhos Direct pre-hybridization reagent in a hybridization oven tube rotating for 1 hr at 55 ºC. After blocking, PfGDPD-YFP-CAD locus was detected by incubating the membrane overnight at 55 ºC with 100 ng probe generated from primers complementary to the 3' end of the gene; forward primer, GGCTTACTAGTCAATATATTCGGTATCATTAATAGGTTC and reverse primer GTACGCCATGGTTGAACTTAAAGGTAACAAAGAAGATCT. Probe was labelled using the AlkPhos Direct protocol and labelling kit (GE Biosciences) and signal was detected by autoradiography.

3.3.5 Parasite Fractionation

To determine if PfGDPD-YFP-CAD protein was present in the parasitophorous vacuole, trophozoite stage parasites expressing PfGDPD-YFP-CAD and PfGDPD-YFP (clone D9) were obtained using a MACS magnetic column (Miltenyi Biotech) [27]. The column was washed with 5mL complete RPMI medium and allowed to flow through. Two 12 mL culture plates were centrifuged were centrifuged for 3 min at 863 x g and the collected pellet was re-suspended in 5 mL complete RPMI medium and loaded onto the column. Trophozoite-infected red blood cells bind to the column due to the presence of significant amounts of hemozoin, while ring stage parasites and un-infected erythrocytes flow through. Bound parasites were eluted 3 mL complete

RPMI medium after the column was removed from the magnet. Parasites were spun for 2 min at 863 X g, re-suspended in 1 mL complete RPMI medium and transferred to a 24-well plate. To determine the number of parasites in each culture, 10 μL was transferred to a hemocytometer and counted in a large 5 x 5 grid with ~ 100 parasites/grid. The cultures had more than 100 parasites/grid and were diluted 20-fold in PBS. The following equation was used to calculate parasite number/mL:

average # of parasites x 10^4 x dilution factor

PfGDPD-YFP culture contained 1.6 x 10^8 parasites/mL and PfGDPD-YFP-CAD culture contained 1.3 x 10^8 parasites/mL.

Purified trophozoite parasites were washed once in 40 mL PBS and spun for 3 min at 863 X g. The pellet volume was estimated and a 2x volume of 1.5 mg/mL cold saponin in PBS was added and allowed to incubate for 15 min on ice, swirly occasionally. The mixture was spun at 1940 X g, 10 min at 4 ^oC and separated into supernatant and pellet fractions kept on ice. Pellet extracts were re-suspended in 24 μL PBS inhibitor cocktail. 1 mL of inhibitor cocktail contained a final concentration of 10 μM pepstatin, 10 μM N-(trans-epoxysuccinyl)-L-leucine 4-guanidinobutylamide (E-64), 0.5 mM 4-(2-aminoethyl)benzenesulfonyl fluoride and 1 mM sodium EDTA. Samples were solubilized in 6 μL 5x SDS-PAGE buffer, boiled in a water bath for 3 min and spun at 16,000 X *g* for 2 min to remove insoluble material. To confirm the presence of PfGDPD-YFP-CAD aggregates in the parasitophorous vacuole, mature trophozoite parasites were cultured to parasitemia between 5-7 %. A 1 ml culture aliquot was spun at 863 X g for 3 min and the pellet was re-suspended in 40 μL 1 mg/mL saponin prepared in complete RPMI medium. The culture was incubated for 10 min at room temperature (RT), diluted with 1 mL media and spun at 1940 X g for 10 min, RT. Pellet was washed twice in 1 mL media and taken up in 200 μL of media into a 96 well plate flat bottom plate and incubated at 37 ^oC prior to imaging.

3.3.6 Western Blot Analysis

A 10 μL aliquot of SDS solubilized supernatant and pellet extracts were loaded on 7.5 % SDS gel at an average of ~1 x 10^7 parasites. Gel was run at 80 volts and transferred onto a nitrocellulose membrane for 40 min at constant current (0.4Amp). Membrane was blocked for 1 hr in 2 % (w/v) bovine serum albumin/Tris-Buffered Saline and Tween 20 (TBST) buffer. anti-

PfGDPD primary antibody incubation (1:5,000 dilution in 2 % (w/v) BSA/TBST) was performed for 1 hour followed by incubation with anti-rat horseradish peroxidase-conjugated secondary antibody (1:10,000 dilution in 2 % (w/v) BSA/TBST) for one hour at room temperature. Following three 5-minute washes in TBST, signal was developed by chemiluminescence using Amersham ECL-Plus kit (GE Biosciences) according to maufacturer's instruction and detected on a STORM 840 imaging system under fluorescence acquisition mode at 750 volts. To evaluate loading controls, membrane was probed with primary antibody anti-SERA (1:38,000 dulition in 2 % (w/v) BSA/TBST) and anti-BiP (1:10,000 dilution in 2 % (w/v) BSA/TBST) and anti-rabbit horseradish peroxidase-conjugated secondary antibody (1:10,000 dilution in 2 % (w/v) BSA/TBST).

3.3.7 Media Preparation

Choline Free Medium (CFM) was prepared using the ingredients listed in Table 3-1. The concentration of components used was based on standard RPMI 1640 media (Invitrogen) with the exception of isoleucine. CFM was prepared as a 250 mL 2x stock and filtered through a .22 μm bottle top filter (Corning). AlbuMAX I free media (RPMI) was prepared as a 500 mL 2x sterile stock supplemented 2.25 g 27 mM sodium bicarbonate, 2 g 11 mM glucose, 3.6 mL 0.37 mM hypoxanthine and 200 μL 500 x gentamicin.

Lipids supplements for CFM and RPMI medium were purchased from Sigma; FFA (Palmitic acid $C_{16:0}$ and oleic acid $C_{18:1\ n\text{-}9}$) and lysophosphatidylcholine (LPC) (1-palmitoyl-2-hydroxy-*sn*-glycero-3-phosphocholine and 1-oleoyl-2-hydroxy-*sn*-glycero-3-phosphocholine). Each LPC and FFA lipid molecule was dissolved in ethanol at concentrations of 15 mM and 30 mM, respectively and stored at -20 ^{o}C until use. Fatty acid free bovine serum albumin powder (ffBSA- Sigma A7511) was dissolved in sterile Dulbecco's-PBS (Sigma) at 40 mg/mL. Lipids pairs were prepared as previously described [6] by drying (24 μl of each FFA and 48 μl of each LPC) under a stream of nitrogen gas. Dried lipid precipitates were reconstituted with the addition of 1.2 ml ffBSA stock solution and sonicated at power level 3 (5 x 12s pulses). 1.1 mL of each BSA complex mixture was diluted 5-fold by combining 4.4 mL of 1x media consisting of 2.75 mL 2x media and 1.65 mL sterile water and filtered through a small .22 μm syringe filter into a 15 mL conical tube. 5 mL of sterilized mixture was diluted in 15 mL 1 x media to obtain a medium with a 2 mg/mL concentration of ffBSA and 30 μM lipid.

Supplements were purchased from Sigma and provided at physiological concentrations; serine 286 μM, choline 21.4 μM, ethanolamine 50 μM, glycerophosphocholine 240 μM. Glycerophosphoserine 290 μM, and glycerophosphoethanolamine 40 μM were generously donated by Dr Larson. Supplements were prepared sterile as 100 x stock and added at 200 μL volume to 20 mL media. AlbuMAX I supplement was prepared at 20 mg/mL in 1 x media, sterile filtered and 5 mL was diluted in 15 mL 1x media at a final concentration of 5 mg/mL, which is similarly found in complete RPMI medium.

3.3.8 Parasite Growth Rate Analysis

To prepare parasites for growth analysis, human O^+ erythrocytes (Interstate Blood Bank), previously maintained in complete RPMI medium, were washed three times in 1x CFM for 12 min at 863 x g to remove traces of AlbuMAX I and choline and soted at 4 ^oC until used. Asynchronous PfGDPD-YFP-CAD and PfGDPD-YFP parasite cultures were inoculated at ~3% parasitemia and washed three times for 3 min at 863 x g. in 1 x media. 1mL aliquots were distributed into sterile 0.5 mL Eppendorf tubes, spun for 30 sec in a small centrifuge and re-suspended in 1mL of appropriate test medium. Parasite cultures were maintained in a 24-well plate placed in a cake jar and gassed with a 5 % O_2, 5 % CO_2 and 90 % N_2 mixture. Cell progression was monitored for 8 days and maintained below 10 % parasitemia by diluting every two days at 2 % hematocrit. 100 μL samples were taken every two days and analyzed for parasitemia by flow cytometery.

Table 3-1. Components of Choline Free Medium.

INORGANIC SALTS	1X (mg/L)	Stock	2 x Media (250 mL)
Calcium Nitrate (Ca ($N0_3$).H2O)	100	5 x salt mix	100 mL
Magnesium Sulfate	48.84	″	″
Potassium Chloride	400	″	″
Sodium Chloride	5850	″	″
Sodium Phosphate Dibasic (anhydrous)	800	″	″
AMINO ACIDS			
Cystine.HCl	65	1000 x	0.5 mL
Glutamic Acid	20	1000 x	0.5 mL
Glutamine	300	100 x	5 mL
Isoleucine	147.5	100 x	5 mL
Methionine	15	1000 x	0.5 mL
VITAMINS			
D-Biotin	0.2	100 x mix	5 mL
D-Panthothenate Ca salt	0.25	″	″
Vitamin B_{12}	0.005	″	″
Myo-inositol	35	″	″
Niacinamide	1	″	″
p-Amino Benzoic Acid	1	″	″
Pyridoxine.HCl	1	″	″
Riboflavin	0.2	″	″
Thiamine.HCl	1	″	″
Folic acid	1	1000 x	0.5 mL
OTHER			
Gentamycin	10,000	500 x	100 μL
Glucose	2000	N/A	1 g
HEPES	5958	5 x salt mix	100ml
Hypoxanthine	13600	0.1 M	1.8 mL
Sodium Bicarbonate	2250	N/A	1.125 g
Phenol Red	5	200 x	2.5 mL
Reduced Glutathione	1	100 x	0.5 mL

3.3.9 Flow Cytometry

To prepare cultures for flow cytometry, culture aliquots were fixed in 0.1 % glutaraldehyde (Sigma) and stored at 4 ^{o}C until use. Fixed samples were permeabilized with 0.25% Triton X-100 for 5 min at RT and stained with 400 nM YOYO-1 (Molecular Probes) in PBS for at least 30 minutes. Labelled samples were diluted 40-fold in PBS and analyzed on a BD mini Accuri C6 flow cytometer. A total of 3 x 10^4 erythrocyte counts were taken for each sample. The FL1 detector records the green fluorescence of YOYO-1 when bound to dsDNA at an

emission wavelength of 530 nm distinguishing infected from uninfected erythrocytes. Data was exported and analyzed using an Excel spreadsheet. The total number of parasites (parasitemia x cumulative dilution factor) was converted to the natural log (y), graphed against time (x) and fitted to the linear equation using KaleidaGraph 4.1 software (Synergy Software). Erythrocyte background values were substracted from calculated % parasitemia.

3.4 RESULTS

3.4.1 Modulation of PfGDPD Sub-Cellular Localization

As described in Chapter 2, our attempts at disrupting the endogenous PfGDPD gene either by gene truncation via single-crossover or gene knockout via double-crossover proved unsuccessful. Our results therefore suggest an important role for PfGDPD in parasite development. To elucidate its biological role, we attempted to modulate the distribution of PfGDPD within the parasite. We employed the use of a conditional aggregation domain system (CAD) that self-aggregates through its multi-domains, which can be reversed in the presence of a small anti-aggregation ligand [24]. CAD is comprised of a four tandem repeats of self-dimerizing mutant protein, FK506 Binding protein (FKBP) [24]. FKBP is a highly abundant cytosolic monomeric protein that functions as the primary receptor for the immunosuppressive ligands, FK506 and rapamycin [28, 29]. A Phe36Met point mutation renders with the unusual property to reversibly dimerize in the presence of a small anti-aggregation ligand, AP21998 [24]. To control the aggregation state of a protein and thereby control protein sub-cellular localization, 2 or more Phe36Met FKBP domains are fused to a protein of interest, and expressed as aggregates, which are retained in the endoplasmic reticulum (ER).

We generated parasites expressing PfGDPD as a fusion to yellow fluorescent protein (YFP) and CAD (PfGDPD-YFP-CAD), by transfecting PfGDPD-YFP-CAD plasmid into synchronous 3D7 ring parasites and enriched for plasmid chromosomal integration through repeated cycling on and off drug media. Successful integration would occur via a single-crossover recombination at homologous PfGDPD regions (Figure 3-1A). To prevent premature aggregation of protein fusion during cycling, parasites were maintained in the presence of the AP21998 ligand. Emerged parasites were genotyped by Southern blot using probes specific to the 3' end of PfGDPD locus. We analyzed genomic DNA isolated from transfected parasites and 3D7 wild-type, which served as a control for non-integration. In the event of plasmid integration,

duplication of the homology region would occur and would be detected as two bands of 4.3 kb and 10 kb, when digested with EcoRI. However non-integration of plasmid would be detected at 5.9 kb similar to the wild-type. As shown in Figure 3-1B, we observed two bands of the appropriate size in –CAD parasites, indicating an integration event of plasmid into PfGDPD gene. 3D7 parasite samples revealed the expected 5.9 kb, which is missing from the –CAD parasite lines. Results confirm the generation of parasites expressing PfGDPD-YFP-CAD, which were used for further analyses.

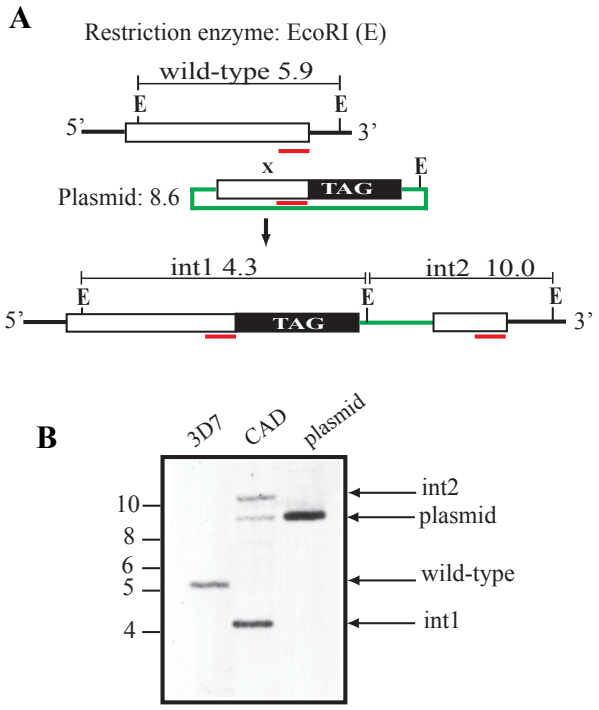

Figure 3-1. **Homologous recombination strategy and Southern analysis of PfGDPD-YFP-CAD.** A) Schematic diagram depicts the fragment sizes in kilobases of the endogenous PfGDPD locus (wild type), YFP-CAD plasmid and the result of a single-crossover integration (int1 and int2). The diagrams are not drawn to scale. The white box represents the PfGDPD coding region, the black box indicates YFP-CAD fusion tag, the green line corresponds with the plasmid backbone and the red bars represent the sites of hybridization with gene-specific Southern probes. Restriction enzyme is designated as EcoRI (E) B) Southern analysis of 2 µg total DNA isolated from PfGDPD-YFP-CAD (CAD) and 3D7 parasite lines and 1µg of YFP-CAD plasmid. The plasmid band in PfGDPD-YFP-CAD line represents the integration of episomal concatemers, which when digested, produces the same size band as the plasmid.

When observed in the presence of anti-aggregation ligand, the cellular distribution of PfGDPD-YFP-CAD was maintained as indicated by observed YFP fluorescence in the cytosol and parasitophorous vacuole (PV) (Figure 3-2A). Surprisingly, the removal of the anti-aggregation ligand did not lead to protein aggregate retention in ER but were instead observed as punctate structures (Figure 3-2B). The ER network surrounds the nucleus and therefore

aggregate retention can easily be observed around the nucleus. However, due to the cytosolic distribution of –CAD fusion protein, it is difficult to discern whether a small fraction of ER retention occurred and also whether the aggregate proteins leaked further into the PV. To assess if a shift in distribution occurred, we permeabilized the PV membrane using saponin, which rendered the membrane porous to the exit movement of macromolecules, resulting in a loss of punctate structures. Shown in Figure 3-2C, is the result of saponin treated PfGDPD-YFP-CAD where YFP fluorescence of punctate structures are less visiblesuggesting that the –CAD fusion aggregates were present in the PV. In addition to saponin treated parasites, we performed immunoblot analysis on fractionated parasites expressing PfGDPD-YFP-CAD to examine the level of fusion protein within parasite compartments. Previously generated parasites expressing PfGDPD-YFP, served as a control to allow multiple detection with antibodies against YFP and PfGDPD. Both parasites lines were cultured to high parasitemia and the number of parasites/mL were calculated for immunoblot loading purposes. Cultures were treated with saponin and the lysate was clarified into pellets and supernatant fractions, in which the supernatant fraction contains contents from the red cell cytosol and PV. SDS solubilized extracts were loaded with ~1 x 10^7 parasites and protein bands were separated by electrophoresis. Probed with anti-PfGDPD, the expected size of PfGDPD-YFP-CAD fusion protein runs ~123 kDa (50 kDa, native PfGDPD; 25 kDa, YFP; 48 kDa, CAD). We observed PfGDPD-YFP as an intact fusion protein (75 kDa) with similar quantities of protein in both supernatant and pellet fraction. However, in -CAD parasite extract, we detected –CAD fusion protein in the supernatant, indicative of PV localization, at levels lower than the pellet extract (Figure 3-2D). These results indicated that although our attempt to modulate PfGDPD localization using the CAD system was not achieved, we obtained a conditional knockdown of PfGDPD in the PV. The shift in protein distribution led us to question if a phenotypic could be observed in parasites expressing the –CAD protein fusion.

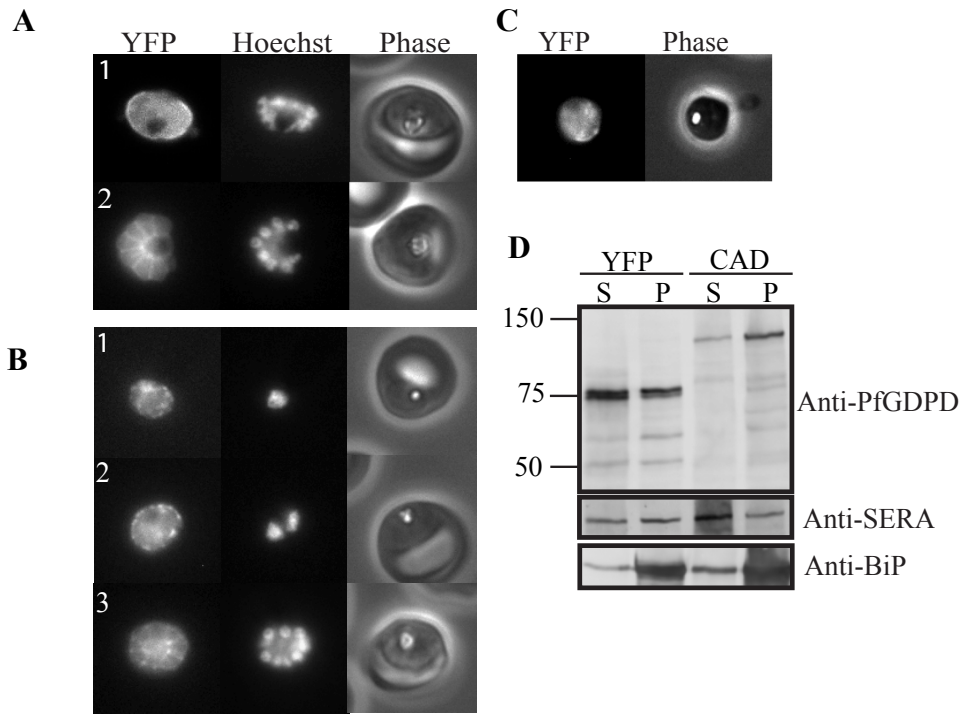

Figure 3-2. Localization of PfGDPD-YFP-CAD in *P. falciparum.* A) YFP fluorescenc of live parasites expressing PfGDPD-YFP-CAD in the presence of anti-aggregation ligand within the parasitophorous vacuole and the parasite cytosol; 1. *Late trophozoite;* 2. *Schizont*. B) YFP fluorescence of PfGDPD-YFP-CAD parasites observed in the absence of anti-aggregation ligand. Fusion proteins are detected a punctate structures within the parasite and diffused within the cytosol;*1. Young trophozoites; 2. Mature trophozoites; 3. Segmenters*. C). Saponin treatment of a trophozoite stage parasite expressing PfGDPD-YFP-CAD fusion protein. YFP fluorescenc is mainly diffused within the parasite cytosol, while punctuts structures are less visible. D) Anti-PfGDPD immunoblot analysis of purified saponin-treated trophozoite stage parasites expressing PfGDPD-YFP (YFP) and PfGDPD-YFP-CAD (CAD). Extracts were separated into supernatant (S) and pellet (P) fractions. An average of ~1 x 10^7 parasites were loaded in each extract. Molecular size markers in kDa are shown on the left. Compartment markers, SERA and BiP, are indicated in the lower panel.

3.4.2 Assessing PfGDPD-YFP-CAD expressing parasites

When observed on Geimsa stained smears, PfGDPD-YFP-CAD parasites showed normal morphology compared to wild-type. To determine if an effect could be observed on parasite proliferation rates, we performed flow cytometry growth assays of PfGDPD-YFP-CAD parasites and parasites expressing PfGDPD-YFP fusion protein in rich complete RPMI medium (CM). The method of flow cytometry analysis enables the quantitation of infected erythrocytes by detecting fluorescently labelled DNA in fixed parasite cultures, which can easily be distinguished from uninfected anuclear erythrocytes [30, 31]. To limit any observed changes in growth rates to presence of CAD, we chose to compare growth rates of parasites expressing the –CAD fusion protein to PfGDPD-YFP parasite lines rather than to 3D7 wild-type. Asynchronous parasites were inoculated at 3 % parasitemia and were monitored for cell cycle progression for 8

days in the CM. Samples aliquots were fixed every 2 days in 0.1 % glutaraldehyde, stained with 400 nM YOYO-1 DNA dye and analyzed by flow cytometry to determine % parasitemia. Cumulative growth rates were calculated and graphed against time and indicated parasites expressing PfGDPD-YFP-CAD grew robustly with identical growth rates to control parasites when cultured in CM (Figure 3-5A). With the lack of a growth phenotype, these results prompted us to critically examine the function PfGDPD in the PV.

The PV is a vacuolar space separating the parasite from the host cell and strategic environment for parasites to scavenge necessary nutrients from the host. The membrane is permeable to metabolites such as choline and serine, which are essential precursors in phospholipid synthesis required for parasite growth and development. Choline can either be taken up by the parasite as free choline or hydrolyzed through sequential steps from choline esters. We hypothesize that PfGDPD localized to the PV, is one of such enzymes that hydrolyzes glycerophosphocholine, generated from the deacylation of lysophosphatidylcholine, which diffuse into the vacuolar space (Figure 3-3). Generated choline is the transported into the parasite via transporter present in the parasite plasma membrane. In addition to choline, serine and ethanolamine are precursors also taken up by the parasite and required in the synthesis of phosphatidylcholine and phosphatidylethanolamine (Figure 3-3). By correlating a function of PfGDPD to phospholipid metabolism in the PV, we sought to develop stringent measures to assess activity of PfGDPD-YFP-CAD in generating choline, in order to detect a distinguishable growth phenotype. The rich culture medium employed in the previous growth assay contains the necessary phospholipid precursors required for successful parasite proliferation that includes a lipid-rich bovine serum albumin (AlbuMAX I) supplement, abundant in fatty acids and phospholipids, and a nutrient source, RPMI, which contains choline, serine, vitamins, amino acids and inorganic salts. Our aim therefore, was to develop a chemically defined media, in which we would force PfGDPD-YFP-CAD parasites to rely on a sole source of exogenous choline. To attain this, we developed a media termed Choline Free Medium (CFM), devoid of choline and serine precursors and a defined source of essential fatty acids.

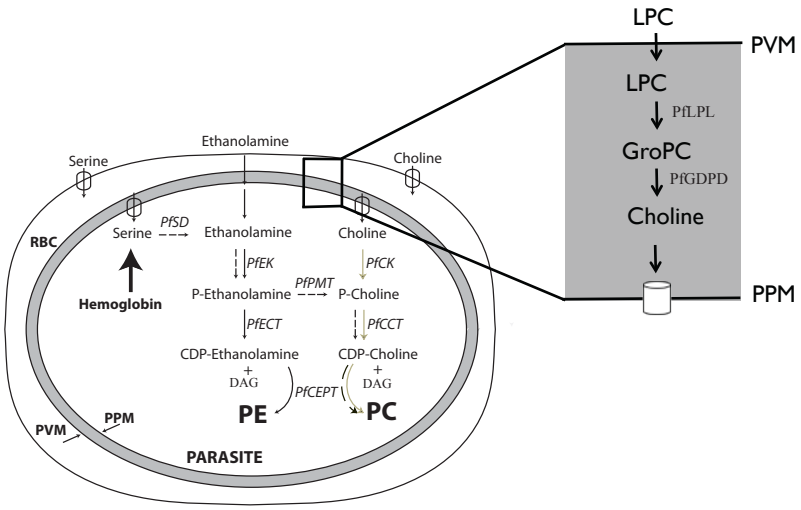

Figure 3-3. Step-wise generation and uptake of phospholipid precursors in *P. falciparum*. Shown in the magnified box insert is the diffusion of lysophosphatidylcholine (LPC) into the parasitophorous vacuole following the sequential hydrolysis to choline, by both lysophospholiase (PfLPL) and glycerophosphodiester phosphodisterase (PfGDPD) activity. Choline is then transporter through choline transporter present in the parasite plasma membrane (PPM). Inside the parasite, choline is incorporated into phosphatidylcholine (PC) through concerted CDP-choline anabolic steps (gold arrows). Serine is taken up from the host through an amino acid permease where it is shuttled into the serine-decarboxylation-phosphoethanolamine methyltransferase pathway (broken arrows), in the synthesis of phosphatidylcholine . Ethanolamine easily diffuses through membranes into the parasite and is incorporated into phosphophatidylethanolamine (PE) through the CDP-ethanolamine pathway (solid arrows). *PfCK*, *P. falciparum* choline kinase; *PfCCT*, *P. falciparum* CTP phosphocholine cytidylyltransferase; *PfEK*, *P. falciparum* ethanolamine kinase; *PfECT*, *P. falciparum* CTP phosphoethanolamine cytidylyltransferase; *PfCEPT*, *P. falciparum* choline/ethanolamine-phosphate transferase; *DAG,* diacylglycerol; *PfPMT*, *P. falciparum* phosphoethanolamine methyltransferase; *PfSD*, serine decarboxylase; *PPM*, parasite plasma membrane; *PVM*, parasitophorous vacuolar membrane; *RBC*, red blood cell.

3.4.3 Constituents of Choline Free Medium

The ingredients used to prepare Choline Free Medium (CFM) were based on standard RPMI 1640 media, which consisted of inorganic salts, amino acids, vitamins, glutathione, glucose and phenol red as the pH indicator (Table 3-1). Except for the absence of choline and serine, the differences in media lay in the number of amino acids used. Of the 20 amino acids present in RPMI medium, only five were included in preparing CFM, namely, cystine, glutamic acid, glutamine, isoleucine and methionine. The importance of these five amino acids has previously been reported to maintain parasite culture in complete RPMI medium [32, 33], unpublished data]. All 5 amino acids were added at concentrations similar to RPMI except isoleucine, which was added at 148 μM (Table 3-1), lower than that found in RPMI, but also validated to sustain parasite growth [34]. As mentioned earlier, AlbuMAX I is the lipid rich growth-promoting component supplied with basal RPMI, containing a variety of lipid species.

However in the context of developing chemically defined CFM, we chose to provide a sole source of essential fatty acids (FFA), palmitic acid ($C_{16:0}$) and oleic acid ($C_{18:1}$), previously established to support parasite growth in culture [6, 9]. We prepared the lipid mix in complex with the fatty acid-free lipid carrier protein, bovine serum albumin (BSA). To summarize, CFM is comprised of source of free fatty acids and all ingredients listed in Table 3-1, which include inorganic salts, vitamins, glutathione, glucose, a pH indicator and five amino acids, cystine, glutamic acid, glutamine, isoleucine and methionine. We tested the sustainability of CFM on parasite growth in CFM to determine if we had successfully deprived parasites of choline. Parasite proliferation was observed using Giemsa stained smears and showed significant growth inhibition over a period of days. This indicated that parasite proliferation rates could indeed be assessed in CFM, and successful growth would only rely on the presence of exogenous supplements i.e choline, serine. During the course of initial validation experiments of supplemented CFM, we discovered the importance of vitamins in the media. Studies have shown that *in vitro* culturing of *P. falciparum* relies significantly on the presence of isoleucine, calcium and D-pantothenate (vitamin B_5) [32, 34-36]. Therefore, our initial media contained all three supplements with D-pantothenate as the sole vitamin. We discovered that D-pantothenate alone could not sustain parasites development as cultures consistently failed to develop past 4 days, even when supplemented with lipid rich AlbuMAX I. However, upon the addition of all vitamins present in RPMI, parasite cultures were consistently maintained. This effect can be attributed to the role vitamins play as precursors to amino acids, of which only five are supplied in CFM. In addition, it is possible that parasites may also rely on scavenging these vitamins from host plasma [37], even though the parasite possesses the machinery to synthesize vitamins such as thiamine (vitamin B_1), pyridoxine (vitamin B_6), folate and its co-factors [37-40].

3.4.4 Growth Rate Analysis in Choline Free Medium

Prior to analyzing the effects of PfGDPD-YFP-CAD fusion on parasite proliferation in CFM, we needed to first establish the growth promoting effects of different CFM supplements with 3D7 wild-type parasites. Supplements used were provided at final concentrations of serine (286 μM), choline (21.4 μM), glycerophosphocholine (GroPC) (240 μM) and 30 μM lysophosphatidylcholine (LPC)/BSA complex. Choline and serine were provided at physiological concentration, while LPC was lower than the concentration reported in human

plasma (120-250 μM) [41-44]. The physiological concentration of GroPC is unclear, therefore, based on the concentration range of choline (10-40 μM), we examined parasite growth rates at GroPC concentrations of 60, 120 and 240 μM and our preliminary results indicated 240 μM GroPC aptly maintained parasite proliferation at levels similar to choline supplementation. As positive controls, we included CM and RPMI supplemented with FFA (FFA/RPMI) and CFM served as a negative control.

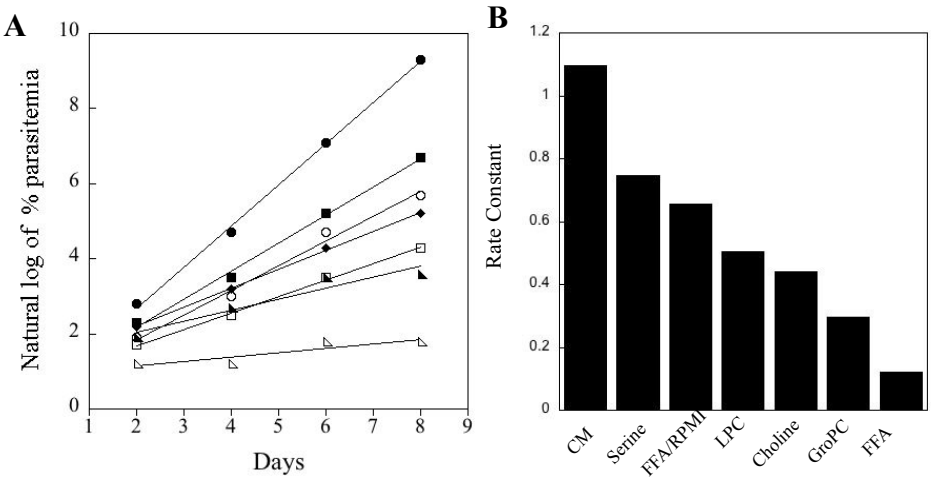

Figure 3-4. Growth analysis of 3D7 in supplemented CFM. Asynchronous 3D7 cultures were monitored for 8 days in supplemented CFM. Sample aliquots were fixed in 0.1 % glutaraldehyde, permeabilized with 0.25% Triton X-100 and stained with 400 nM YOYO-1 DNA fluorescent dye. % Parasitemia was calculated on a flow cytometer. A) Graph shows a linear representation of natural log of % parasiteima against time (Days). Filled circles indicate complete RPMI medium; filled squares indicate serine in CFM; open circles indicate free fatty acids in RPMI; filled diamonds indicate lysophosphatidylcholine in CFM; open squares indicate choline in CFM; filled triangles indicate glycerophosphocholine in CFM; open triangles indicate CFM with no supplements. B) Bar graph represents the rate constants derived from the slope of each growth assay in presented in graph B. Graphs are representative of duplicate experiments.

In preparation for growth analysis, asynchronous 3D7 parasites were washed in CFM to remove traces of choline and AlbuMAX, seeded at ~3 % parasitemia and monitored for cell cycle progression in each CFM supplemented media. After 8 days, we assessed parasite growth using flow cytometry. The rank for each CFM supplement on growth rate is as follows: serine > LPC > choline > GroPC (Figure 3-4). The preferential selectivity of serine-CFM is validated in its incorporation into the synthesis of both phoshpatidylcholine and phosphatidylethanolamine (Figure 3-3). However, it is surprising that growth rates in serine-CFM were higher than control medium FFA/RPMI, since the only difference lie in the number of amino acids present in the medium. The preference for choline ester LPC over un-esterified choline was also interesting to

note. This observation suggests the ability of parasites to scavenge LPC as a source of both fatty acid and choline, setting a rationale in examining the function of lysophospholipases in the pathway of generating choline (Chapter 4). As mentioned earlier, growth rates in GroPC-CFM were similar to choline-CFM. Our data therefore validates the use of CFM in assessing the hydrolytic capabilities of PfGDPD-YFP-CAD parasites in comparison to control PfGDPD-YFP parasites. Asynchronous parasite cultures were monitored in CFM supplemented with GroPC and LPC in the absence of the stabilizing ligand. As a positive control, serine-CFM was included in the assays. The results of our assays were unexpected, as we observed no growth inhibition in either media in parasites expressing the –CAD fusion protein (Figure 3-5), suggesting that the observed shift in PfGDPD-YFP-CAD localization in the PV was insufficient in eliciting a phenotype. We have shown that PfGDPD is also expressed in cytosol. Therefore, it is possible that the lipid molecules diffused through the membranes into the parasite and were subsequently hydrolyzed in the cytosol.

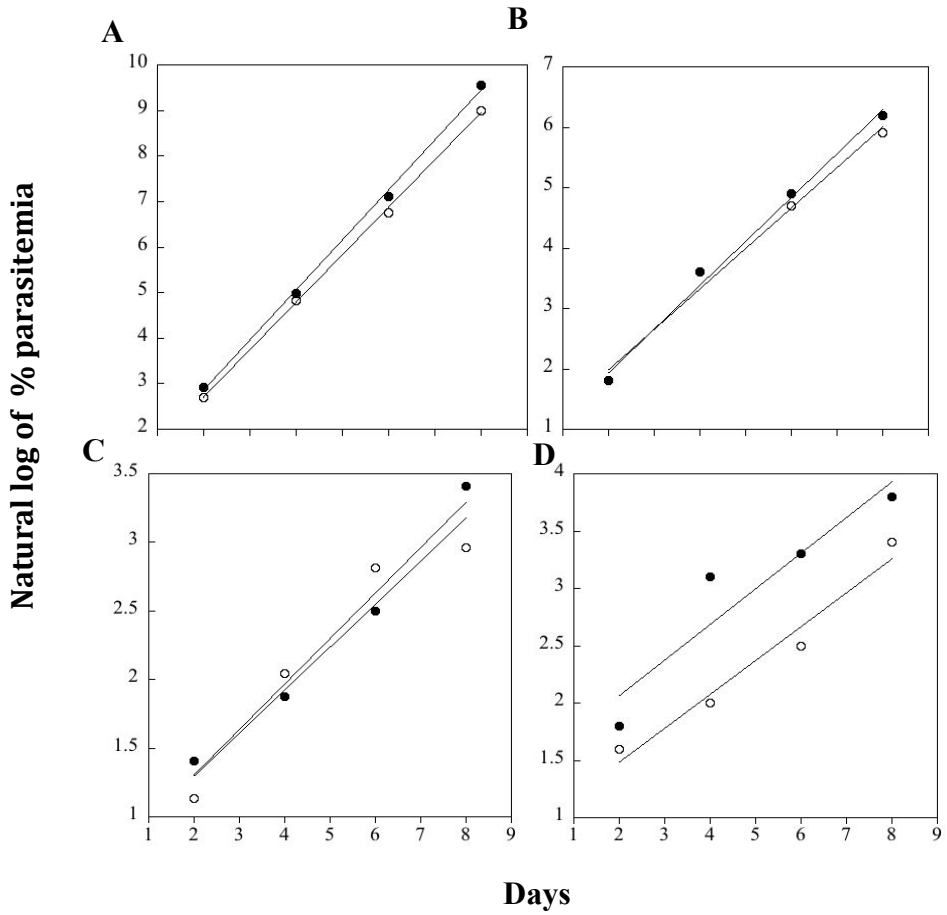

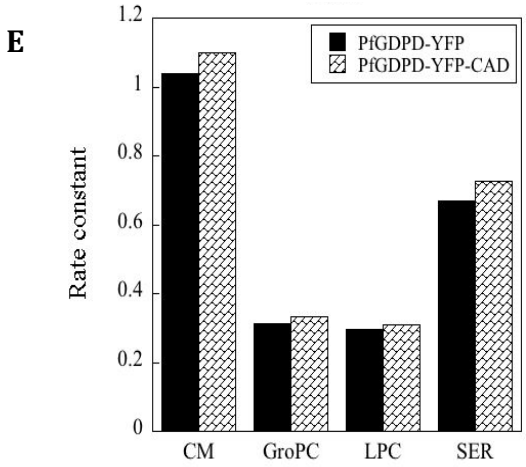

Figure 3-5. Comparative growth analysis of PfGDPD-YFP-CAD and PfGDPD-YFP parasites. Asynchronous cultures were monitored for 8 days and sample aliquots were fixed in 0.1 % glutaraldehyde, permeabilized with 0.25% Triton X-100 and stained with 400 nM YOYO-1 DNA fluorescent dye. % Parasitemia was calculated on a flow cytometer and growth rates are shown as a linear representation of natural log of % parasiteima against time (Days) of parasites cultured in A) Complete RPMI medium, B) Serine in CFM, C) Glycerophosphocholine (GroPC) in CFM and D) Lysophosphatidylcholine in CFM. Filled circles represent PfGDPD-YFP-CAD parasites and open circles represent PfGDPD-YFP parasites. E) Bar graph represents the rate constants derived from the slope of each growth assay in presented in graph A-D. Graphs are representative of duplicate experiments.

3.5 DISCUSSION

PfGDPD gene knockout attempts were unattainable (Chapter 2), which indicate the protein plays a role during blood stages, however, the role is yet to be determined. Our attempt to perturb sub-cellular localization of PfGDPD using a reversible conditional aggregation domain (CAD) system did not allow for protein modulation, as fusion proteins were presents aggregates in the cytosol, which further leaked into the PV. This method has previously been validated [24] and been employed in several studies as a system for the pharmalogical control of insulin secretion in mammalian cells [45], a conditional export control system for protein trafficking in *P. falciparum* [26] and *Toxoplasma gondii* [46]. Recently, the CAD system has proven efficient in perturbing the cellular location of *P. falciparum* hemoglobin degradative enzyme, plasmepsin IX, (Klemba and Dalal, unpublished data). In spite of the inefficiency of CAD, we probed the effect of CAD fusion protein on parasite proliferation. Our assessment of growth rates in rich complete media revealed no growth phenotype, which prompted the development of Choline Free Medium in an attempt to provide a more stringent environment to which we could obtain a growth phenotype. Growth rates were similarly uninhibited probably due to unimpaired function of PfGDPD as aggregates, or diffusion of lipid substrates to the cytosol, where PfGDPD fusion proteins were more abundant than in the PV.

The development of Choline Free Medium (CFM), however, proved to be successful. Several groups have employed the use of RPMI medium free of choline [47, 48], however, we have not only removed un-esterified choline but have also eliminated lysophosphatidylcholine as a source of choline. We achieved this by replacing lipid-rich AlbuMAX supplement with a defined source of free fatty acid (palmitic and oleic acid) used to supplement the basal medium, containing inorganic salts, vitamins, glutathione, glucose, phenol red and five amino acids, cystine, glutamic acid, glutamine, isoleucine and methionine. In the preparation of CFM, we reached a "bump", where parasite culture could not be sustained for more than 4 days. Recent studies had validated the use of minimally required free fatty acid and the five essential amino acids. Therefore, we deduced that the problem lay in the lack of other vitamins, where initially, D-pantothenate (vitamin B_5) was provided as the sole vitamin. The requirement for D-pantothenate in culture medium has been established [36], however, vitamins such as thiamine (vitamin B_1), pyridoxine (vitamin B_6), folate and its co-factors, can be synthesized from the host [37-40]. Though these *de novo* pathways exist, the malaria parasite may complement synthesis by acquiring these nutrients from the host [37, 40]. In addition, the eliminated vitamins also serve as precursors and co-factors in amino acid metabolism in reactions such as the conversion of serine to glycine.

Our analysis of CFM supplementation with serine, choline compounds revealed a higher preference for serine. The robust growth rate of parasites in serine-CFM is due to its incorporation in the synthesis of the two most abundant phospholipids, phosphatidylcholine (PC) via the SDPM pathway and phosphatidylethanolamine (PE) via the CDP-ethanolamine pathway. The precursor can not only be acquired from the host but also through the degradation of host hemoglobin [23]. In contrast, parasites can only utilize choline to synthesize PC, though serine from hemoglobin degradation is also available. Our studies suggest that amino acid acquisition from hemoglobin degradation is insufficient in sustaining parasite growth. We also discovered a preference for the utilization of choline ester, lysophosphatidylcholine (LPC) over free choline. LPC deacylation has been reported to occur at rapid rates upon *Plasmodium* infection [49], and our studies indicated that LPC can also serve as a source of free fatty acids for parasite phospholipid metabolism, which readily provides a substrate for PfGDPD hydrolysis to generate free choline. Though growth rates in glycerophosphocholine-CFM were similar to choline-CFM, the concentration provided was not physiological, but served a purpose in our studies.

Ethanolamine is also a phospholipid precursor that freely enters the cell through passive diffusion. This precursor however, was excluded from our analysis because of the low plasma concentration [50, 51] and its absence in RPMI medium [52], thus rendering it an unphysiological metabolite.

3.6 REFERENCES

1. Jensen, J.B., *Some aspects of serum requirements for continuous cultivation of Plasmodium falciparum.* Bulletin of the World Health Organization, 1979. **57**((Suppl. 1)): p. 27-31.
2. Schuster, F.L., *Cultivation of Plasmodium spp.* Clinical Microbiology Reviews, 2002. **15**(3): p. 355-364.
3. Trager, W. and J. Jensen, *Human malaria parasites in continuous culture.* Science, 1976. **193**(4254): p. 673 - 675.
4. Binh, V.Q., A.J.F. Luty, and P.G. Kremsner, *Differential Effects of Human Serum and Cells on the Growth of Plasmodium falciparum Adapted to Serum-Free in Vitro Culture Conditions.* Am J Trop Med Hyg, 1997. **57**(5): p. 594-600.
5. Cranmer, S.L., et al., *An alternative to serum for cultivation of Plasmodium falciparum in vitro.* Trans R Soc Trop Med Hyg, 1997. **91**(3): p. 363-5.
6. Mitamura, T., et al., *Serum factors governing intraerythrocytic development and cell cycle progression of Plasmodium falciparum.* Parasitology International, 2000. **49**(3): p. 219-229.
7. Wene, J.D., W.E. Connor, and L. DenBesten, *The development of essential fatty acid deficiency in healthy men fed fat-free diets intravenously and orally.* The Journal of Clinical Investigation, 1975. **56**(1): p. 127-134.
8. Mi-ichi, F., S. Kano, and T. Mitamura, *Oleic acid is indispensable for intraerythrocytic proliferation of Plasmodium falciparum.* Parasitology, 2007. **134**(12): p. 1671-1677.
9. Mi-ichi, F., K. Kita, and T. Mitamura, *Intraerythrocytic Plasmodium falciparum utilize a broad range of serum-derived fatty acids with limited modification for their growth.* Parasitology, 2006. **133**(04): p. 399-410.
10. Asahi, H., et al., *Investigating serum factors promoting erythrocytic growth of Plasmodium falciparum.* Experimental Parasitology, 2005. **109**(1): p. 7-15.
11. Asahi, H., et al., *Plasmodium falciparum: Differing effects of non-esterified fatty acids and phospholipids on intraerythrocytic growth in serum-free medium.* Experimental Parasitology, 2011. **127**(3): p. 708-713.
12. Vial, H.J. and M.L. Ancelin, *Malarial Lipids: an overview.* Subcell. Biochem, 1992. **18**: p. 259-306.

13. Waller, R.F., et al., *Nuclear-encoded proteins target to the plastid in Toxoplasma gondii and Plasmodium falciparum.* Proceedings of the National Academy of Sciences, 1998. **95**(21): p. 12352-12357.
14. Surolia, N. and A. Surolia, *Triclosan offers protection against blood stages of malaria by inhibiting enoyl-ACP reductase of Plasmodium falciparum.* Nat Med, 2001. **7**(2): p. 167-73.
15. Vial, H.J., Thuet, M. J, Broussal, J. L, Philippot ,J. R., *Phospholipid biosynthesis by Plasmodium knowlesi-infected erythrocytes: the incorporation of phospohlipid precursors and the identification of previously undetected metabolic pathways.* journal of parasitology, 1982. **68**(3): p. 379-391.
16. Krishnegowda, G. and D.C. Gowda, *Intraerythrocytic Plasmodium falciparum incorporates extraneous fatty acids to its lipids without any structural modification.* Molecular and Biochemical Parasitology, 2003. **132**(1): p. 55-58.
17. Vaughan, A.M., et al., *Type II fatty acid synthesis is essential only for malaria parasite late liver stage development.* Cellular Microbiology, 2009. **11**(3): p. 506-520.
18. Yu, M., et al., *The Fatty Acid Biosynthesis Enzyme FabI Plays a Key Role in the Development of Liver-Stage Malarial Parasites.* Cell Host & Microbe, 2008. **4**(6): p. 567-578.
19. Kirk, K., *Membrane Transport in the Malaria-Infected Erythrocyte.* Physiological Reviews, 2001. **81**(2): p. 495-537.
20. Biagini, G.A., et al., *Characterization of the choline carrier of Plasmodium falciparum: a route for the selective delivery of novel antimalarial drugs.* Blood, 2004. **104**(10): p. 3372-7.
21. Lehane, A.M., et al., *Choline uptake into the malaria parasite is energized by the membrane potential.* Biochem Biophys Res Commun, 2004. **320**(2): p. 311-317.
22. Francis, S.E., R. Banerjee, and D.E. Goldberg, *Biosynthesis and Maturation of the Malaria Aspartic Hemoglobinases Plasmepsins I and II.* Journal of Biological Chemistry, 1997. **272**(23): p. 14961-14968.
23. Goldberg, D.E., *Hemoglobin degradation.* Current Topics in Microbiology and Immunology, 2005. **295**: p. 275-91.

24. Rollins, C.T., et al., *A ligand-reversible dimerization system for controlling protein–protein interactions.* Proceedings of the National Academy of Sciences, 2000. **97**(13): p. 7096-7101.
25. Lambros C, V.J., *Synchronization of Plasmodium falciparum erythrocytic stages in culture.* Journal of parasitology, 1979. **65**(3): p. 418-420.
26. Saridaki, T., et al., *A conditional export system provides new insights into protein export in Plasmodium falciparum-infected erythrocytes.* Cellular Microbiology, 2008. **10**(12): p. 2483-2495.
27. Ribaut, C., et al., *Concentration and purification by magnetic separation of the erythrocytic stages of all human Plasmodium species.* Malaria Journal, 2008. **7**(1): p. 45.
28. Kay, J.E., *Structure-function relationships in the FK506-binding protein (FKBP) family of peptidylprolyl cis-trans isomerases.* Biochemistry Journal, 1996. **314 (Pt 2)**: p. 361-85.
29. Schreiber, S., *Chemistry and biology of the immunophilins and their immunosuppressive ligands.* Science, 1991. **251**(4991): p. 283-287.
30. Jiménez-Díaz, M.B., et al., *Improvement of detection specificity of Plasmodium-infected murine erythrocytes by flow cytometry using autofluorescence and YOYO-1.* Cytometry Part A, 2005. **67A**(1): p. 27-36.
31. Janse, C.J. and P.H. Van Vianen, *Flow cytometry in malaria detection.* Methods in Cell Biology, 1994. **42 Pt B**: p. 295-318.
32. Divo AA, G.T., Davis NL, Jensen JB., *Nutritional requirements of Plasmodium falciparum in culture. I. Exogenously supplied dialyzable components necessary for continuous growth.* Journal of Protozoology, 1985. **32**(1): p. 59-64.
33. Liu, J., et al., *The role of Plasmodium falciparum food vacuole plasmepsins.* Journal of Biological Chemistry, 2005. **280**(2): p. 1432-7.
34. Liu, J., et al., *Plasmodium falciparum ensures its amino acid supply with multiple acquisition pathways and redundant proteolytic enzyme systems.* Proceedings of the National Academy of Sciences, 2006. **103**(23): p. 8840-8845.
35. Saliba, K.J., I. Ferru, and K. Kirk, *Provitamin B5 (Pantothenol) Inhibits Growth of the Intraerythrocytic Malaria Parasite.* Antimicrobial Agents and Chemotherapy, 2005. **49**(2): p. 632-637.

36. Brackett, S., E. Waletzky, and M. Baker, *The relation between pantothenic acid and Plasmodium gallinaceum infections in the chicken and the antimalarial activity of analogues of pantothenic acid.* journal of parasitology, 1946. **32**(5): p. 453-62.
37. Wrenger C, E.M., Müller IB, Laun NP, Begley TP, Walter RD., *Vitamin B1 de novo synthesis in the human malaria parasite Plasmodium falciparum depends on external provision of 4-amino-5-hydroxymethyl-2-methylpyrimidine.* Biological Chemistry, 2006. **387**(1): p. 41-51.
38. Gengenbacher, M., et al., *Vitamin B6 biosynthesis by the malaria parasite Plasmodium falciparum: biochemical and structural insights.* J Biol Chem, 2006. **281**(6): p. 3633-41.
39. Ferone, R., *Folate metabolism in malaria.* Bull World Health Organ, 1977. **55**(2-3): p. 291-8.
40. Wang, P., et al., *Utilization of exogenous folate in the human malaria parasite Plasmodium falciparum and its critical role in antifolate drug synergy.* Molecular Microbiology, 1999. **32**(6): p. 1254-1262.
41. Psychogios, N., et al., *The Human Serum Metabolome.* PLoS ONE, 2011. **6**(2): p. e16957.
42. Aoki, J., et al., *Serum Lysophosphatidic Acid Is Produced through Diverse Phospholipase Pathways.* Journal of Biological Chemistry, 2002. **277**(50): p. 48737-48744.
43. Croset, M., Brossard, N., Polette, A., and Lagarde, M., *Characterization of plasma unsaturated lysophosphatidylcholines in human and rat.* Biochemistry Journal, 2000. **345**: p. 61-67.
44. Okita, M., et al., *Elevated levels and altered fatty acid composition of plasma lysophosphatidlycholine(lysoPC) in ovarian cancer patients.* International Journal of Cancer, 1997. **71**(1): p. 31-34.
45. Rivera, V.M., et al., *Regulation of protein secretion through controlled aggregation in the endoplasmic reticulum.* Science, 2000. **287**(5454): p. 826-30.
46. DeRocher, A., et al., *Dissection of brefeldin A-sensitive and -insensitive steps in apicoplast protein targeting.* Journal of Cell Science, 2005. **118**(3): p. 565-574.
47. Le Roch, K.G., et al., *A systematic approach to understand the mechanism of action of the bisthiazolium compound T4 on the human malaria parasite, Plasmodium falciparum.* BMC Genomics, 2008. **9**: p. 513.

48. Ahiboh H, D.A., Yapi FH, Edjeme-Aké A, Hauhouot-Attoungbré ML, Yayo ED, Monnet D, *Uptake and kinetic properties of choline and ethanolamine in Plasmodium falciparum.* Tropical Journal of Pharmaceutical Research, 2008. **7**: p. 953-959.
49. Zidovetzki, R., et al., *Inhibition of Plasmodium falciparum lysophospholipase by anti-malarial drugs and sulphydryl reagents.* Parasitology, 1994. **108 (Pt 3)**: p. 249-55.
50. Perry, T.L., S. Hansen, and J. Kennedy, *CSF amino acids and plasma--CSF amino acid ratios in adults.* Journal of Neurochemistry 1975. **24**(3): p. 587-9.
51. Kruse, T., H. Reiber, and V. Neuhoff, *Amino acid transport across the human blood-CSF barrier. An evaluation graph for amino acid concentrations in cerebrospinal fluid.* Journal of the Neurological Sciences, 1985. **70**(2): p. 129-38.
52. Jensen, J.B. and W. Trager, *Plasmodium falciparum in culture: use of outdated erthrocytes and description of the candle jar method.* Journal of Parasitology, 1977. **63**(5): p. 883-6.

Chapter 4

Examining the source of glycerophosphocholine production in *P. falciparum*

4.1 ABSTRACT

Phosphatidylcholine is the most abundant lipid required for cellular membrane synthesis in *Plasmodium falciparum*. Necessary precursors for lipid synthesis i.e. choline, can either be scavenged from the host milieu as free choline or from choline esters i.e. lysophosphatidylcholine or glycerophosphocholine, which are derived from the degradation of phosphatidylcholine. The parasitophorous vacuole is an ideal environment for choline scavenging, in which the semi-permeable membrane allows the diffusion of choline into the vacuolar space that separates the parasite from the extracellular red cell cytosol. Choline is then actively taken up by the parasite via transporters present in the parasite plasma membrane. We have previously characterized a *P. falciparum* glycerophosphodiester phosphodiesterase localized to the parasitophorous vacuole, involved in releasing choline by hydrolyzing glycerophosphocholine, a substrate generated downstream in phosphatidylcholine degradation pathway. As a first step in developing this pathway in *P. falciparum*, we identified a lysophospholipase (PfLPL1) involved in the intermediary steps of phosphatidylcholine hydrolysis generating glycerophosphocholine as a product. Fluorescent tagging of the endogenous copy revealed PfLPL1 around the parasite periphery within the parasitophorous vacuole and diffused within the parasite cytosol. Localization to the parasitophorous vacuole was confirmed by saponin treatment, which resulted in a loss of rim of fluorescence. To characterize the role of PfLPL1 in erythrocytic parasites, PfLPL1 gene was disrupted and generated knockout parasites were cloned and further analyzed. Gene disruption was confirmed by Southern and PCR analysis. Compared to wild-type parasites, PfLPL1 knockout parasite clones developed normally, maintained the same morphology and multiplication rates in standard culture medium. To observe a phenotype, the growth rate PfLPL1 knockout parasites were analyzed by forcing parasites to rely on hydrolyzing the choline ester substrate, lysophosphatidylcholine as a sole source of choline. Growth analysis indicated no growth inhibition in two of the knockout clones and significant growth impairment in one clonal line, which was due to clonal variation and not an effect of PfLPL1 knockout. Our results indicate PfLPL1 does not contribute to parasite fitness during the erythrocytic stages of parasite replication.

4.2 INTRODUCTION

Intra-erythrocytic replication of *Plasmodium falciparum* is accompanied by a drastic increase in phosphatidylcholine required for membrane biogenesis. Synthesis of phosphatidylcholine requires the precursor choline, which is actively scavenged from the host plasma either as free choline or in an esterified form i.e lysophosphatidylcholine and glycerophosphocholine, derived from the stepwise or concerted removal of fatty acids from phospholipids (Figure 4-1).

Glycerophosphocholine is a major intracellular metabolite derived directly from the hydrolysis of lysophosphatidylcholine (LPC) by lysophospholipases (LPL). Lysophosphatidylcholine represents between 5-20 % of total PL in plasma, found bound in complex with serum albumin [1] [2] and lipoproteins [3-6]. The structure of LPC is comprised of a glycerol backbone with a long hydrophobic acyl chain esterified at the *sn*-1 position and a large hydrophilic polar head group. Due to their amphipathic structure, they possess cytotoxic effects on membranes at high concentrations and as a result, are tightly regulated [7]. Lysophospholipases (EC number 3.1.1.5) are one way in which to regulate the availability of LPC. These enzymes have also been implicated in the attenuation of signal transduction process and host mediated destruction of parasites [8-10]. Lysophospholipases have been characterized in both eukaryotes and prokaryotes [2, 11-13], generally classified as either large enzymes (60 kDa) that exhibit hydrolytic and transacylase activities or in the form of small enzymes of molecular weights between 16.5 and 28 kDa, possessing singular hydrolytic activity [14]. In *Plasmodium* studies have detected LPL activity in infected erythrocytes [15, 16]

We have previously characterized a *P. falciparum* enzyme, glycerophosphodiester phosphodiesterase (PfGDPD) that hydrolyzes glycerophosphocholine, available as one form of choline ester. Genetic studies indicated PfGDPD is important during asexual intrra-erythrocytic replication and abundantly expressed in the parasite cytosol and parasitophorous vacuole. To build a pathway for choline acquisition within the parasite through the degradation of host phospholipid, we have identified a *P. falciparum* lysophospholipase (PfLPL1) that generates the alternative choline ester, lysophosphatidylcholine, and report the genetic characterization of PfLPL1 and the effects of gene knockout on parasite growth and development. Of the nine putative lysophospholipases within the *Plasmodium* genome database (PlamoDB.org), PfLPL1 shared similar distribution with PfGDPD, expressed within the parasite cytosol and

parasitophorous vacuole, thus providing a concerted mechanism in generating choline as precursor for parasite phospholipid synthesis.

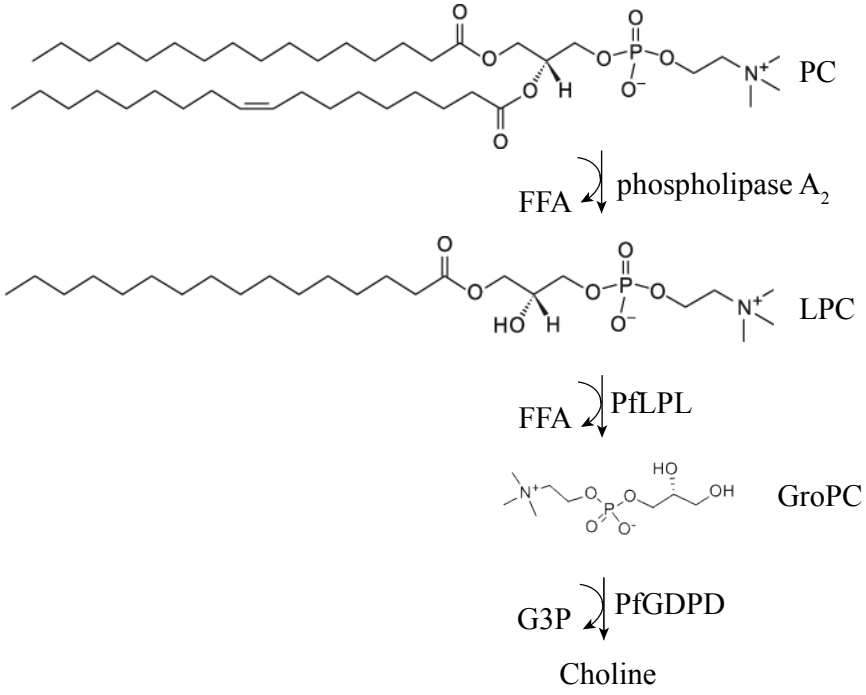

Figure 4-1: Pathway for phosphatidylcholine hydrolysis. Phosphatidylcholine (PC) is hydrolyzed by phospholipase A_2 to generate lysophosphatidylcholine (LPC) and oleic acid as the free fatty acid. Glycerophosphocholine (GroPC) and palmitic acid are generated from the hydrolysis of lysophosphatidylcholine by lysophospholipase (PfLPL). *P. falciparum* glycerophosphodiester phosphodiesterase (PfGDPD) catalyzes the hydrolysis of glycerophosphocholineto yield choline and glycerol-3-phosphate (G-3-P)

4.3 EXPERIMENTAL PROCEDURES

4.3.1 Generation of Constructs

P. falciparum lysophospholipase (gene ID: PF14_0738) was expressed as C-terminal YFP fusion tag from 3D7 genomic DNA by amplifying a 1-kb fragment at the 3' end excluding the stop codon. Products were digested and cloned into XhoI/AvrII restriction sites of pPM2CIT2 vector to yield PfLPL1-YFP. Knockout (KO) constructs were generated using a double crossover disruption plasmid by PCR amplifying two PfLPL1 sequences between bases 8-516 at the 5' end and bases 605-1116 at the 3' end. The 5' and 3' fragments were digested and cloned respectively into SacII/SpeI and MfeI/NcoI sites, positioned to flank human *dihydrofolate*

reductase (h*dhfr*) cassette in pCC1 vector. Primer sequences used in cloning are listed below in Table 4-1.

Table 4-1. PCR primers for vector construction and knockout analysis. [a] Primers used for Southern analysis

Description	Direction	Sequence	Restriction site
YFP Fusion	Forward	GCACGCTCGAGCTTTTTGTAACAAAGATGGTTTACG	XhoI
	Reverse	GCACGCCTAGGTTTCTTTTCTTTTTCTTTTTGCTTCTT	AvrII
KO Disruption			
[a] 5' fragment	Forward	GTACGCCGCGGAAAGTAATATTATTAATGATGAGAATAC	SacII
	Reverse	GTACGACTAGTATTTGCACCCATAGAAAAACCTGC	SpeI
3' fragment	Forward	GTACGCAATTGGAATGTTTTCTATTAAGGCAGTTGG	MfeI
	Reverse	GTACGCCATGGTCATTTCTTTTCTTTTTCTTTTTGCTTC	NcoI
KO Confirmation			
P1	Forward	TGCAAATATAATGTTAAGAGCTATGG	
P2	Reverse	GATAGTGACACAAGTCCTTTTATAC	
P3	Forward	TATATATATTAATATATTTACCATGACAG	
P4	Reverse	TATATTATTTAAAATGTTAATTCTATGATG	

4.3.2 Parasite Culture

All tissue culture experiments were performed under aseptic conditions in a biosafety cabinet. Unless stated otherwise, parasite cultures were maintained in a 5 % CO_2 incubator, cultured in human O^+ erythrocytes (Interstate Blood Bank) at 2% hematocrit in complete RPMI 1640 (CM) medium supplemented with 27 mM sodium bicarbonate, 11 mM glucose, 0.37 mM hypoxanthine, 10 μg/mL gentamycin and 5 g/L AlbuMAX I (Invitrogen) [17]. Synchronous *P. falciparum* 3D7 ring stage parasites were transfected with 75-100 μg of PfLPL1-YFP and KO plasmid using low voltage electroporation conditions. Positive selection with 10 nM WR99210 drug (Jacobus Pharmaceuticals) began 48 hours after transfection. To allow plasmid integration, parasites emerging after 18-24 days were cycled whereby WR99210 was removed from media for 21 days and reapplied until resistant parasites appeared. Parasites expressing PfLPL1-YFP were observed after 2 cycles. KO parasites were cycled three times after negative selection with 5-fluorocytosine. Generated parasite lines were cultured and maintained in human O^+ erythrocytes (Interstate Blood Bank) at 2% hematocrit in complete RPMI 1640 medium supplemented with 27 mM sodium bicarbonate, 11 mM glucose, 0.37 mM hypoxanthine, 10 mg/ml gentamicin and 5 g/litre AlbuMAX I (Invitrogen).

To generate parasite clones expressing PfLPL1-YFP and PfLPL1 KO, parasitemia of each line was determined by Giemsa staining and depending on the parasitemia, cultures were

diluted between 2-4 %. The cultures were further diluted 10^4-fold and inoculated into mixture of 24 mL media and 1mL 50 % red blood cell according to the formula below:

volume (μL) of 10^4-fold diluted culture = [25000/(80 x % parasitemia)] x 2.5

Diluted cultures were mixed thoroughly and 200 μL of culture was aliquoted into round bottom 96 well plates. Media was changed every two days and resuspended in ~ 170 μL of fresh media. Every 6 days, parasites were split 1:1 with media containing fresh red blood cells at 2 % hematocrit. Individual clones appeared after 10 days and were identified by Giemsa stained smears. PfLPL1-YFP clone C6 and PfLPL1 KO clones F8, B11, E7, were generated and used in this study.

To confirm the presence of PfLPL1 in the parasitophorous vacuole, parasites were cultured to parasitemia between 5-7 %. A 1 mL culture aliquot was spun at 863 x g for 3 min and the pellet was re-suspended in 40 μL saponin (1 mg/mL) prepared in RPMI 1640 complete media. The culture was incubated for 10 min at room temperature (RT) then diluted with 1 mL media and spun at 1940 x g for 10 min, RT. Pellet was washed twice in 1 mL media and taken up in 200 μL of media into 96 well plate flat bottom plate and incubated at 37 ^{o}C prior to imaging.

4.3.3 Fluorescence Microscopy

Live images of parasites expressing PfLPL-YFP were collected by incubating 40 μL of culture with 1 μL 5 μM nuclear stain Hoechst 33342 for 5 min at 37 ^{o}C. Cells were mounted under a coverslip and images were collected on a Zeiss AxioImager M1 equipped with an MRm Axiocam digital camera using a 100x/1.4NA objective lens. Images were converted to TIFF files and contrast was adjusted using Adobe Photoshop CS4.

4.3.4 Southern Blot Analysis

To obtain parasites for genomic DNA (gDNA) extraction, 24 mL culture of PfLPL1 knockout clones and 3D7 wild-type parasites, were washed in 40 mL PBS, centrifuged for 3 min at 863 x g. Collected ellet cultures were treated with 40 mL cold 0.1 % saponin in PBS and mixed by inverting the tube several times. The culture was incubated for 10 min on ice and centrifuged at 1940 x g, 10 min at 4 ^{o}C. Parasite pellet was washed in cold PBS at 1940 x g, 10 min at 4 ^{o}C and stored at -80 ^{o}C. To confirm gene knockout, gDNA was extracted from PfLPL1 KO clones using the QiaAmp DNA blood mini kit (Qiagen). 50 μL of gDNA (2 μg) and KO

plasmid (1 μg) were digested in a 100 μL reaction containing 10 μL10x NEB Buffer 4, 10 μL 10x bovine serum albumin (BSA), 1 μL EcoRI and 4 μL ClaI restriction enzymes and 25 μL MilliQ-H_20. Reaction was incubated for 3 hrs at 37 ºC and purified using the QiaAmp nucleotide removal kit kit (Qiagen) in 30 μL elution buffer. DNA fragments were resolved on a 0.6 % agarose gel (200 mL) without ethidium bromide, run overnight at 30 volts for ~17 hours. 1kb markers were loaded in an edge lane and after electrophoresis, the marker lane was cut off, stained for 20 minutes in 0.5 μg/mL ethidium bromide and photographed with a fluorescent ruler. Following separation, DNA fragments were depurinated in 0.25 M HCl for 15 min, denatured in 0.5 M NaOH, 1.5 M NaCl for 30 min and neutralized in 1 M Tris-HCl pH 8, 1.5 M NaCl for 30 min and rinsed in water after each step. DNA was transferred to an Immobilon Nytran$^+$ membrane (Millipore) using a Turboblotter for a minimum of 3 hrs in 20x SSC buffer containing 3.0 M NaCl and 0.3 M sodium citrate. Membrane was blocked using 20 μL AlkPhos Direct pre-hybridization reagent in a hybridization oven tube rotating for 1 hr at 55 ºC. After blocking, the PfLPL1 locus was detected by incubating the membrane overnight at 55 ºC with the probe generated from the 5' amplification of the gene (Table 4-1). 100 ng of probe was labelled using the AlkPhos Direct protocol and labelling kit (GE Biosciences) and signal was detected by autoradiography.

4.3.5 PCR Analysis

PfLPL1 KO parent and clonal lines were analyzed by PCR to confirm gene disruption using 4 different primers (Table 4-1). gDNA from each PfLPL1 KO parent and clones (F8, B11 and E7) and wild-type 3D7, were extracted using the QiaAmp DNA blood mini kit (Qiagen). A volume of 13.3 μL of gDNA (88 ng) was used in the PCR reaction containing 2 μL 10x buffer, 2 μL 10 μM primers, 0.5 μL 10 mM deoxynucleotide Triphosphates (dNTPs) and 0.2 μL Taq polymerase. Reaction conditions included 30 cycles with a denaturation temperature at 95 ^{o}C an annealing temperature of 50 ^{o}C and a 2 min extension time at 55 ^{o}C.

4.3.6 Preparation of Lipid and Media

AlbuMAX free RPMI 1640 medium, simply termed RPMI, was used for growth analysis, which was prepared using commercially available RPMI 1640 medium (Invitrogen)

supplemented with 2.25 g 27 mM sodium bicarbonate, 2 g 11 mM glucose, 3.6 mL 0.37 mM hypoxanthine and 200 μL 500 x gentamicin. RPMI was prepared as a 500 mL, 2x stock, and sterile filtered though a 0.22 μm bottle top filter (Corning). Working media solution was diluted to 1x and supplemented with lysophosphatidylcholine (LPC) (1-palmitoyl-2-hydroxy-*sn*-glycero-3-phosphocholine and 1-oleoyl-2-hydroxy-*sn*-glycero-3-phosphocholine) purchased from Sigma. LPC pairs were dissolved in ethanol at 15 mM concentration and stored at -20 ^{o}C until use. Fatty acid free bovine serum albumin powder (ffBSA- Sigma A7511) was dissolved in sterile Dulbecco's-PBS (Sigma) at a concentration of 40 mg/ml. LPC was prepared by drying 48 μL of each LPC under a stream of nitrogen gas. Dried lipid precipitates were reconstituted by adding addition 1.2 ml ffBSA stock solution and sonicated at power level 3 (5 x 12s pulses). Each BSA complex mixture was diluted 5-fold by combining 1.1 mL of BSA mix to 4.4 mL of 1x RPMI consisting of 2.75 mL 2x RPMI and 1.65 mL sterile water. The mixture was filtered through a small .22 μm syringe filter into a 15 mL conical tube and 5 mLs of sterilized mixture was diluted in 15 mL 1 x RPMI to obtain a medium with a 2 mg/mL concentration of ffBSA and 30 μM LPC.

4.3.7 Parasite Growth Rate Analysis

To prepare parasites for growth analysis, PfLPL1 KO clones were washed 3 times RPMI for 3 min at 863 x g to remove traces of AlbuMAX I present in complete RPMI1640 medium (CM) and maintained in human O^{+} erythrocytes previously washed in RPMI. After washing, 1 mL cultures were aliquoted into sterile 50 mL Eppendorf tubes, spun for 30 sec in a mini centrifuge and re-suspended in 1mL RPMI. Parasite cultures were maintained in a 24-well plate placed in a cake jar and gassed with 5 % O_2, 5 % CO_2 and 90 % N_2 mixture. Growth assays were monitored in both CM and RPMI containing LPC. Three independent asynchronous starter cultures were inoculated at ~3% parasitemia, determined by Giemsa stained smears and maintained below 10 % by sub-culturing every two days. Parasites were grown for a total of 8 days and sample aliquots were taken every two days and analyzed for parasitemia by flow cytometery.

4.3.8 Flow Cytometry

100 μL of *P. falciparum* cultures were fixed in 100 μL 0.1% glutaraldehyde (Sigma) and stored at 4 ^{o}C until use. Fixed samples were washed in 200 μL phosphate buffered saline (PBS) and permeabilized in 200 μL 0.25% Triton X-100 for 5 min at room temperature. Cultures were washed again in 200 μL PBS stained with 100 μL 400 nM YOYO-1 (Molecular Probes) in PBS for at least 30 minutes and diluted 40-fold in PBS for flow cytometry analysis on a BD mini Accuri C6 flow cytometer. A total of 3 x 10^4 erythrocyte counts were taken for each sample. The FL1 detector records the green fluorescence of YOYO-1 when bound to dsDNA at an emission of 530 nm, distinguishing infected from uninfected erythrocytes. Data was exported and analyzed using an Excel spreadsheet. The total number of parasites (parasitemia x cumulative dilution factor) was converted to the natural log (y), graphed against time (x) and fitted to the linear equation using KaleidaGraph 4.1 software (Synergy Software). Erythrocyte background values were substracted from calculated % parasitemia.

4.3.9 Statistical Analysis

Two-tailed Student t-tests were employed to analyze the significance of growth rates of clones compared to wild-type. T- test was performed under the different variance assumption. *p* values are listed in Table 4-2.

4.4 RESULTS

4.4.1 Lysophospholipase PfLPL1 in *P. falciparum*

Pf14_0738 is a 1.1 kb single-exon gene on chromosome 14 that encodes a 377 amino acid homologue of lysophospholipase, termed PfLPL1. A search for conserved domains indicate that PfLPL1 belongs to a multi-domain family called the *Plasmodium* subtelomeric family (PST-A), where the genes are located in the subtelomeric regions of the chromosome. They represent an evolutionary diverse family of genes in phylum Apicomplexa (*Plasmodium spp, Toxoplasma* and Theileria), pathogenic *fungi (Candida), Trypanosomatids* and diplomonads i.e. *Giardia.* Homologues of PfLPL1 were found in other *Plasmodium* species including *P. vivax, P. chabaudi, P. berghei* and *P. yeolli* as well as in other apicomplexans, *Babesia bovis* and *Neospora caninum* and as hypothetical proteins in *Toxoplams gondii* and *Theileria parva*. Analysis of the first 70 residues of PfLPL1 using the signal peptide prediction algorithm SignalP

4.0 indicates no signal peptide sequence or transmembrane domains. All members of the *P. falciparum* lysophospholipase family lack signal peptides.

4.4.2 Cellular distribution of PfLPL1

The result of a text search for lysophospholipases in the *Plasmodium* database, PlasmoDB.org, shows a total of nine putative lysophospholipases in *P. falciparum* 3D7 strain. To determine the protein distribution within the parasite, all nine encoding genes were tagged with yellow fluorescent protein (YFP) at the C-terminus. Protein expression reflected a variety of fluorescent levels in different cellular compartments. However, one gene product, PfLPL1, was highly expressed and had similar localization to *P. falciparum* glycerophosphodiester phosphodiesterase PfGDPD. Generated clones showed PfLPL1-YFP expression in the parasite cytosol and parasitophorous vacuole (PV) (Figure 4-2A). Our interest in this protein serves to build a mechanism for generating precursors for parasite phospholipid (PL) synthesis (Figure 4-1). The localization of the enzymes to the parasitophorous vacuole (PV) serves as a strategic environment to scavenge lipids from the host to release choline, which can then be shuttled into the parasite via choline transporters present in the plasma membrane. To confirm the presence of PfLPL1 in the PV, parasites were treated with 40 μL 1mg/mL saponin, a detergent that permeabilizes both the red cell membrane and PV membrane. After centrifugation, the parasite pellet was resuspended in media and PfLPL1 fluorescence was assessed under an epifluorescence microscope. PV localization was confirmed as shown by the loss of the distinct PV rim fluorescence (Figure 4-2B)

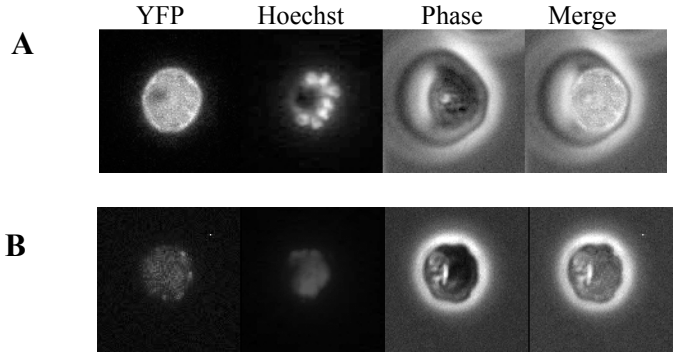

Figure 4-2. Localization of PfLPL1 in *P. falciparum.* A) Fluorescence microscopy of live late stage trophozoite parasites (clone C6) expressing PfLPL1-YFP in the parasitophorous vacuole and diffused in the cytosol. B) Saponin treated trophozoite stage parasites showing cytosolic fluorescence with a concurrent loss of rim fluorescence within the parasitophorous vacuole.

4.4.3 Disruption of PfLPL1 Gene

To assess the importance of PfLPL1 in parasite development, PfLPL1 gene was targeted for disruption using the double crossover technique illustrated in Figure 4-3A. After 3 cycles on and off negative drug selection pressure, resistant parasites emerged and were cloned as described in 4.3.2: Parasite Culture, to generate clones E7, F8 and B11. Knockout parasite clones were gentoyped by Southern blot and PCR analysis. Genomic DNA from KO clones and 3D7 wild-type (WT) parasites were isolated and digested with restriction enzymes, EcoRI and ClaI. Probes to detect PfLPL1 locus were generated using primers specific to the 5' end of the gene. Separation and detection of PfLPL1 gene locus would result in a 1.9 kb size, representing an intact gene, a 4.0 kb size indicative of KO plasmid integration into the chromosome and the presence of the KO plasmid within the parasite at 4.4 kb (Figure 4-3A). Results from Southern analysis confirm disruption of PfLPL1 gene, which is indicated with the presence of a 4 kb band in the KO parasite clones and the absence of the WT intact copy (Figure 4-3B). The KO plasmid is also not detected in the clones, confirming its integration into the chromosome. However, a band of 1.8 kb was detected in both the WT and PfLPL1 clones, which we identified as a PF14_0737, present on the same chromosome as the PfLPL1 encoding gene. PF14_0737 encodes a lysophospholipase and is located adjacent to PfLPL1 encoding gene (PF14_0738) on chromosome 14. Analysis of PF14_0737 gene revealed the presence of ClaI and EcoRI restriction sties that would result in a 1.8k kb fragment, which we observed in our analysis.

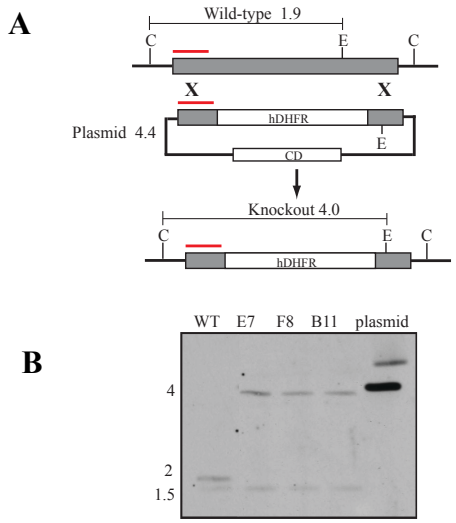

Figure 4-3. Generation of PfLPL1 knockout parasite clonal lines E7, F8 and B11. A) Schematic diagram showing the double crossover homologous recombination technique of PfLPL1 knockout plasmid into the *P. falciparum* genome. The gray box represents the wild-type gene coding for PfLPL1, the red line indicates the site of probe hybridization. The sites of the restriction enzymes, EcoRI (E) and ClaI (C) and the expected size of bands after digestion are indicated. hDHFR, human dihydrofolate reductase positive selection cassette; CD, cytosine deaminase, negative selection cassette. Sizes of boxes are not to scale. B) Southern blot of 2 µg of genomic DNA extracted from PfLPL1 knockout clones E7, F8 and B11 and 3D7 wild-type parasites. Sizes of detected bands are in kilo bases and are indicated on left.

To corroborate PfLPL1 gene KO from Southern analysis, PCR analysis was employed using three different sets of paired primers. Four primers were designed to target PfLPL1 gene and not the KO plasmid, thereby distinguishing between an integration event at PfLPL1 gene locus. Figure 4-4A shows the position of the 4 primers used; P1 and P2 are internal primers, specific to WT gene sequences and primers P3 and P4 are specific to the 5' and 3' un-translated regions (UTR) respectively. If our results are similar to that obtained using Southern blot, then primers P1/P4 and P2/P3, would result in the amplification of only the WT gene with band sizes of ~0.7 kb. In contrast, primers P3/P4 would amplify both WT and KO genes but with distinguishable sizes of 1.1 and 3.0 kb, respectively. Isolated genomic DNA from all three KO clones, the parental KO and WT parasites were analyzed using equal amounts of DNA in each sample. As expected, amplification of PfLPL1 KO parasites were not detected with primers P1/P4 and P2/P3. However, clear size shift between PfLPL1 KO parasites and WT was observed using primers P3 and P4 (Figure 4-4B), which further validate the gene disruption of PfLPL1.

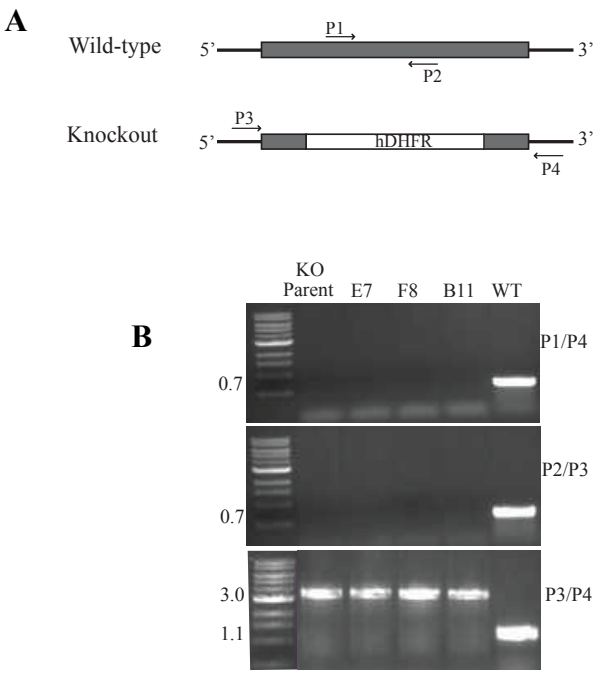

Figure 4-4. PCR Analysis of PfLPL1 knockout parasites. A) Schematic diagram of wild type and knockout PfLPL1 gene showing primer positions. B) 0.8 % agarose gel of PCR reaction using 88 ng of genomic DNA from PfLPL1 knockout parasites (parent and clones E7, F8 and B11) and wild-type (WT) parasites. Primer combinations used in each PCR reaction are indicated on the right. 10 μL of 1-kilobase ladder was used and the sizes of resulting bands are indicated on the left.

4.4.4 Analysis of Growth Rates

PfLPL1 KO parasites were assessed by Giemsa stained smears and maintained normal morphology. To determine if an effect from the loss of PfLPL1 could be detected on cell cycle progression, KO clones and WT parasites were monitored for 8 days and analyzed by flow cytometry. Asynchronous parasites were cultured in complete RPMI 1640 medium (CM) and fixed sample aliquots, taken every other day were stained with DNA dye YOYO-1 and analyzed by flow cytometry to calculate % parasitemia. The cumulative parasitemia was calculated over the 8-day period and graphed as linear function against time. Our analysis showed similar growth rates between clones F8 and B11 with WT, but a slightly slower growth of clone E7 (Fig 4-5A) in CM. The lack of growth inhibition could be attributed to the lipid-rich bovine serum albumin (BSA) supplement, AlbuMAX I, found in CM. AlbuMAX I contains an abundance of fatty acids [18], readily available for parasite use and capable of maintaining long term parasite growth [19-21]. PfLPL1 is a lysophospholipase that generates free fatty acid (FFA) as one of the products, it is therefore probable that the lack of PfLPL1 activity in generating FFA is complemented by the presence of FFA present in AlbuMAX I.

To directly assess the lack of PfLPL1 lysophospholipase activity, parasites were forced to rely on lysophosphatidylcholine (LPC) as the sole source of FFA available for parasite replication. Standard RPMI medium was prepared and supplemented with LPC in place of AlbuMAX I. In the event that PfLPL1 plays a role in parasite fitness, our analysis should indicate a level of growth inhibition in all knockout parasite clones. LPC was introduced as a containing FFA, palmitic acid and oleic acid esterified at *sn*-1 position in complex with fatty acid-free BSA. Palmitic acid and oleic acid were chosen because their growth promoting activity has been established in *P. falciparum* [19, 21]. Asynchronous cultures at ~3 % starting parasitemia were grown for 8 days and fixed samples taken every two days were analyzed for parasitemia by flow cytometry. Analysis revealed similar growth patterns seen previously in CM (Figure 4-5B). Clones F8 and B11 were found to have comparable growth rates to WT, while clone E7 exhibited a significant growth phenotype (Table 4-2). Growth inhibition was only observed in E7 and is therefore not an effect of PfLPL1 knockout, but rather resulted from clone variation due to a single-nucleotide polymorphism in the DNA sequence. These results suggest PfLPL1 does not contribute to parasite replication within the erythrocytic stages.

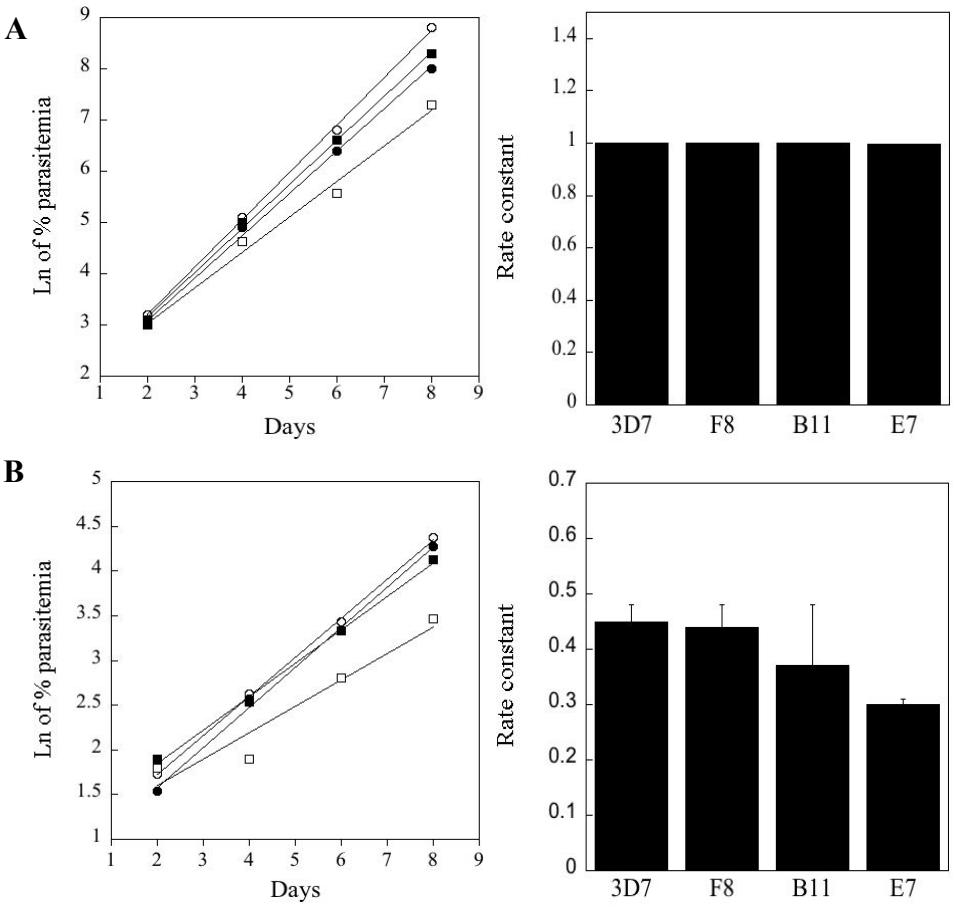

Figure 4-5: Growth rates of *P. falciparum* PfLPL1 knockout parasites. Asynchronous parasites were grown in 1 mL culture medium containing (A) complete RPMI 1640 medium and (B) AlbuMAX-free RPMI medium supplemented with 30 μM lysophosphatidylcholine. Cultures were grown for 8 days where 100 μL sample aliquots were taken every two days and fixed in 100 μL 0.1 % glutaraldehyde for at least 30 minutes. Fixed samples were permeabilized in 200 μL 0.25% Triton X-100 for 5 min at room temperature and stained with 100 μL 400 nM YOYO-1. % parasitemia was measured on a flow cytometer and expressed as the natural log of % parasitemia graphed against time, which are shown on the left panel. Shown on the right panel are bar graph representations of rate constants against parasite cultures 3D7 and PfLPL1 knockout clones, F8, B11 and E7. Filled circle represents 3D7; open circle represents clone F8; filled square represents clone B11 and open square represents clone E7. Graphs (A) are representative of duplicate experiments and graphs (B) represent an average of triplicate experiments.

Table 4-2. Growth rates of PfLPL1 knockouts clones compared with 3D7. Cultures were monitored in RPMI medium supplemented with lysophosphatidylcholine. Standard deviation was calculated from the rate constants (slope). *P* values are from a 2-tailed t-test.

	Parasite culture			
Replicate #	F8	B11	E7	3D7
1	0.46	0.55	0.31	0.48
2	0.45	0.445	0.33	0.42
3	0.53	0.315	0.335	0.445
Mean	0.48 (±0.04)	0.44 (±0.11)	0.32 ±0.01	0.45 ±0.03
p value	0.37	0.88	0.0097	

4.5 DISCUSSION

Our interest in characterizing PfGDPD prompted the identification of a source of glycerophosphocholine (GroPC) in parasite blood stages. PfGDPD is involved in the downstream degradation pathway of phosphosphatidylcholine, releasing choline and glycerol-3-phosphate, which are taken up and respectively utilized either in phospholipid metabolism or shuttled into glycolysis as an energy source. In this study, we attempted to build a pathway for phospholipid degradation by identifying lysophospholipases, which are involved in the intermediary steps releasing free fatty acids (FFA) and GroPC. Nine putative lysophospholipases were identified in the *Plasmodium* genome and of these, only one protein, PfLPL1 revealed similar distribution patterns to PfGDPD located within the parasite cytosol and the parasitophorous vacuole (PV). The presence of both enzymes in the PV designates a step-wise process in the phosphatidylcholine hydrolysis and the subsequent generation of choline.

We targeted PfLPL1 for gene disruption in order to assess its role during parasite intra-erythrocytic development. PfLPL1 knockout experiments generated parasites which we examined by Southern and PCR and confirmed the loss of PfLPL1 gene. Moreover, our Southern analysis detected the presence of an adjacent gene, PF14_0737, located on the same chromosome as PfLPL1 encoding gene. PF14_0737 encodes a putative lysophospholipase with a 53 % amino acid sequence identity to PfLPL1, and is also a member of the multi-domain *Plasmodium* subtelomeric family.

The knockout of PfLPL1 gene was easily achieved because the loss of this protein did not confer significant disadvantages to parasite. PfLPL1 knockouts retained normal parasite morphology and replicated at rates similar to 3D7 wild-type parasites when monitored in complete RPMI medium (CM). We attributed the results of our growth analysis to the abundance of fatty acid molecules available in AlbuMAX I, the lipid-rich bovine serum albumin component of CM, which would supplement the lack of available fatty acids resulting from the loss of PfLPL1 activity. We therefore modified CM by replacing AlbuMAX I with lysophosphatidylcholine (LPC), as the sole source of free fatty acids. Our analysis showed no difference in growth rates compared to wild-type in two of the three PfLPL1 knockout clones, F8 and B11, whereas clone E7 revealed a significant growth phenotype. The slow growth phenotype in clone E7 was an isolated event resulting from clone genetic variation and therefore not a direct effect of PfLPL1 knockout. Despite the observed slow growth phenotypes PfLPL1 knockout

parasites could continuously grown in culture. PfLPL1 is one of the nine lysophospholipases in the *Plasmodium* 3D7 isolate. Seven of these enzymes belong to the multi-domain Plasmodium subtelomeric family (PST-A), located in the subtelomeric region of the chromosome and consists of repetitive blocks of sequences that are highly polymorphic and species-specific [22]. In *P. falciparum*, this region consists of variable number of species-specific repeats between 10-40 kb, which are associated with many gene families involved in parasite virulence and evading the host immune system [23]. Some of the well-studied variable genes include *var* [24-26] *rif* [27, 28] and *stevor* [29] genes. PfEMP1, encoded by *var* genes, is exposed on the erythrocytes surface and mediates adherence to various endothelial receptors in the human contributing substantially to chronic disease and transmission [24, 30, 31]. It is interesting to note the presence of lysophospholipases present within this region. Further studies will extend to analyze the functional roles of the other predicted lysophospholipases in *P. falciparum.* Single knockout strategy presented here as well as double or triple lysophospholipase knockout parasites may prove valuable in characterizing this uncharted multi-domain family of lysophospholipases.

4.6 REFERENCES

1. Switzer, S. and H.A. Eder, *Transport of lysolecithin by albumin in human and rat plasma.* Journal of Lipid Research, 1965. **6**(4): p. 506-511.
2. Croset, M., Brossard, N., Polette, A., and Lagarde, M., *Characterization of plasma unsaturated lysophosphatidylcholines in human and rat.* Biochemistry Journal, 2000. **345**: p. 61-67.
3. Thiès, F., et al., *Unsaturated Fatty Acids Esterified in 2-Acyl-1-Lysophosphatidylcholine Bound to Albumin Are More Efficiently Taken up by the Young Rat Brain than the Unesterified Form.* Journal of Neurochemistry, 1992. **59**(3): p. 1110-1116.
4. Portman, O.W. and D.R. Illingworth, *Lysolec1thin binding to human and squirrel monkey plasma and tissue components.* Biochimica et Biophysica Acta (BBA) - Lipids and Lipid Metabolism, 1973. **326**(1): p. 34-42.
5. Nelson, G., *The phospholipid composition of plasma in various mammalian species.* Lipids, 1967. **2**(4): p. 323-328.
6. Psychogios, N., et al., *The Human Serum Metabolome.* PLoS ONE, 2011. **6**(2): p. e16957.
7. Weltzien, H.U., *Cytolytic and membrane-perturbing properties of lysophosphatidylcholine.* Biochimica et Biophysica Acta (BBA) - Reviews on Biomembranes, 1979. **559**(2–3): p. 259-287.
8. Asaoka, Y., et al., *Role of lysophosphatidylcholine in T-lymphocyte activation: involvement of phospholipase A2 in signal transduction through protein kinase C.* Proceedings of the National Academy of Sciences, 1992. **89**(14): p. 6447-6451.
9. Golan, D.E., et al., *Schistosomula of Schistosoma mansoni use lysophosphatidylcholine to lyse adherent human red blood cells and immobilize red cell membrane components.* Journal of Cell Biology 1986. **103**(3): p. 819-828.
10. Meyer zu Heringdorf, D. and K.H. Jakobs, *Lysophospholipid receptors: Signalling, pharmacology and regulation by lysophospholipid metabolism.* Biochimica et Biophysica Acta (BBA) - Biomembranes, 2007. **1768**(4): p. 923-940.
11. Sugimoto, H., H. Hayashi, and S. Yamashita, *Purification, cDNA cloning, and regulation of lysophospholipase from rat liver.* J Biol Chem, 1996. **271**(13): p. 7705-11.

12. Wang, A., R.A. Deems, and E.A. Dennis, *Cloning, expression, and catalytic mechanism of murine lysophospholipase I.* Journal of Biological Chemistry, 1997. **272**(19): p. 12723-9.
13. Toyoda, T., H. Sugimoto, and S. Yamashita, *Sequence, expression in Escherichia coli, and characterization of lysophospholipase II.* Biochimica et Biophysica Acta (BBA) - Molecular and Cell Biology of Lipids, 1999. **1437**(2): p. 182-193.
14. Waite, M., *Biochemistry of lipids, lipoproteins and membranes.*1991, Amsterdam: Elsevier BV.
15. Vial, H.J., et al., *Phospholipid metabolism in Plasmodium-infected erythrocytes: guidelines for further studies using radioactive precursor incorporation.* Parasitology, 1989. **98 Pt 3**: p. 351-7.
16. Zidovetzki, R., et al., *Inhibition of Plasmodium falciparum lysophospholipase by anti-malarial drugs and sulphydryl reagents.* Parasitology, 1994. **108 (Pt 3)**: p. 249-55.
17. Trager, W. and J. Jensen, *Human malaria parasites in continuous culture.* Science, 1976. **193**(4254): p. 673 - 675.
18. Frankland, S., et al., *Serum Lipoproteins Promote Efficient Presentation of the Malaria Virulence Protein PfEMP1 at the Erythrocyte Surface.* Eukaryotic Cell, 2007. **6**(9): p. 1584-1594.
19. Mi-ichi, F., K. Kita, and T. Mitamura, *Intraerythrocytic Plasmodium falciparum utilize a broad range of serum-derived fatty acids with limited modification for their growth.* Parasitology, 2006. **133**(04): p. 399-410.
20. Asahi, H., et al., *Investigating serum factors promoting erythrocytic growth of Plasmodium falciparum.* Experimental Parasitology, 2005. **109**(1): p. 7-15.
21. Mitamura, T., et al., *Serum factors governing intraerythrocytic development and cell cycle progression of Plasmodium falciparum.* Parasitology International, 2000. **49**(3): p. 219-229.
22. Mefford, C., and Trask J., *The complex structure and dynamic evolution of human subtelomeres*

. Nat Rev Genet, 2002. **3**(2).
23. Miller, L., M. Good, and G. Milon, *Malaria pathogenesis.* Science, 1994. **264**(5167): p. 1878-1883.

24. Su, X.-z., et al., *The large diverse gene family var encodes proteins involved in cytoadherence and antigenic variation of plasmodium falciparum-infected erythrocytes.* Cell, 1995. **82**(1): p. 89-100.
25. Baruch, D.I., et al., *Cloning the P. falciparum gene encoding PfEMP1, a malarial variant antigen and adherence receptor on the surface of parasitized human erythrocytes.* Cell, 1995. **82**(1): p. 77-87.
26. Smith, J.D., et al., *Switches in expression of plasmodium falciparum var genes correlate with changes in antigenic and cytoadherent phenotypes of infected erythrocytes.* Cell, 1995. **82**(1): p. 101-110.
27. Kyes, S.A., et al., *Rifins: A second family of clonally variant proteins expressed on the surface of red cells infected with Plasmodium falciparum.* Proceedings of the National Academy of Sciences, 1999. **96**(16): p. 9333-9338.
28. Fernandez, V., et al., *Small, Clonally Variant Antigens Expressed on the Surface of the Plasmodium falciparum–Infected Erythrocyte Are Encoded by the rif Gene Family and Are the Target of Human Immune Responses.* The Journal of Experimental Medicine, 1999. **190**(10): p. 1393-1404.
29. Cheng, Q., et al., *stevor and rif are Plasmodium falciparum multicopy gene families which potentially encode variant antigens.* Molecular and Biochemical Parasitology, 1998. **97**(1–2): p. 161-176.
30. Leech, J.H., et al., *Identification of a strain-specific malarial antigen exposed on the surface of Plasmodium falciparum-infected erythrocytes.* The Journal of Experimental Medicine, 1984. **159**(6): p. 1567-1575.
31. Kyes, S., P. Horrocks, and C. Newbold, *Antigenic variation at the infected red cell surface in malaria* Annual Review of Microbiology, 2001. **55**(1): p. 673-707.

CHAPTER 5

Summary and Conclusions

Plasmodium falciparum has evolved the ability to remain undetected within the human erythrocyte as it grows and multiplies while actively engaging in lipid metabolism and utilizing a vast number of precursors scavenged from the host milieu. Parasite lipids are required in the synthesis of membranes that serve as barriers between the parasite and host, membranes of sub-cellular organelles, cytoplamic membrane networks and lipid derived signalling molecules. Enzymes that hydrolyze host-derived lipids play key roles in parasite growth, virulence, differentiation, cell-signaling and hemozoin formation. The work presented in this dissertation characterizes glycerophosphodiester phosphodiesterase (PfGDPD), an enzyme that is involved in the downstream hydrolysis of phosphatidylcholine generating choline and glycerol-3-phosphate through the hydrolysis of glycerophosphocholine (GroPC).

Through homology and text search for phospholipases and lipases in the *Plasmodium* database, we identified possible gene candidates, which were endogenously tagged with a fluorescent probe to assess parasite cell distribution. Only one candidate gene, PF14_0060, encoded a protein, glycerophosphodiester phosphodiesterase (PfGDPD), with high fluorescence intensity expressed in the parasitophorous vacuole, cytosol and weakly expressed in the food vacuole. PfGDPD is a 56 kDa protein sharing similar TIM barrel structure with the unique GDPD insertion domain. Similarly, conserved residues at the N-terminal domain revealed two putative catalytic histidine residues (His29 and His78) and three metal binding residues (Glu63, Asp65 and Glu168).

The inability to disrupt the endogenous gene either by truncation or knockout strategies implicates an unidentified role for PfGDPD during the erythrocytic stages of the parasite. Biochemical characterization of purified native and recombinant species indicated efficient hydrolysis of glycerophosphocholine at the neutral pH of the parasitophorous vacuole, implicating a catalytic function in that compartment, in contrast to the acidic environment of the food vacuole where low activity was observed. Similar to other GDPD homologues, our kinetic analyses confirmed PfGDPD as a metalloenzyme, maximally active in the presence of Mg^{2+}, which was also required during expression and purification processes of recombinant protein to obtain an active enzyme. Evolutionary studies indicated a divergence of *Loxosceles* sphingomyelinase D (SMaseD) from GDPD domain family, which hydrolyze sphingomyelin and lysophosphatidylcholine (LPC). PfGDPD activity against two species of LPC with varying

lengths of fatty acid, C6:0 and C12:0, revealed hydrolysis LPLC6:0, though glycerophosphocholine is still the preferred substrate.

To gain insight into the role of PfGDPD, we attempted to modulate protein distribution in parasites in order to elicit a functional phenotype. We employed a ligand reversible conditional aggregation system (CAD), and generated parasites expressing PfGDPD-YFP-CAD. Fusion protein would be expressed as aggregates trapped in the ER, which can be dissociated in the presence of an anti-aggregation ligand. Though our studies revealed in the absence of ligand, fusion protein distribution in the cytosol, and leakage in the parasitophorous vacuole, we assessed effects of mis-localized PfGDPD on parasite growth rates. We took advantage of the choline-generating properties of PfGDPD, which is an important precursor for phospholipid synthesis and attempted to force parasite reliance on a single source of choline-containing compounds, glycerophosphocholine and lysophosphatidylcholine. This led to the development of Choline Free Media, a medium free of any metabolite precursors. Growth analysis in Choline Free Media elicited no phenotype, which may be due to the diffusion of lipid substrates to the cytosol, where PfGDPD-YFP-CAD fusion proteins were also present. Nonetheless, the successful development of Choline Free Media should be highlighted as the only medium in which lysophosphatidylcholine was eliminated as a source of choline.

We furthered our studies with PfGDPD by attempting to elucidate a pathway for phospholipid degradation in the parasite parasitophorous vacuole. We identified putative lysopholipases, involved in the upstream production of glycerophosphocholine, and only one *P. falciparum* lysophospholipase (PfLPL1), was localized to the same parasitophorous vacuole compartment as PfGDPD. Gene disruption experiments generated knockout parasites, which were subsequently cloned and genotyped, confirming the loss of the encoding gene. The effects of PfLPL1 knockout on parasite clones were not toxic to parasites and elicited no growth phenotype, as all clones retained normal morphology and could be continuously cultured.

Though a defined role for PfGDPD was not attributed, evidence persists for an important function of PfGDPD in erythrocytic replication. The complex distribution confounds studies to delineate a specific function for the protein beyond involvement in the downstream phospholipid degradative pathway. At this juncture, characterization of PfGDPD has been concluded, until more applicable techniques can overcome this hurdle.